UNIVERSITY OF CALIFORNIA,
IRVINE

Modeling Disruptions to Roadway Network Bridges, Restoration Workforce, and Vehicle-carried Information Flow for Infrastructure Management

DISSERTATION

submitted in partial satisfaction of the requirements
for the degree of

DOCTOR OF PHILOSOPHY

in Civil Engineering

by

Pierre Milton Caluna Auza

Dissertation Committee:
Professor R. Jayakrishnan, Chair
Professor Wenlong Jin
Professor Wilfred W. Recker

2018

DEDICATION

To Diana,
my red, red rose,
my muse's well,
my fondest kiss,
my forever girl,

"We are not bound forever in the circles of the world,
and beyond them is more than memory."

– J.R.R. Tolkien
LOTR, Appendix A(v)

Neither angels, nor demons,
nor wide-roaring oceans
can sever my soul from thee.

and to Margaret,
mi hija,

whose soul dwells

"in the house of tomorrow,
which (I) cannot visit,
not even in (my) dreams…"

– Kahlil Gibran
"On Children"

In the house of tomorrow,
I pray I be worthy
of enshrinement
in your heart.
If I be worthy,
remember me.

TABLE OF CONTENTS

LIST OF FIGURES

Page

LIST OF TABLES

Page

ACKNOWLEDGMENTS

The first order of thanks goes to my parents, Alex and Cynthia. They kept me out of trouble – not an easy or trivial task in my hometown in the 1990s. In addition, by defraying my rent costs and purchasing an automobile on my behalf, they afforded me opportunities since graduation that I would not have otherwise been able to pursue.

I thank the Transportation Research Board for their peer review of and for their permission to include my two Transportation Research Board Annual Meeting papers in this dissertation (one accepted for presentation in 2010, the other accepted for publication in the *Transportation Research Record* in 2018). Moreover, I thank the UC Irvine Regents' Scholarship, the former University of California Transportation Center (UCTC, now UC Connect), and the METRANS Transportation Center of the University of Southern California and California State University Long Beach. Their support gave me the financial peace of mind to complete my studies.

The CEE181 (Senior Design Practicum) and CEE81 (Introduction to Civil Engineering) Teaching Assistantships provided financial support for several years, though they have meant more to me than that. I am proud of the legacy I left in shaping the student experience for both courses. I thank April Heath for her help navigating UCI's bureaucracy – both as the CEE181 TA and afterwards. I thank CEE181 Professor C. Stephen "Steve" Bucknam for his kind, prayerful guidance that impressed upon me the humanity of the civil engineering profession – its potential for good and its poignant imperfections. I also thank my advisor for giving me the opportunity to design the final project for CEE81, and thus better prepare the students upstream of Senior Design.

I will forever admire the patience and genius of my advisor, Professor R. Jayakrishnan. He has shown me his genius in helping me simplify the problems I studied for this dissertation so that I could feasibly analyze them. He has shown me his patience in giving me the space to deal with my personal struggles and thus finish my dissertation.

I thank my committee members (Professors Wilfred W. Recker and Wenlong Jin). Their scholarship is profound and steadfastly rigorous, yet they have always been approachable to discuss research. They were similarly gracious even back when I was just another student needing their help in both undergraduate and graduate courses. They balance collegiality and scholarship, which is my favorite aspect of UC Irvine's Institute of Transportation Studies (ITS-UCI).

Like my advisor and committee, my dissertation would not have been possible without several mentors who helped me grow professionally, helped shape my views, and continued to see potential in me, even in those hard years when I had difficulty believing so myself. *Andreas Kaiser, mein Deutschlehrer, hat mir die Augen an eine Welt geöffnet, die größer als die Kleingeistigkeit in der ich erzogen geworden war.* I owe much to Herby Lissade and Dana Hendrix of Caltrans, who give me a valuable perspective into one major stakeholder's priorities, which in turn informed my dissertation's motivations. *Mwen reve yon jou nou twa kap kanbe ansanm nan lonbraj yon legliz St Rose de Lima rebati, epi tounen lakay pou manje lanbi ak sòs pwa.* I thank both Herby and Dr. Yuko J. Nakanishi for introducing me to the ABR10 (formerly ABE40) Critical Transportation Infrastructure Protection TRB committee. This experience gave me insight into the priorities of multiple sectors (private, public, nonprofit, academic).

The greatest keys to my recent success in bringing my dissertation to a close have been my mental health providers and my emotional support network. The improvements in mental health necessary to finish my dissertation were not immediate, but through my providers and network, I gained the ability to care for my mental health and thereby advance my studies a day at a time.

First, I must thank my spiritual advisors (Fr. Pat, Fr. John Francis, and Rev. Martha) who first saw I needed help, and who gently directed me to professional counseling. Dr. Julie Bartlett, thank you for teaching me that if I could break down my grief into smaller pieces, I can set goals to deal with them one at a time. Dr. Annie Ahn, thank you for making me aware of the childhood roots

of my irrationally harsh internal critic, and thank you for always reminding me that my future self-talk need not be distorted like in my past. Thank you also for referring me to Dr. David D. Burns' *Feeling Good* (now my go-to reference work for cognitive behavioral therapy, or CBT). Finally, thank you for recognizing when I was not progressing, and thus referring me to the battery of tests that determined my needs would be best served by long-term care outside the UCI Counseling Center.

To the kind Albanian Psy.D. who administered those tests to me, thank you. We met only once, and I have regretfully lost your name, yet you've helped me more than you can know. Dr. Malcolm Miller, thank you for clarifying for me and guiding me through the nuts and bolts of implementing CBT: the journaling and data-gathering, the precise identification of distorted thoughts, and their disputation. And to Holly Gil-Navarrete, LCSW, thank you for being my counselor as I finish my dissertation and as I embark on fatherhood. Thanks to you, guided meditation and affirmation lists are now tools in my anti-depression and anti-anxiety toolkit.

Friends, family, and even several important literary and public figures have been a necessary emotional support for my mental health (without which I couldn't have completed this journey). First of all, I thank my friends at ITS UCI: Drs. Daji Yuan, Ankoor Bhagat, and Dr. Sarah Aly. In particular, Dr. Sarah Aly, your perseverance, your commitment to your family, and your faith in God are lodestars for me. I aspire to reach where you are, and to do so as gracefully as you have.

I thank several literary and public figures who provided me a mental health lifeline: PBS host Huell Howser, Scottish poet Robert Burns, Rwandan-Quebecois artist Corneille Nyungura, professors CS Lewis and JRR Tolkien, author John Green, Catholic satirist Stephen Colbert, and Rev. Fred Rogers. Along with CBT, I found in each of these figures' works different tools that allowed me to deal with consuming grief and a harsh internal critic in healthier, less destructive ways.

Thank you to the choir at Corpus Christi Catholic Community in Aliso Viejo (particularly Dean Calvano, John White, Chris Tran, and Shelby Mocnik) and to my various support groups at SHARE Center Culver City. You gave me a welcoming, nonjudgmental venue to re-tell the story of my life in a way that was more accepting and forgiving of myself.

Thank you to my closest living friends: Patrick Huu, Kyle and Alec Kimmel, and Chad Kim. Thank you for being people I could trust when my mental health was most vulnerable; for inspiring me; or even just for sharing your food, drink, and company with me on days when I had to fight depression to get out the door.

Thank you to my cousin Jason and my friend Ralph. They have passed before me, but I could feel them with me at my most mentally vulnerable moments during my doctoral studies. *Ralph, mon frère libanais, j'avais toujours cru que vos enfants et les miens iraient grandir ensemble. Je regrette que le bon Dieu avait eu d'autres desseins. Vous me manquez toujours. Attendez-moi dans l'Au-Delà.* Jason, I haven't brought Maggie down to the river to see you yet. We will bring your favorite drink as libation. And on the day when air, land, and sea are compelled to give up their dead, I'll see you again, face-to-face, with the same sharp, living vision with which I see the hairs on the back of my hand, or on my daughter's head. Wait for me, Jason. Wait for me.

Diana, my beloved, first of all, thank you for showing me how ArcGIS and SAS were superior for the applications at hand, and for supporting me when I had questions with either. But beyond that, thank you for your patience with the dissertation, and with me. Thank you for trusting me enough to share your life with me, and my feet of clay. I love you so much.

Maggie, I have not been your father for long. But I have learned painfully that the voices with which we will speak to our future selves often find their roots in the words our parents first spoke to us. When you are older and need to listen to your inner voice for strength or guidance, I pray that the voice that speaks back to you is kind, encouraging, and forgiving. I pray for wisdom to choose carefully the words I say to you. And I pray you forgive me when my choices fall short.

CURRICULUM VITAE

Pierre Milton Caluna Auza

2007	B.S. in Civil Engineering, Structures, University of California, Irvine
2007-12	Teaching Assistant, CEE181 Senior Design Project Practicum and CEE81A Introduction to Civil Engineering
2009	M.S. in Civil Engineering, Transportation Systems, University of California, Irvine
2011-14	Research Coordinator, TRB Standing Committee of Critical Transportation Infrastructure Protection
2012-18	Graduate Student Researcher, Institute of Transportation Studies, University of California, Irvine
2014-2018	Secretary, TRB Standing Committee of Critical Transportation Infrastructure Protection
2018	Ph.D. in Civil Engineering University of California, Irvine

FIELD OF STUDY

Resilience of Transportation Infrastructure Systems
Modeling Disruptions to Transportation Systems and Workforces

PUBLICATIONS

Auza, P. and D. Lavery, R. Jayakrishnan, Y. Nakanishi. (2018). "Telecom, Traffic Cones, and The Big One: Identifying Transportation and Communications Emergency Support Workforces, and Calculating Their Exposure to Seismic Peak Ground Accelerations" *Transportation Research Record: Journal of the Transportation Research Board*. Washington, DC. DOI: http://dx.doi.org/10.1177/0361198118787937

Auza, P. and R. Jayakrishnan, M. Shinozuka. (2010). "Using Mesoscopic Traffic Simulation in a Seismic Risk Analysis (SRA) Framework Applied to a Downtown Los Angeles Network" (Paper 10-4007). The 89th Annual Meeting of the Transportation Research Board, Washington, DC.

ABSTRACT OF THE DISSERTATION

Modeling Disruptions to Roadway Network Bridges, Restoration Workforce, and Vehicle-carried Information Flow for Infrastructure Management

By

Pierre Milton Caluna Auza

Doctor of Philosophy in Civil Engineering

University of California, Irvine, 2018

Professor R. Jayakrishnan, Chair

The ability to model the disruptions of adverse events on various systems, such as infrastructural and social, is an important tool to assessing these systems' resilience. While previous research on system resilience concentrated on physical infrastructure such as transportation systems, two recent research topics include social resilience and dependencies across many infrastructure systems. For example, transportation is dependent on such systems as power, communications, and the workforces that are key to restoring these infrastructure systems. This dissertation contains three disruption modeling studies that have followed the evolution of resilience research over the past decade from physical systems to interrelated topics. The first study uses mesoscopic traffic simulation to evaluate seismic risk of potential travel time increases from earthquake damage to bridges in a roadway network. This analysis successfully obtained system risk curves of network-wide travel time increases. The second study shifts focus towards workforces that participate in restoring infrastructure systems. It identifies transportation and communications workers and calculates these workers' exposure to the Peak Ground

Accelerations (PGAs) of a 7.8 magnitude Southern California scenario earthquake. Indeed, for this scenario, transportation workers are exposed to statistically significant higher PGAs than non-transportation workers, and communication workers to significantly lower PGAs. The third study proposes a model for the travel time of information along communication-equipped vehicles physically traveling in a network. Vehicles are sampled as equipped vehicles, then their trajectories are analyzed to (1) estimate equipped vehicle link flow and turning movement counts and (2) estimate the frequency of equipped vehicles encountering each other on links and at nodes. This study compares two scenarios: the baseline scenario and a work zone scenario that corresponds to a bridge being damaged in the network. It is hypothesized that there would arise a difference in expected path travel times when (1) the representation of a specified subpath within the sample is increased and (2) when vehicles are routed along currently unused subpaths. This dissertation concludes with a discussion of the contributions of all three studies, as well as suggestions for future work.

1 INTRODUCTION

The ability to model the disruptions of adverse events on various systems (such as infrastructural and social) is an important tool to assessing these systems' resilience. While previous resilience research concentrated on physical infrastructure (such as transportation systems), two recent research topics include social resilience and dependencies among infrastructure systems. Social resilience at the individual, community, and national scales is an important determinant of positive resilience outcomes (such as during response or recovery). Transportation is itself dependent on such systems as power, communications, and the workforces that are key to restoring these infrastructure systems. This dissertation contains three disruption modeling studies that have followed the evolution of resilience research over the past decade from physical systems to interrelated topics.

The first study (or "Study 1") is entitled "*Using mesoscopic traffic simulation in a seismic risk analysis (SRA) framework applied to a West Los Angeles network*". It evaluates seismic risk of potential travel time increases from earthquake damage to bridges in a roadway network. It is the earliest of the three studies, accepted for presentation at the 89th Annual Meeting of the Transportation Research Board in 2010. It introduces the use of mesoscopic traffic simulation in a seismic risk analysis (SRA) framework. The study area incorporates the site of the West Los Angeles bridge failures during the 1994 Northridge earthquake. The analysis successfully obtained system risk curves of network-wide travel time increases. The study also took advantage of vehicle trajectory output to obtain risk curves of travel time increases for specific OD pairs.

The second study (or "Study 2") is entitled "*Identifying transportation and communications emergency support workforces, and calculating their exposure to seismic peak ground accelerations*". It shifts focus towards workforces that would participate in restoring infrastructure systems, though it concentrates on transportation and communications. The study's goals are 1. to identify such workers and 2. to calculate these workers' exposure to the Peak Ground Accelerations (PGAs) of a 7.8 magnitude Southern California scenario earthquake. These exposures are then compared to the rest of the working population's exposure, to determine if the difference is statistically significant. This study finds that for this scenario, transportation workers are exposed to statistically significant higher PGAs than non-transportation workers, and communication workers to significantly lower PGAs. For practioners, knowing which worker categories a disaster disproportionately affects could justify pre-event investments in preparedness and recovery planning efforts for specific workforce categories.

The third study (or "Study 3") is entitled "*Modeling expected travel time changes in vehicle-carried information flow along selected routes under network disruptions*". It proposes a model for the travel time of information along communication-equipped vehicles that are physically traveling in a network. The study compares the expected travel time of information flowing along multiple paths connecting a specified pair of one sender and one receiver node in the fictional AZVille network. To estimate the information travel time, the methodology samples different proportions of simulated vehicles (10%, 20%, and 30%) as equipped vehicles. These samples' trajectories are analyzed to estimate link flow and turning movement counts of equipped vehicles, and to estimate the frequency of equipped vehicles encountering each other as they travel on links and through nodes. This

study compares two scenarios: the baseline scenario and a work zone scenario that corresponds to a bridge being damaged in the network. It is hypothesized that there would arise a difference in expected path travel times when 1. the representation of a specified subpath within the sample is increased and 2. when vehicles are routed along currently unused subpaths.

1.1 Motivations

1.1.1 Resilience and Infrastructure-Related Core Capabilities

The evolution of the concept "Resilience" is a running thread in the studies of this dissertation. One definition can be found in Presidential Policy Directive 8:

> "The ability to adapt to changing conditions, and withstand and rapidly recover from disruption due to emergencies."

For example, after a complex disaster like a large earthquake, or a major terrorist attack, or a Category V hurricane, all levels of government will need to respond: Federal, State, Regional, and Local. In the short-term response, these governments must cooperate to restore Emergency Support Functions like Transportation, Communications, Firefighting, Public Health, and others (as defined in the *National Response Framework* (2016)). During the mid- to long-term recovery, there are Recovery Support Functions (as defined in the *National Disaster Recovery Framework* (2016)) that focus on restoring Community Planning, the Economy, Health & Social Services, Housing, Infrastructure, and Natural and Cultural Resources.

But Response and Recovery are not the whole picture. If these are to succeed, governments must also commit to the other Mission Areas that precede the event: Protection, Prevention, and Mitigation. These Mission Areas are defined in the *National Preparedness Goal* (2017):

- **Prevention.** "Prevent, avoid or stop an imminent, threatened or actual act of terrorism."
- **Protection. "**Protect our citizens, residents, visitors and assets against the greatest threats and hazards in a manner that allows our interests, aspirations and way of life to thrive."
- **Mitigation.** "Reduce the loss of life and property by lessening the impact of future disasters."
- **Response.** "Respond quickly to save lives, protect property and the environment, and meet basic human needs in the aftermath of a catastrophic incident."
- **Recovery.** "Recover through a focus on the timely restoration, strengthening and revitalization of infrastructure, housing and a sustainable economy, as well as the health, social, cultural, historic and environmental fabric of communities affected by a catastrophic incident."

These Mission Areas include Core Capabilities, including those related to infrastructure: Infrastructure Systems (Response and Recovery), Physical Protective Measures (Protection), Long-Term Vulnerability Reduction (Mitigation), and Critical Transportation (Response). Ideally, engagement in developing and maintaining these Core Capabilities across all Mission Areas is ongoing and continuous, long before an event occurs and is detected.

1.1.2 California Natural Hazards, and a focus on Earthquakes

In California, the natural hazards of most interest are earthquake, flooding, and fire. These are the first three hazards listed in the *State of California Emergency Plan* (2017). However, this dissertation's long-term focus is on seismic hazards. Study 1 of this dissertation is an extension of the seismic risk analysis work performed in Shinozuka et al (2005), a study to estimate the potential reductions in post-earthquake travel delays of a seismic retrofit program of Southern California highway bridges. Study 2 and Study 3 continue to use earthquake as its hazard of focus.

Flood is the second listed hazard in the 2017 *State of California Emergency Plan*. The plan notes that "over five million Californians, or approximately 15 percent of the total population, live in a Flood Insurance Rate Map (FIRM) designated floodplain" and that "the potential direct flood damages in the Sacramento area alone could exceed $25 billion". Of the 17 major disaster declarations between January 2010 and August 2018 within the state of California on the Federal Emergency Management Agency (FEMA) archive of disaster declarations ("Disasters | FEMA.gov", n.d.), there have been eight declarations which involve flood: Resighini Rancheria Flooding (DR-4312); Severe Storms, Flooding, Mudslides (DR-4308, DR-4305, DR-4301, DR-1952, DR-1884); and severe winter storms that affected the Hoopa Valley (DR-4302) and Soboba Band of Luiseño Indians (DR-4206) tribal governments. Between 2010 and 2014, the California Governor's Office of Emergency Services (Cal OES) has published After Action Reports (AARs) for five storms with flooding: 2014 December Storm, July 2013 Inyo County Thunderstorms, 2011 March Severe Storms, 2010 December Statewide Storms, and 2010 January Statewide Storms ("After Action-Corrective Action Reporting", n.d.).

Fire is the third listed hazard in the 2017 *State of California Emergency Plan*. The plan notes that from 1954 to 2017:

- "seventy-three (73) percent of presidentially declared disasters in California were the result of wildfires",
- wildfires claimed "97 lives, resulted in 1,504 injuries, and $2.1 billion in [Cal OES] administered disaster costs",
- "approximately 37 million acres within California are at risk from wildfire, with 17 million acres at high risk", and that
- "a total of 11.8 million homes are located in the Wildland-Urban Interface (WUI)."

The plan also notes that the state of California established the California Fire Service Task Force on Climate Impacts in July 2014, recognizing the connection between climate change and increased wildfire severity. One responsibility of the Task Force is "as necessary, (to) develop new or updated recommendations related to wildfire preparedness and mitigation needed to *successfully adapt to California's changing climate*" (emphasis added).

Of the 17 major disaster declarations between January 2010 and August 2018 in California, six involve fires ("Disasters | FEMA.gov", n.d.): California Wildfires And High Winds (DR-4382); California Wildfires, Flooding, Mudflows, And Debris Flows (DR-4353); California Wildfires (DR-4344); California Valley Fire and Butte Fire (DR-4240); California Rim Fire (DR-4158); and the Karuk Tribe Wildfire (DR-4142). Between 2010 and 2014, the California Governor's Office of Emergency Services (Cal OES) has published AARs for three wildfires: 2014 Fire Season, 2013 Fire Season, and 2012 Chips Ponderosa Fires. However, of the 21 AARs published online since 2003, fires comprise the largest proportion with seven totals ("After Action-Corrective Action Reporting", n.d.). In addition to the three

mentioned above, Cal OES has created AARs for the following fires: 2008 Southern California Fires, 2008 Mid-Year California Fires, 2007 Southern California Wildland Fires, and the 2003 Southern California Fires.

Since the most recent fire-related Cal OES AAR in 2014, other fires have made the top 20 lists of the most structure-destroying ("Top 20 Most Destructive California Wildfires," 2018), deadliest ("Top 20 Deadliest California Wildfires," 2018), and largest ("Top 20 Largest California Wildfires," 2018) California fires. In July 2018, the Mendocino Complex fire became the largest California wildfire, while the Carr fire became the 7th largest and 6th most destructive. In December 2017, the Thomas fire became the 2nd largest and the 8th most destructive California wildfire. October 2017 saw several fires enter these lists: the Tubbs fire (3rd deadliest, 1st most destructive), the Redwood Valley fire (10th deadliest, 18th most destructive), the Atlas fire (14th deadliest, 12th most destructive), Cascade (20th deadliest), and the Nuns fire (7th deadliest). September 2015 had two fires on the Most Destructive list: Valley (#4) and Butte (#11).

Yet despite the devastation wrought by floods and fires, earthquake remains the first hazard listed in the 2017 *State of California Emergency Plan*. The plan notes that "although infrequent, major earthquakes have accounted for and continue to have the greatest potential for loss of life, injury, and damage to property." There remains a lot at stake just from seismic hazards alone. For example, Corelogic (2016) found that an 8.3 magnitude San Andreas earthquake could result in 1.6 to 3.5 million damaged homes (potentially costing $289 billion). The landmark 2008 USGS ShakeOut Scenario report (Jones et al, 2008) simulated a 7.8-Mw San Andreas earthquake and found $213 billion in economic losses.

The 2017 *State of California Emergency Plan* notes that more than 70 percent of California's population resides within 30 miles of a fault where strong ground shaking could occur in the next 30 years, and that in 17 counties, more than 90 percent of the population lives where shaking can be strong. Since January 2010, California has experienced two earthquakes that have received major disaster declarations ("Disasters | FEMA.gov", n.d.): the 6.0-magnitude Napa earthquake (DR-4193) and the 7.2 magnitude Baja California earthquake (DR-1911). Both of these earthquakes also resulted in Cal OES publishing After-Action Reports, although Cal OES also published an AAR for the 6.5-magnitude January 2010 Eureka earthquake in Humboldt county ("After Action-Corrective Action Reporting", n.d.).

1.1.3 The State of U.S. Bridge Infrastructure

The state of bridge infrastructure over the past decade has been a motivating factor in the three studies of this dissertation.

There were 614,387 bridges in the 2016 National Bridge Inventory. The 2017 ASCE Infrastructure Report Card (ASCE, 2017) notes that of these bridges, almost 4 in 10 were 50 years or older, and 9.1% (56,007) were structurally deficient. On average, the Report Card estimates that 188 million trips occur across a structurally deficient bridge each day.

Study 1 is a seismic risk analysis study. Bridges are the infrastructure for which the risk of post-earthquake travel time increases are being assessed.

The original motivations for Study 3 lay in exploring the possibility of using vehicles equipped with communication equipment as a means of transferring data on the structural health of bridges from sensors to receivers, especially when wireless communication systems are disrupted. Disaster events like earthquake, fire, or inundation can severely

disrupt wireless communication systems in addition to bridges and other transportation system elements. In such a scenario, what if communications-equipped vehicles could be enlisted or routed in order to physically carry information on critical infrastructure systems, such as bridges, from remote sensors to receiver stations? From this consideration grew the attempt in Study 3 to model the flow of information based upon the physical travel of equipped vehicles.

Study 2 relates not to physical infrastructure such as bridges, but to the workforces tasked with maintaining it. Bridge maintenance workers are among the worker categories included in the analysis for identifying workers critical to restoring transportation infrastructure, and subsequently estimating their exposure to the Peak Ground Accelerations (PGAs) of a scenario earthquake.

1.1.4 Growth in Connected Vehicles and Related Infrastructure

The growing ubiquity of connected vehicles forms part of the motivations for Study 3. The near future will see an increase in both connected vehicles and connected vehicle infrastructure. In 2016, the National Highway Traffic Safety Administration (NHTSA) published its highly anticipated *Federal Automated Vehicles Policy*. In December 2013, the Intelligent Transportation Society of America published a Market Report which found the following: 54% of survey respondents said their department has developed a regional or agency-specific Intelligent Transportation Systems (ITS) architecture, 63% of state governments have an ITS strategy in place, and 71% of survey respondents that have a state ITS plan said their agency implemented ITS to reduce congestion and traffic delays (ITS America, 2013b). Meanwhile, the 2013 National ITS Deployment Tracking survey suggests there is a strong commitment to continued growth in ITS investment. One-half to

three-fourths of the surveyed agencies planned to expand current deployments or deploy new technologies (ITS America, 2013a).

In light of the interest in newer concepts in ITS, and the expected near-term development of a data-rich mobility environment with connected vehicles, Study 3 grew from an attempt to develop schemes to use connected vehicles to efficiently enhance the mobility of data in these systems. This use of connected vehicles was itself rooted in an exploration of mules. A "mule" is an entity which physically carries computer data between locations to create a data communication link. Coined by Shah et al (2003), "mule" was originally an acronym for Mobile Ubiquitous LAN Extension (MULE). Researchers in computer science no longer capitalize the acronym for this now-established term.

Mule-based systems can reduce the fixed communication infrastructure needed for monitoring traffic and the health of large infrastructure systems such as bridges and wind farms. To the writer's knowledge, there has been no recognition in the literature of the importance of mule communication in other critical areas such as management of network traffic disruptions, specifically under disaster conditions. However, such disasters may often cause serious jamming of the infrastructural and wireless communication systems, and mules might even be necessary to carry information from point to point. Furthermore, the studies on mules in the past have focused on the technical and computational details, rather than on the mobility aspects and on efficiency in the mobile deployment of mules.

Study 3 is an important step in developing a methodology for efficient network deployment and movements of mules and the information they carry. The study also has a specific focus on disrupted states under scenarios such as disasters. Though Study 3 does not solve for an optimum set of routes for equipped vehicles, it measures changes in

information flow on those paths over which equipped vehicles are routed. This contribution could be critical in formulating an optimization scheme.

1.1.5 Restoration-Critical Workforces

The resilience of infrastructure systems is often dependent upon more than merely the physical assets themselves. The resilience of social systems may also affect an infrastructure system. For example, certain worker categories will be critical to the restoration of transportation and communication systems after a disruptive event. This dissertation labels these workforces as "restoration-critical workforces". Some obvious critical workforces would include Maintenance & Operations (M&O) personnel from a state or local DOT; police, fire, or other public safety personnel; and technicians who maintain and repair telecommunications utilities.

At the federal level, frameworks and plans from the Department of Homeland Security define Emergency and Recovery Support Functions and Critical Infrastructure Sectors that can in turn determine if a worker category is critical to restoration. Specifically, the *National Response Framework (NRF)* (2016) defines Emergency Support Functions (ESFs), the *National Disaster Recovery Framework (NDRF)* (2016) defines Recovery Support Functions (RSFs), and the *National Infrastructure Protection Plan (NIPP)* (2013) defines Critical Infrastructure Sectors (CISs).

However, the very workers that would be relied upon to restore infrastructure could themselves be badly affected by natural hazards. That is, if the homes of M&O or telecommunications workers are badly damaged by an earthquake, then their ability to return to work and repair roads or communication systems is hindered. For example, in their case studies of the Port of New York and New Jersey, Southworth et al (2014)

highlighted several actions that would assist in recovery. One example action was to arrange on-site housing for critical staff, emergency responders, and relief workers.

1.2 Overview of Dissertation

This dissertation contains three studies that share a common theme of modeling disruptions for infrastructure management:

- Chapter 2: Study 1, *Using Mesoscopic Traffic Simulation in a Seismic Risk Analysis (SRA) Framework Applied to a West Los Angeles Network*.
- Chapter 3: Study 2, *Identifying Transportation and Communications Emergency Support Workforces, and Calculating their Exposure to Seismic Peak Ground Accelerations*.
- Chapter 4: Study 3, *Modeling Expected Travel Time Changes in Vehicle-carried Information Flow along Selected Routes under Network Disruptions*).

The dissertation concludes in Chapter 5 with a summary of the contributions of the three studies and with suggestions for future work.

2 STUDY 1: USING MESOSCOPIC TRAFFIC SIMULATION IN A SEISMIC RISK ANALYSIS (SRA) FRAMEWORK APPLIED TO A WEST LOS ANGELES NETWORK

Previous efforts to quantify and estimate the effect of seismic disruptions on the performance of the transportation network have relied on traditional trip-based static traffic assignment methods to estimate and compare network flows under base and damaged cases. Such static assignments with the well-known problem of unrealistically high volume/capacity ratios on congested links, are questionable for predicting the post-earthquake peak-period travel times when links are disabled. This paper introduces the use of mesoscopic traffic simulation in a seismic risk analysis (SRA) framework. This study assesses seismic risk in terms of potential travel time increases in a study area incorporating the site of the West Los Angeles bridge failures during the 1994 Northridge earthquake. This study successfully obtained system risk curves of network-wide travel time increases, and took advantage of vehicle trajectory output to obtain risk curves of travel time increases for specific OD pairs.

2.1 Introduction

In Southern California, significant media attention has fallen upon the USGS press release claiming that the probability of an earthquake of magnitude ≥6.7 is greater than 99% (USGS, 2009). In the scenario earthquake considered for the California ShakeOut earthquake drill, an earthquake of 7.8 on the San Andreas fault can cause 2,000 deaths, 50,000 injuries, and $200 billion in damage (Jones et al, 2008). The same study also estimates $5 billion in damage to transportation lifelines alone over the year following the disaster, although it praises the mitigation efforts of the state's 20-year bridge retrofit

program. In addition, the 1994 Northridge earthquake resulted in 72 deaths, $25 billion in damage, and major disruptions to the freeway network at four locations (DeBlasio et al, 2002). Shinozuka et al (2005) cites the 1994 Northridge and the 1989 Loma Prieta earthquakes as having lent urgency to the Caltrans bridge retrofit program. That study attempted to quantify the program's benefits in the Los Angeles highway network by comparing the cost of the retrofits against (1) the restoration and repair costs avoided by retrofits and (2) the equivalent monetary costs of the travel time increases on the damaged network. Indeed, the study concluded that when both the avoided restoration/repair costs and the avoided travel time increases are considered, the retrofits yielded a net benefit (i.e. had benefit-cost ratios exceeding 1.00).

In order to calculate network travel times for both the base case and to calculate travel time increases for several earthquake scenarios, Shinozuka et al (2005) uses a user equilibrium (UE) variable demand traffic network model that includes only the freeways and major highways of the LA Basin. The model is somewhat unconventional in that it performs simultaneous trip distribution and traffic assignment via the Evans algorithm rather than perform those steps sequentially perhaps with feedback (inherited from Cho et al (2003)). Nevertheless, this model suffers from two "inherent weaknesses" of traditional trip-based UE-based static traffic assignment models: as a 2007 TRB Special Report points out, the traditional methods (1) lack "a coherent theory of travel behavior" on the demand side and (2) are "unable to represent dynamic conditions" on the supply side (Wachs et al, 2007).

This paper does not address the demand-side shortcomings of the analysis in Shinozuka et al (2005). Instead, this paper explores the use of a more advanced supply

model for seismic risk analysis (SRA) applications. In particular, flows are modeled using a mesoscopic traffic simulation software, namely, DYNASMART (**DY**namic **N**etwork **A**ssignment **S**imulation **M**odel for **A**dvanced **R**oadway **T**elematics). By modeling individual vehicles, this paper most immediately demonstrates the advantages of being able to disaggregate results by subsets of vehicles. Specifically, this paper evaluates the risk of travel time increases for two specified OD pairs. Just as importantly, these models can potentially incorporate future advances in path-based decision-making behavior.

2.2 Background

This paper and Shinozuka et al (2005) are indebted to research efforts to adapt SRA methods to spatially distributed lifeline systems. Some examples are highway networks, domestic water and sewage, power grids, and even hospitals (critical to delivering post-event health care). In these systems, continuous system functionality depends upon ground motion and the resulting damage at multiple geographical locations in the system (Chang et al, 2000). Prior to Chang et al (2000), SRA research had concentrated on facilities at a single location (e.g. nuclear plants). Whereas Chang et al (2000) devises a scenario earthquake set selection method to approximate the seismic hazard in the LA basin, Cho et al (2003) applies these earthquake scenario sets to a traffic network model that sustains varying degrees of seismic damage. These studies culminate in the REDARS (**R**isks from **E**arthquake **DA**mage to **R**oadway **S**ystems) methodology, which separates the earthquake scenario selection, transportation infrastructure fragility, and network flow models into separate modules to facilitate future improvements in SRA (Werner et al (2006) and Werner et al (2008)).

Sisiopiku et al (2007) reviews three mesoscopic traffic simulation models: DynaMIT, DYNASMART, and VISTA (Visual Interactive System for Transport Algorithms). Although that study ultimately employs VISTA, the study in this paper considers DYNASMART sufficient to implement the SRA framework from Shinozuka et al (2005). The DYNASMART model first appears in Jayakrishnan et al (1993), and its purpose from its inception has been to provide a platform to evaluate information supply strategies, information/control systems (e.g. ATMS, ATIS), and similar information-based elements of Intelligent Transportation Systems (ITS). Under the FHWA's Dynamic Traffic Assignment program, in 1998 the DYNASMART model was adapted at the University of Texas at Austin for traffic prediction, creating DYNASMART-X (Mahmassani et al, 2004a). The FHWA continued its support of DYNASMART, and at the University of Maryland the DYNASMART model was adapted for planning and traffic operations applications; the first version of DYNASMART-P was released in 2004 (Mahmassani et al, 2004b). Lastly, another offline planning package using the DYNASMART model was released in 2008, named DynusT [0]. Its strength is integration with two well-known microscopic traffic simulation models (VISSIM and CORSIM).

Although the strength of DYNASMART is its ability to perform dynamic traffic assignment, those features are not exploited in the present study. Nevertheless, the potential improvements of simulation over static traffic assignment methods could be significant in managing post-earthquake congestion. To this end, a discussion of these improvements is appropriate. However, for this study the most immediate benefit of using simulation is the ability to disaggregate the results by subsets of individual vehicles. This paper includes a brief note discussing this benefit.

2.2.1 Need for Simulation Instead of Static Traffic Assignment Methods

Though traffic assignment based on user equilibrium principles has been the predominant supply-side model used in transportation planning and forecasting for nearly four decades, its deficiencies in modeling congested conditions, especially those that exist over elongated periods (through a three-hour peak-period, for instance) are often not well-appreciated by transportation practitioners and even researchers, even though the basic reason is rather simple.

The assignment models use a network equilibrium paradigm of a flow split across paths between each origin-destination, such that all used paths have equal travel times. The formulation to find equilibrium however uses only one simplistic model for the network supply modeling, which is a function (the well-known 4th power function, BPR, function) that describes the travel times on any network link to be monotonically increasing with respect to the flow (vehicles crossing a point per unit time). While this appears intuitively appealing, any driver stuck in congestion knows that the flow is drastically low during heavily congested periods due to the very high density (vehicles per lane mile) and the very low average speed. As in very basic traffic flow theory, flow is a product of speed and density, and is thus a function that increases and decreases beyond a maximum flow, as more and more vehicles occupy road space (high density), though speed itself is monotonically decreasing (or strictly non-increasing) with density.

The effect of speed being monotonically non-increasing with respect to density causes the basic traffic behavior that the travel time (inverse of speed) function initially increases with flow but then "turns back" and goes to infinity as the flow drops to lower values and the traffic completely jams up (nearly zero speed and zero flow). This behavior

may occur on a point on a highway only for a short period before the conditions change dynamically in stop and go traffic. It was however established from field observations, as far back as the 1950s, that the travel time curve showing two values for any flow value (for congested and uncongested conditions) can be seen if data is aggregated over short period less than 5 to 10 minutes. The curve rarely shows the behavior when average travel times are observed and averaged for hourly flows and thus for static planning models using hourly flows, a BPR-like function was quite acceptable.

It has been known to planners that the assignment models do not replicate flows and travel times on links (such as on a few freeway links in congested networks during peak hours), but many have often not appreciated the real reason, the supply model errors, as explained above. The planning models simply assume that flows are over capacity and that travel times are high due to the high volume over capacity ratio (over even 2.0, while even values over 1.2 are physically impossible on the network links). Thus, while the congested links show high travel times, many alternate links on to which the flows would need to divert would be modeled not to receive adequate traffic and would show very low travel times. Consequently, the true network-wide delays could be very wrongly predicted, especially in the congested portions of the network.

It is worth noting why the above issue is particularly relevant under earthquake traffic scenarios. Post-earthquake, while the traffic does readjust among alternate paths to tackle the situation of unavailable links, it is quite possible that highly congested conditions would exist on several links for significant periods during the perk-periods (technically due to lack of sufficient alternative paths for dynamic redistribution during the peak period). This implies that the “turned back” portion of the travel time curve, showing high values at

low (congested) traffic flows would be in effect. The assignment models, as they do not include this portion of travel time curve will simply assume most of the traffic to stay on the predominant alternate path around the link disabled due to a bridge or structural failure.

The only proper method to predict the congested conditions that exist for longer (for more than 15 minutes of the peak-period) with associated high travel times and low flow, is to use traffic models that are predicated upon the primary variable, traffic density. The primary conceptual reason is the monotonically increasing travel times, with respect to density. This can be accomplished with analytical/numerical traffic models, which are differential equations capturing time dynamics, or a loosely equivalent simulation based on short (discrete) time period updates. This is the primary new supply-modeling concept that is introduced to post-earthquake traffic analysis in this paper.

As is well-known, traffic simulation can be macroscopic (purely based on fluid-like models), microscopic (based on individual vehicles' acceleration, deceleration, lane-changing, etc.) or mesoscopic, which has better driver-decision and path-dynamics capabilities than the fluid (macro) models, without the extreme computational requirements of a micro-model. Due to the need that path level traffic readjustment based on driver decisions on travel times is a necessity in earthquake research, this paper selects a mesoscopic model that is computationally efficient for large-enough network simulation.

2.2.2 Employing Disaggregation of Simulation Results in SRA

One of the benefits in employing simulation in SRA is the ability of simulations to yield much richer data at the disaggregate level, in terms of the systems costs for any origin-destination pair, for any class of vehicles, or any class of users of different behavioral

characteristics, such as regular commuters versus freight operators. The simulation also allows disaggregated results by time periods, either within day or day to day, if the analysis is done in a framework that allows day-to-day travel demand adjustments. Admittedly, the traditional planning programs based on network equilibrium also can yield some of the disaggregate results, though only at the equilibrium state.

The simulation studies in this paper does not delve into all the possibilities and only focuses on comparing the results at the OD pair level to demonstrates the capability and emphasize the need to carry out SRA at the disaggregate level.

2.3 Methodology

The goal of the present study is to assess seismic risk in a traffic network using a mesoscopic traffic simulation model in place of a static traffic assignment model. The risk is measured in terms of potential increases in travel time for an earthquake scenario with respect to a base case (i.e. an undamaged network). The research goals of Shinozuka et al (2005) required the conversion of these travel delays into monetary equivalents in order to compare the cost of travel delay against the costs of restoration and repair. The present study is less ambitious and seeks merely to demonstrate that mesoscopic models can be used effectively in SRA, thus obviating the need to convert potential travel delays into monetary risk.

2.3.1 Overview of Framework (Two Major Phases)

Figure 1 shows the framework of the current study. Input and output are represented by parallelograms. Rectangles indicate individual steps in the framework.

The steps are organized into the two phases required to implement the study framework. The objective of the first phase is to establish the base case model. The steps for the first phase are indicated by rectangles with italicized text in Figure 1.

The assessment of seismic risk occurs in the second, main phase. The steps for this phase are indicated by rectangles with non-italicized text. The results of the main phase are system risk curves.

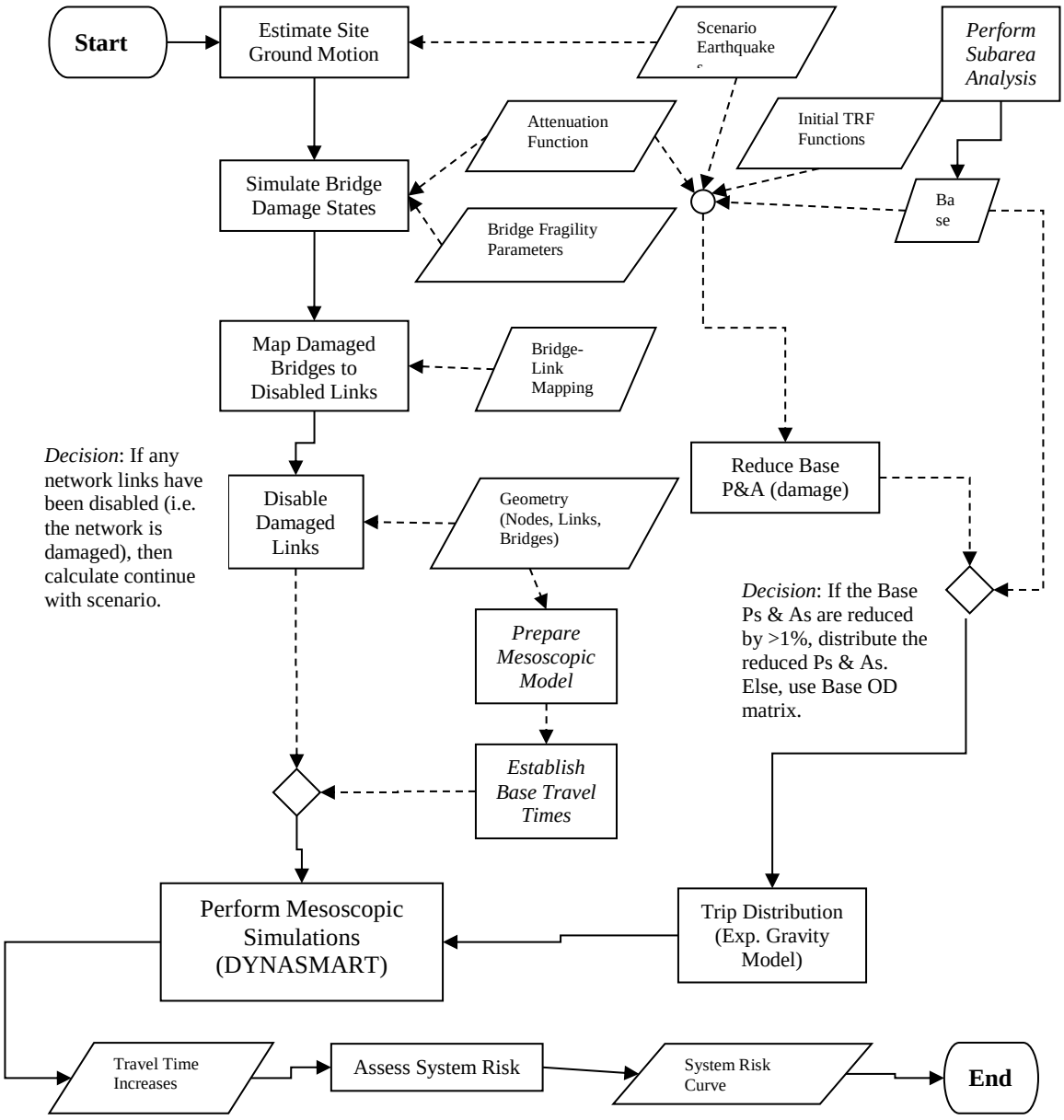

Figure 1: Framework of Study

2.3.2 Input Data

2.3.2.1 Geometry of Study Area

Figure 2 shows the extent of the West LA study area for the present analysis. It includes the site of the bridge collapse that occurred in the 1994 Northridge event, as well as the I10-I405 and I405-SR90 interchanges. To simplify the analysis, the University of California at Los Angeles centroids are not included in the network, and the I405 only extends as far south as La Tijera Boulevard and Howard Hughes Parkway.

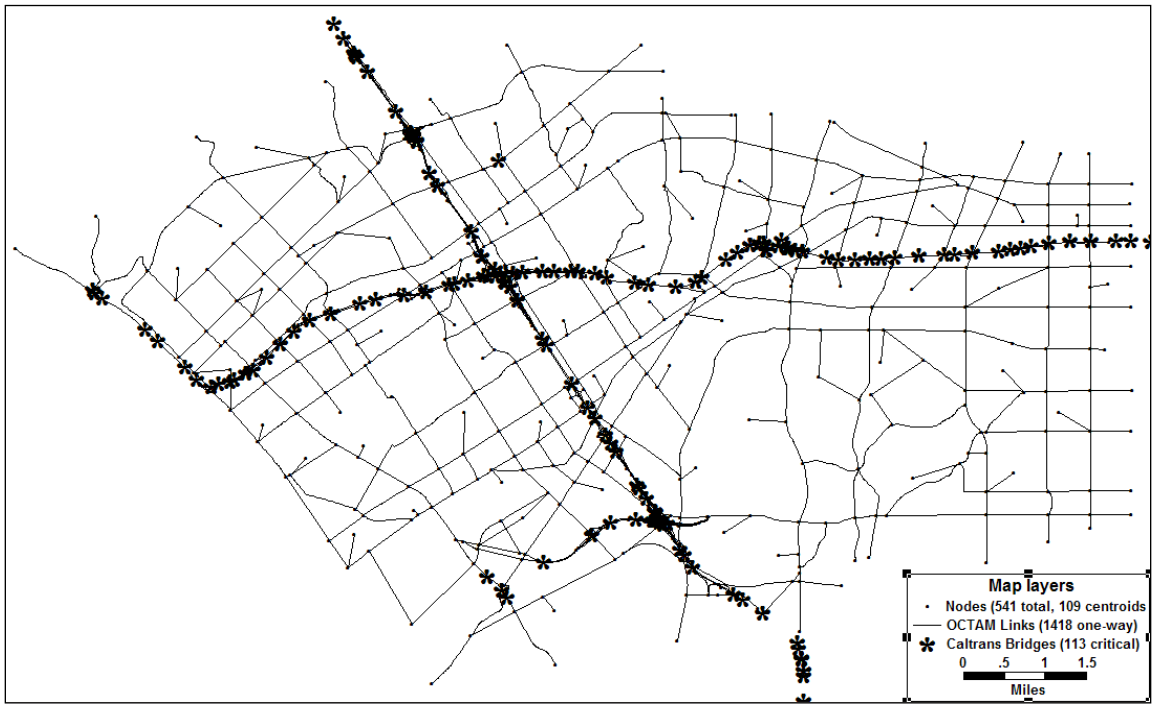

Figure 2: Study Area Near West Los Angeles

The geometry is taken from the Orange County Transportation Authority Model (OCTAM), version 3.0. The network includes the freeways and most arterial streets, but no residential streets. Originally configured for TransCAD, the DynaBuilder tool has been used to convert the TransCAD dataset into a DYNASMART-P network. However, to complete the base model, signalization has been added to the arterial intersections. Ultimately, the base

DYNASMART-P network consists of 1418 one-way links and 541 nodes (of which 109 are centroids).

This study has access only to the dataset of 3133 Caltrans bridges that comprised the LA Basin transportation network at the time of the study in Shinozuka et al (2005). Of these 3133 bridges, 170 are located in the study area in Figure 2. Of these 170, 113 carry flow on links in the network model; the majority of the remaining 57 bridges are on secondary arterials or collectors not found in the model. The Caltrans District 7 Bridge Log has been indispensable to distinguishing bridges in close proximity to each other (e.g. at interchanges) (Caltrans, 2009).

2.3.2.2 Scenario Earthquakes

Forty-seven (47) earthquake scenarios are taken from Shinozuka et al (2005), which approximate the seismicity of the LA basin.

2.3.2.3 Attenuation Function

This study assumes the following ground motion attenuation function (Campbell, 2007) –

$$\begin{aligned}\ln(a_H) = {} & -3.512 + 0.904 \cdot M - \\ & -1.328 \cdot \ln\left(\sqrt{D^2 + \left(0.149 \cdot e^{0.647M}\right)^2}\right) \\ & + \left[0.405 - 0.222 \cdot \ln(D)\right] S_{HR} + \left[0.440 - 0.171 \cdot \ln(D)\right] S_{SR} + \\ & + \left[1.125 - 0.112 \cdot \ln(D) - 0.0957M\right] F\end{aligned} \tag{2-1}$$

Where: a_H PGA

M Earthquake Magnitude

D Distance between epicenter and bridge site

F Fault Type: 1 for reverse thrust, 0 for strike slip

S_{hr} 1 for hard rock, 0 otherwise

S_{sr} 1 for soft rock, 0 otherwise

This attenuation function has been superseded by the function in Campbell and Bozorgnia (2006), but is nonetheless suitable for the present study. Other attenuation functions would also have been appropriate. For example, HAZUS-MH currently employs 34 attenuation functions, demonstrating the variety that exists. The *HAZUS-MH Technical Manual* (2003) enjoins users to consult ground motion estimation experts, keeping in mind that the choice of attenuation function must be in accordance with the conditions under which it was developed (e.g. fault mechanism, location in USA).

However, the variability that would be introduced by comparing multiple attenuation functions is beyond the scope of the present study. The 1997 Campbell attenuation function is chosen simply for compatibility with software components that had been created for the study in Shinozuka et al (2005).

2.3.2.4 Initial Trip Reduction Factor (TRF) Functions

In Shinozuka et al (2005), the productions and attractions in the model are reduced according to the average ground motion at a particular centroid. The primary assumption in applying initial TRFs is that reductions of travel demand at a centroid (in terms of productions and attractions from the trip generation step) are proportional to the square footage loss of different land uses in the zone.

To obtain this relationship, Shinozuka et al (2005) assumed that reductions of travel demand at a centroid are proportional to the square footage loss of different land uses in Southern California. For each land use type, HAZUS-MH had an estimated mapping to building stock types (*HAZUS-MH Technical Manual,* 2003). For example, according to the

default HAZUS-MH data, roughly 99% of single-family dwellings (RES1) in Southern California are light frame wood construction (W1), and the remaining 1% is reinforced masonry bearing wall construction (RM1). Since each building stock type has its own fragility characteristics, the HAZUS-MH land-use-to-building-type mapping can convert functions that relate ground motion and building stock loss into functions that relate ground motion and land use square footage loss. These losses of land use square footage are then linearly related to reductions in productions and attractions.

Figure 3 visually depicts the relationship between trip reductions for Home-Work trips and ground motion at a centroid. The TRFs themselves are obtained by linear interpolation (Table 1). Shinozuka et al (2005) had modeled the recovery of productions and attractions to base case levels; this analysis is beyond the scope of this paper.

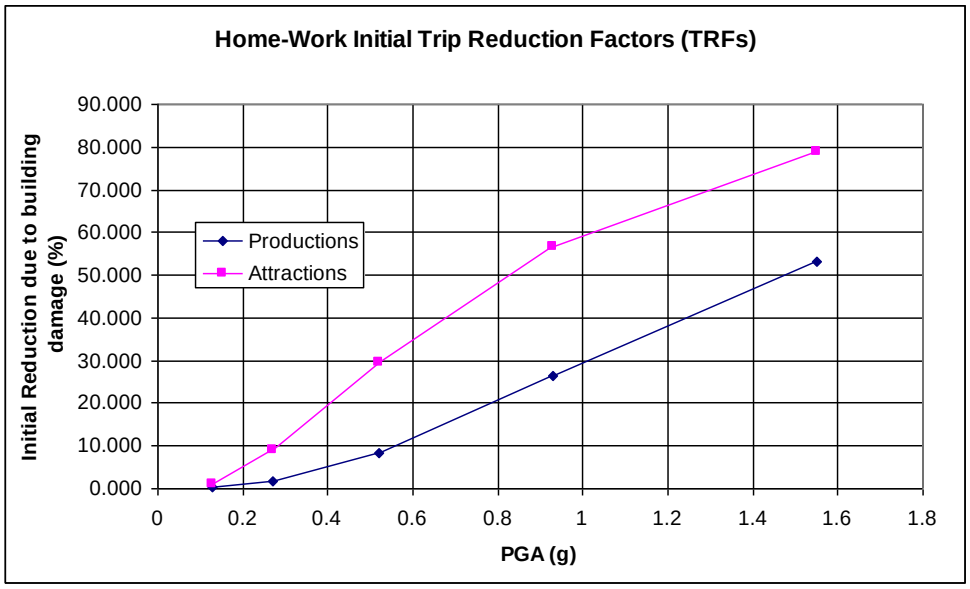

Figure 3: Example Initial Trip Reduction Factor function

Table 1: Initial TRF interpolation table

MMI	MMI6	MMI7	MMI8	MMI9	MMI10
PGA (g)	0.13g	0.27g	0.52g	0.93g	1.55g
Productions	0.24	1.83	8.35	26.26	53.07
Attractions	1.15	8.91	29.39	56.75	78.78

2.3.2.5 Bridge Fragility Parameters

When subjected to seismic ground motion, bridges in the study area are assumed to enter one of five damage states: (0) No Damage, (1) Minor Damage, (2) Moderate Damage, (3) Major Damage, and (4) Collapse (Shinozuka et al, 2005). These damage states are roughly equivalent to the damage states used by HAZUS-MH (*HAZUS-MH Technical Manual,* 2003). For the present study, a bridge is considered incapable of carrying flow when it suffers at least Major Damage; at this point, HAZUS no longer considers the bridge "structurally sound" (*HAZUS-MH Technical Manual,* 2003).

The cumulative probability of entering a specific damage state *j* is lognormally distributed and given by the following equation (Shinozuka et al, 2005) –

$$F_j(a_i; c_j, \zeta_j) = \Phi\left(\frac{\ln(a_i / c_j)}{\zeta_j}\right) \tag{2-2}$$

Where a_i Peak Ground Acceleration (g) at bridge site *i*

c_j Fragility curve median (g)

ζ_j Fragility curve log-standard deviation

$\Phi(\cdot)$ Standard normal distribution

Figure 4 shows each damage state's respective cumulative probability distribution, also known as a fragility curve –

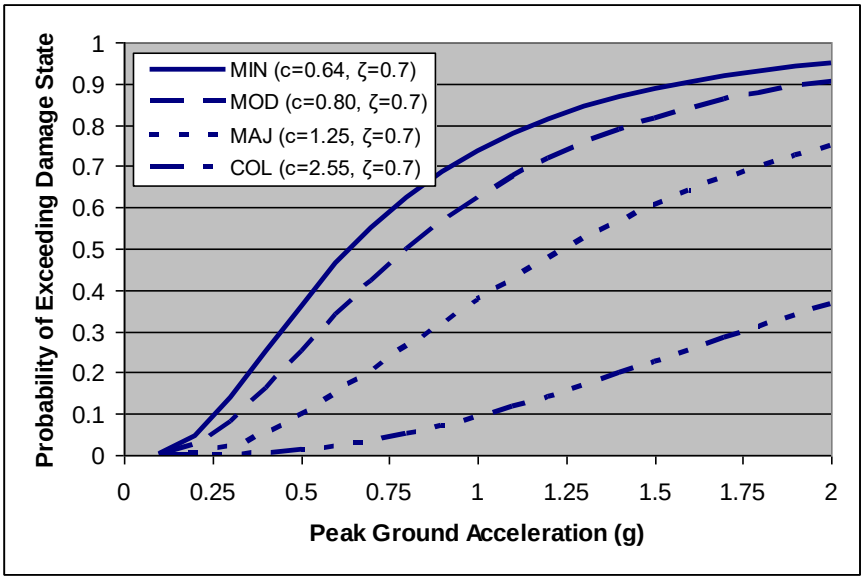

Figure 4: Bridge fragilities assumed for all West LA study area bridges

These parameters were estimated from the entire dataset of 1998 Caltrans bridges which were inspected following the 1994 Northridge earthquake. For the present study, it will be sufficient to assume that all bridges share the same fragility characteristics regardless of span, skew, or soil type. In addition, although the Caltrans bridge retrofit program has enhanced the fragility characteristics of links in the study area, the current study does not incorporate the improvements found in Shinozuka et al (2005), since the focus of this study is the mesoscopic model.

2.3.2.6 Bridge-Link Mapping

The bridge-link mapping is a matrix of n bridges x m links which indicates if a specific bridge i is located on a specific link j. This mapping is required to determine which links become disabled in each scenario.

2.3.3 First Phase: Establish Base Case Model

2.3.3.1 Perform Subarea Analysis

A Subarea Analysis is performed on the West LA subarea network of the OCTAM in order to obtain base case productions and attractions from the subarea OD matrix marginals. The subarea OD matrix output cannot itself be used because the seismic risk analysis must ensure that trip distribution is performed identically for the base case network as well as the damaged networks.

The simplest doubly-constrained trip distribution gravity model (i.e. one with an exponential impedance function) is employed. A parameter of c=0.2 in the function $f(d_{ij}) = \exp(-c \cdot d_{ij})$ is found to minimize the error with respect to the OD matrix output from the subarea analysis. The free-flow interzonal travel times are used as the distance parameter d_{ij}; no feedback has been performed.

2.3.3.2 Prepare Mesoscopic Model

The subarea network must be exported into a format compatible with the DynaBuilder conversion tool (version 0.91). The OD matrix must be given in 5-min increments; the matrix loading pattern is assumed to be uniform throughout the 120-min simulation period. Statistics are collected between 30 to 90 minutes into the simulation. For proper simulation, it is imperative to ensure sufficient capacity on the centroid connectors in terms of link length and number of lanes.

2.3.3.3 Establish Base Case Performance Measures (Average Travel Time)

After running 10 DYNASMART-P simulations with 10 different random seeds, the average travel time for vehicles in the base case model is found to be 46.7 min. Any increases in travel time percentage are calculated from this base case average travel time. Roughly assuming that the 0.68-min standard distribution of these 10 base case simulations would

hold for the damaged networks, three (3) simulations are deemed sufficient (to 90% confidence) to obtain sample average travel times for each damaged case.

2.3.4 Main Phase: Assess Seismic Risk

2.3.4.1 Estimate Site Ground Motion

The attenuation function in Equation (2-1) is employed to estimate the peak ground acceleration at all bridges and centroids.

2.3.4.2 Simulate Bridge Damage States

The fragility curves in Figure 4 serve as input to a Monte Carlo simulation program. This program outputs 50 vectors indicating the damage state for each bridge (0=No Damage, 1=MIN, 2=MOD, 3=MAJ, 4=COL). Each vector has dimensions 113x1, since there are 113 bridges in the study network.

2.3.4.3 Map Severely Damaged Bridges to Disabled Links

The bridges with the MIN and MOD damage states are filtered out (i.e. set to ZERO). The bridges with the MAJ and COL damage states are set to ONE, resulting in a set of 50 vectors which indicate the bridges that cannot be traversed. Then, via the bridge-link mapping, these 50 vectors are mapped to a set of 50 vectors that indicate whether a specific network link is disabled. The bridge damage simulation resulting in the greatest number of disabled links is chosen for simulation.

2.3.4.4 Disable Damaged Links

If any network links are disabled, an "infinite" length (999999 ft, approx. 189 miles) is applied to the corresponding link in the base-case model. Even when applied to freeway links (70 mph), the travel time over one of these links exceeds the 120-min simulation period. These infinite link costs increase the time required to perform a simulation, but they facilitate the coordination of multiple scenarios.

2.3.4.5 Trip Distribution

The next step is to apply the Trip Reduction Factors to productions and attractions. To save time in simulation, the factors were only applied for those scenario earthquakes where the PGAs at the centroids resulted in a reduction of productions or attractions larger than 1%. This was the case in three of the 47 scenario earthquakes. Reduced attractions are balanced against the reduced productions. This time-saving measure was the result of observing that decreasing the loading proportion of the base OD matrix by 1% was found to have a statistically insignificant effect on the simulation results.

2.3.4.6 Perform Traffic Simulations

For each scenario earthquake that results in network damage and/or the distribution of reduced production and attraction vectors, three DYNASMART simulations are performed using three different random seeds. The summary statistics and the vehicle trajectories are retained after each simulation for post-processing.

2.4 Results

The results of a seismic risk analysis are generally summarized in a system risk curve. The system risk curve for network-wide travel time increases in the West LA study area is presented in Figure 5. Of the 47 scenario earthquakes, only 19 of them produced any network damage. That such a small fraction of the set results in network damage is not surprising because the West LA study area comprises only 8 of the 148 zones in Shinozuka et al (2005). Of these 19, only 17 resulted in any time travel increases when using base-level (i.e. not reduced) productions and attractions, and only 15 resulted in time travel increases when using reduced productions and attractions. Negative average travel delays cannot be incorporated into a risk curve and have been neglected.

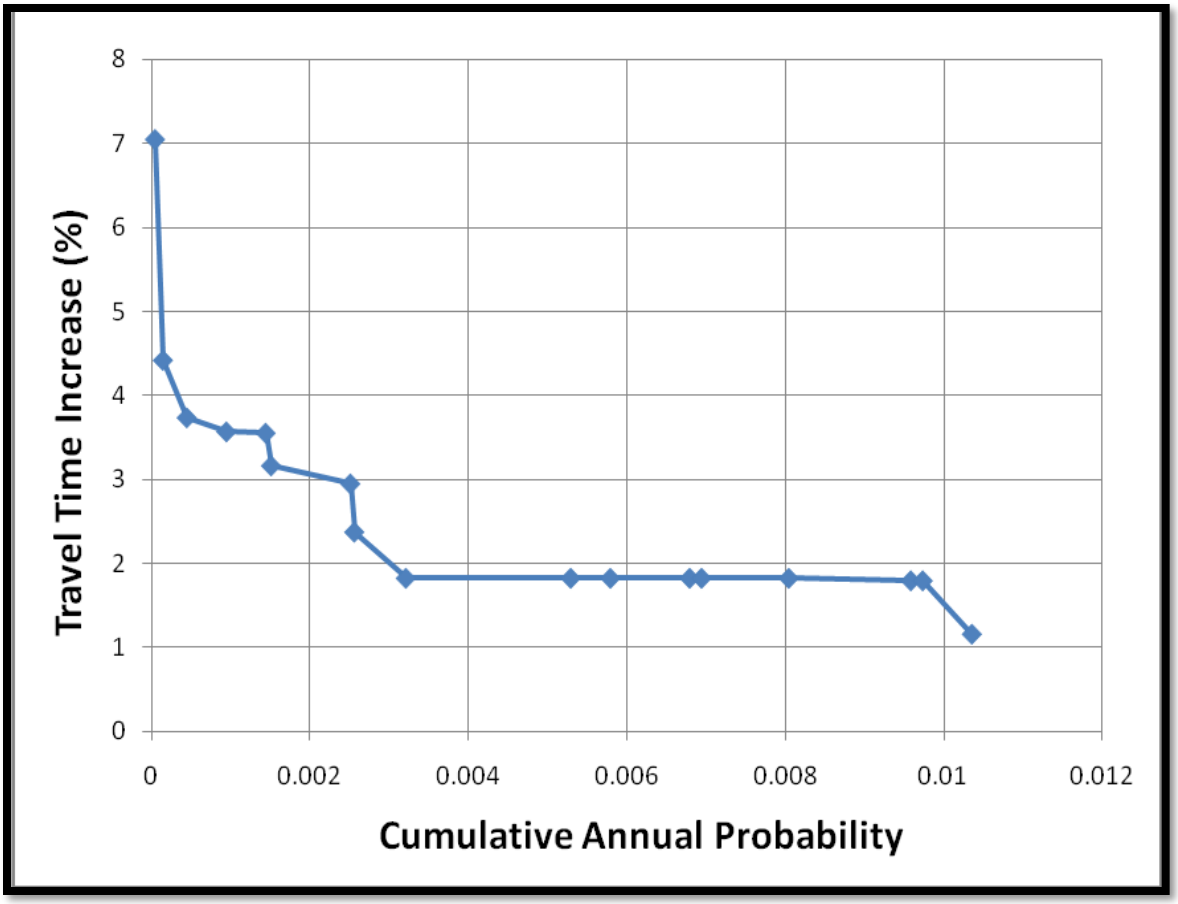

Figure 5: System risk curve for network-wide travel time increases

If one were to take the inverse of the risk curve, it would be nonetheless revealing. When considering travel time increases across all OD pairs, the average network travel time increases range between +1% to +4.5% over the base case. The trend is appropriate: the probability of an earthquake causing large network-wide travel time increases should be smaller than that of an earthquake causing smaller travel time increases.

These increases are less than the travel time increases noted in DeBlasio et al (2002), which noted that while motorists experienced individual delays of as much as one hour in January and February, by March the average travel delays were only 10-15 minutes during the morning commute, and 5-10 minutes in the afternoon commute. In this study,

travel time for vehicles in the base case model is found to be 46.7 min. A +1% to +4.5% increase corresponds to a half-minute to 2.1-minute increase.

2.4.1 Results Disaggregated by OD pair

Admittedly, the travel time increases in Figure 5 are not dramatic. However, some OD pairs have paths that (at least in the base case) travel through portions of the network which are either directly susceptible to travel time increases due to disruption of infrastructure, thus disabling links; or may be indirectly susceptible due to upstream shockwave propagation from nearby disabled links. For example, Figure 6 considers two OD pairs for which vehicles were observed to pass through the I10-I405 interchange in the base (undamaged) case. These OD pairs should expect travel time increases larger than the network-wide travel time increases in Figure 5 at each level of annual probability.

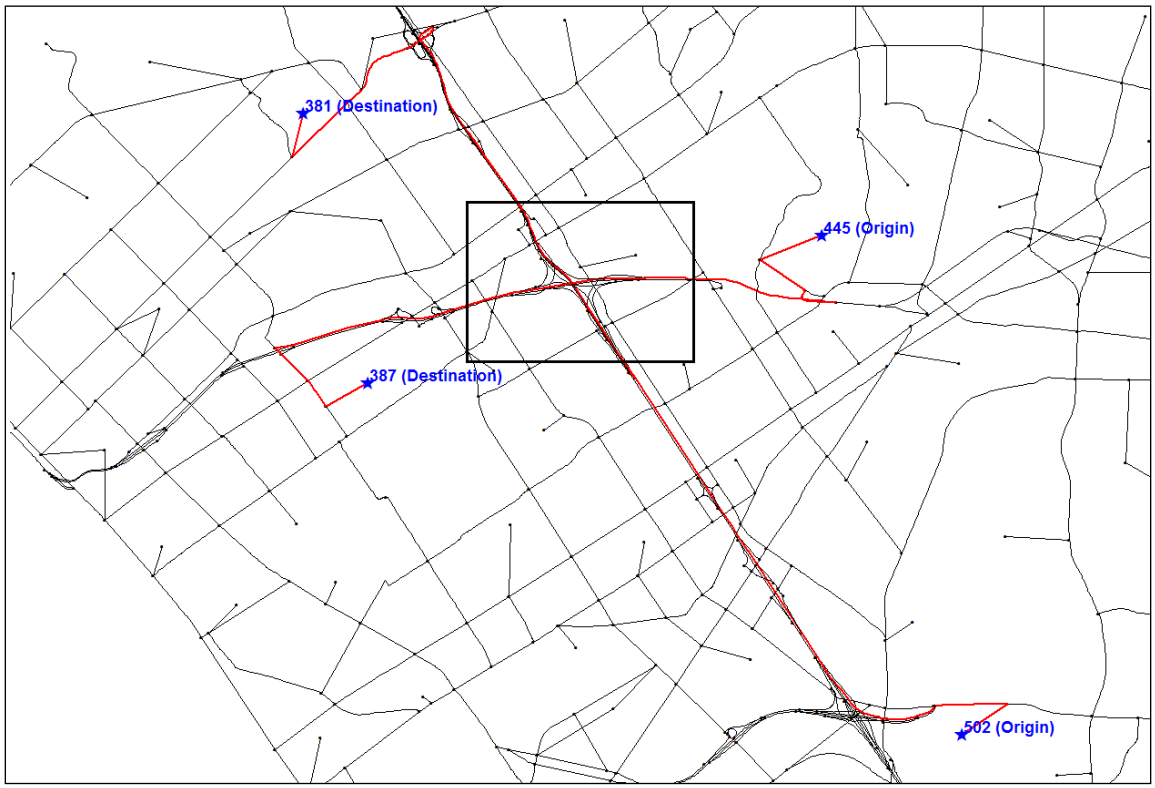

Figure 6: Two OD pairs (445→387 & 502→381) susceptible to delays

To generate risk curves for a specific OD pair, the travel times for that OD pair must be extracted from the vehicle trajectory files created by DYNASMART-P. The average travel time for the base case simulation is compared against the average travel times of the eight earthquakes that resulted in the greatest network-wide travel time increases in Figure 5.

The risk curves for these susceptible OD pairs are presented in Figure 7. Indeed, they exhibit travel time increases larger than the network-wide travel time increases at each level of probability. For example, Figure 5 shows that there is an annual probability of 0.0015 of experiencing an earthquake that results in a ~3.2% network-wide travel time increase, corresponding to an earthquake with a 667-year expected return period. For this level of annual probability, the OD pair traveling westbound through the I10-I405 interchange has a ~10% travel time increase (Figure 7(a)). The OD pair traveling northbound through the interchange exhibits an ~8.5% travel time increase (Figure 7(b)).

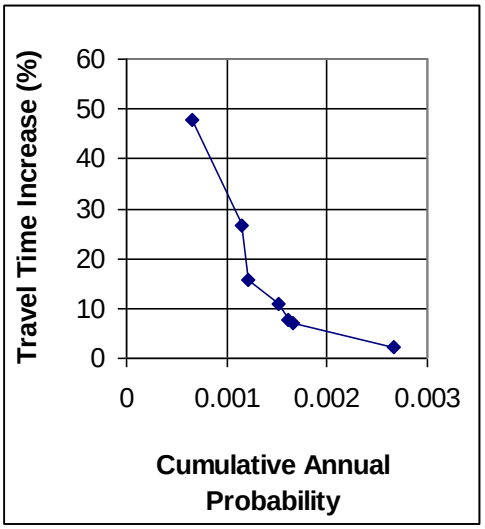

(a)

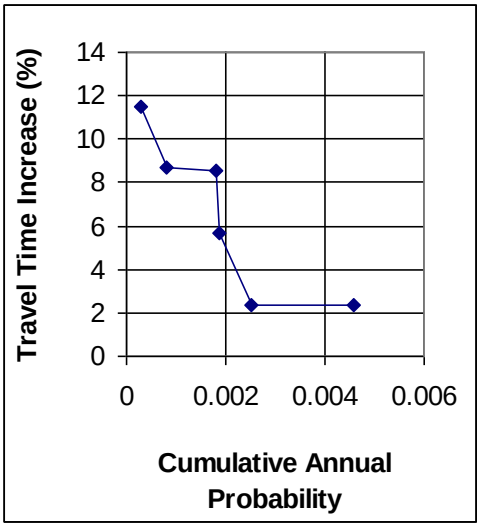

(b)

Figure 7: Risk curves for the susceptible OD pairs (a) 445→387 (b) 502→381

DeBlasio et al (2002) notes that in the aftermath of the 1994 Northridge earthquake, some motorists experienced travel time increases by as much as one hour in January and February. By comparison, the ~10% and ~8.5% travel time increases in Figure 7(a) and (b) would correspond to travel time increases of 4.7 min and 4.0 min (for a base case model travel time of 46.7 min). However, it is important to note that the West LA study area has many potential detours. DeBlasio et al (2002) notes that the most drastic increases corresponded with areas of the network for which there were fewer detours, such as the network close to the SR-14 bridge collapse.

2.4.2 Effect of Initial Trip Reduction Factors

Initial trip reduction factors were applied to only 8 of the 17 scenario earthquakes that comprise the system risk curve. For the remaining 9 earthquakes, the overall productions and attractions were decreased by less than 1%, and no trip distribution of the reduced productions and attractions was performed. However, the former 8 cases resulted in travel time increases smaller than those of the latter 9. This is most clear when the system risk curve is shown with the travel time increases for the cases in which the initial TRFs were applied Figure 8.

There was one scenario which resulted in a negative travel time increase (i.e. a travel time decrease). In this scenario, one of the disabled links had been connected to a centroid connector. This prevented that centroid from being able to clear its outflow, which then caused the simulation to fail. In order to allow the simulation to run successfully, the origin flows for this centroid were redistributed equally to nearby OD pairs on arterials that could plausibly be used for detours during reconstruction. This crude fix unfortunately resulted in an inexplicable decrease.

When base-level productions and attractions are not reduced, the intuitive result is that network-wide travel times will increase as the quantity of network lane-miles disabled by the earthquake increases. The present analysis is consistent with this suspicion Figure 9. However, the trend in Figure 8 suggests that decreasingly smaller travel delays are related to increasing levels of damage. These decreasingly smaller travel delays could be attributed to increasingly larger reductions of overall travel demand (in productions/attractions). Since the initial TRF methodology posits that travel demand will decrease as building stock damage increases, the implication is that decreasing travel delays and increasing building stock damage are related. This in turn implies that network damage and building stock damage may not be independent of each other; indeed, Figure 10 would support such an implication.

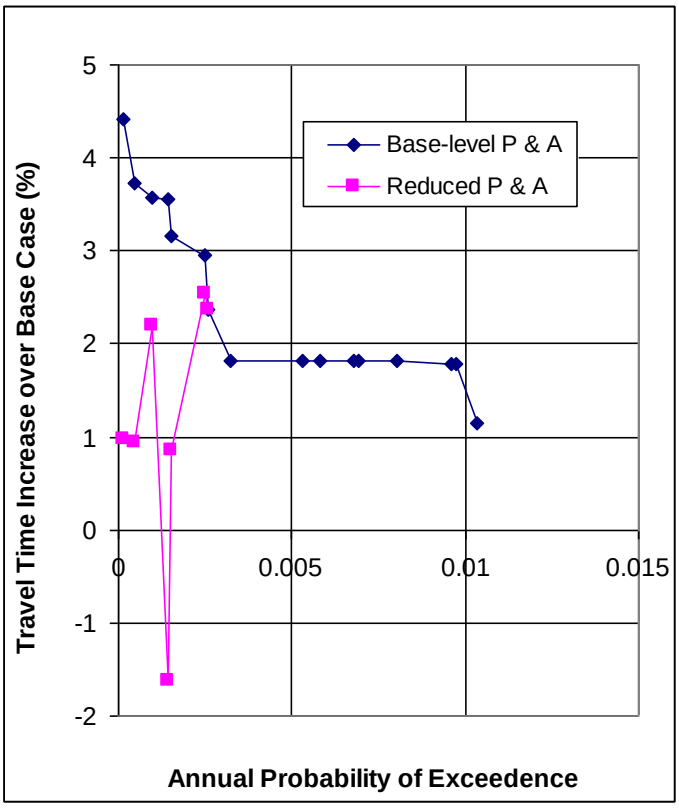

Figure 8: The effect of initial TRFs

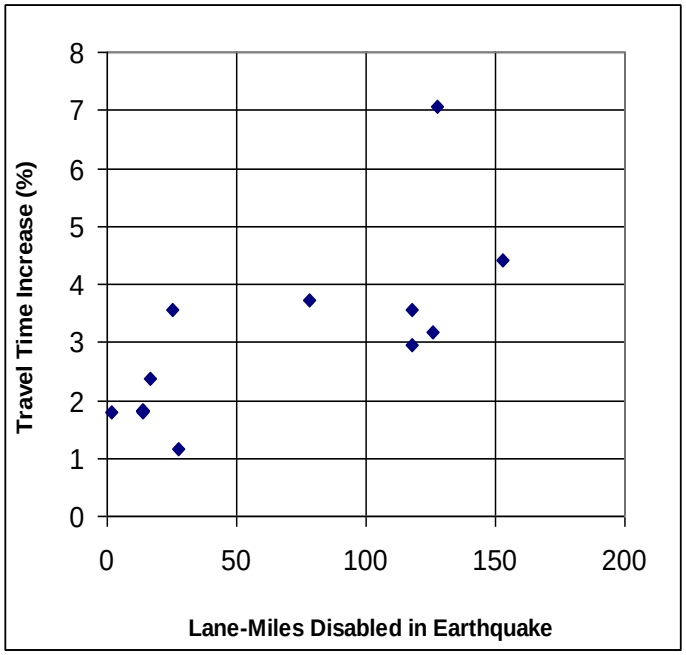

Figure 9: Lane-miles disabled v. network-wide travel time

In hindsight, the positive relationship between network damage and overall travel demand decreases (due to building stock damage) could be attributed to geographic proximity of the study area to a scenario earthquake. At the very least, ground motion attenuation conditions in the study area should affect both transportation infrastructure and building stock similarly. This conjecture does not take into account local variations in building stock, which show differing levels of resilience at different levels of ground motion (e.g. unreinforced masonry v. steel moment frame structures). In addition, DeBlasio et al (2002) cites that following the 1994 Northridge earthquake, media dissemination had played a key role in advising motorists to avoid the most damaged portions of the network. Ultimately, the evaluation of this conjecture is beyond the scope of the present study.

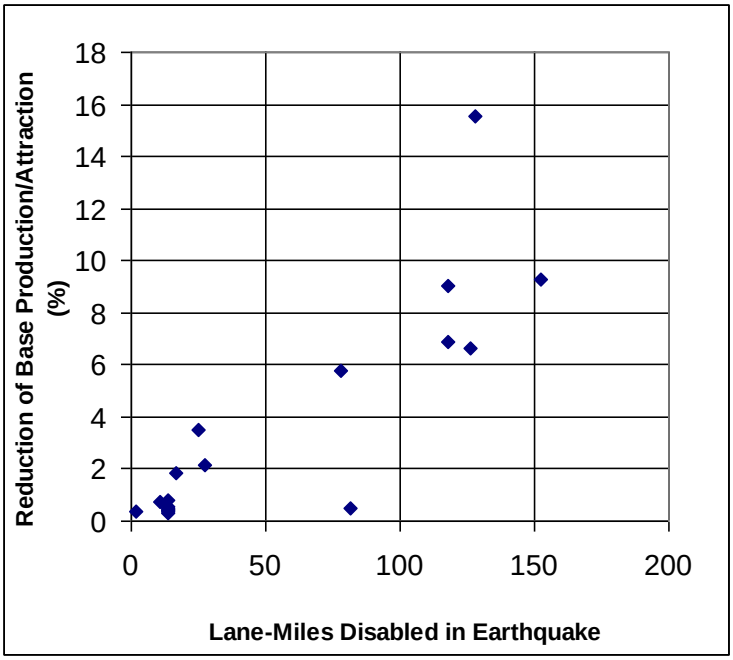

Figure 10: Lane-miles disabled v. percent reduction in productions and attractions

2.5 Conclusions

The goal of the present study has been to demonstrate that a mesoscopic traffic simulation model can be feasibly incorporated into a seismic risk analysis framework. The modified SRA framework has successfully yielded a system risk curve for the network-wide travel time increases. In addition, by using vehicle trajectories to generate risk curves for specific OD pairs, this study has extended the methodology of Shinozuka et al (2005), achieving an unprecedented level of disaggregation in the seismic risk analysis of transportation lifelines.

Nevertheless, this dissertation recommends restraint in applying the findings. The risk curves in this study are predicated on the following assumptions. First of all, travel demand is assumed to have returned to pre-quake levels, which may not be the case if the event is exceedingly destructive. Secondly, none of the disabled links are assumed to have

been repaired; this assumption could still hold a month into the recovery period, but perhaps not much longer if authorities implement an accelerated bidding process. Thirdly, the ground motion attenuation function in this study is quite outdated. Lastly, and perhaps most importantly, the study uses the empirical fragility curves from the 1994 Northridge event, and have not been enhanced to account for the continuing bridge retrofit program.

This dissertation also regards the lack of a convincing travel demand model as being particularly problematic. The traditional doubly-constrained gravity model technique applied in this study is not particularly appropriate for mesoscopic models like DYNASMART, and more advanced OD estimation methods exist that account for time-dependent changes in travel demand. In addition, while initial trip reduction factors have been successfully applied to more traditional trip-based static traffic assignment models, a seismic risk analysis framework that uses a mesoscopic traffic simulation model should strive to modify for earthquake events the OD estimation methods intended for use with mesoscopic models.

3 STUDY 2: IDENTIFYING TRANSPORTATION AND COMMUNICATIONS EMERGENCY SUPPORT WORKFORCES, AND CALCULATING THEIR EXPOSURE TO SEISMIC PEAK GROUND ACCELERATIONS

After a disaster, successful response and recovery depends on prompt restoration of infrastructure, including transportation or communications. However, the disaster can impact the workforce responsible for restoring infrastructure, e.g. by damaging their homes. This study has two goals: 1. Identify workers likely to participate in restoring transportation and communications infrastructure. 2. Calculate these workers' exposure to the Peak Ground Accelerations (PGAs) of a 7.8 magnitude Southern California scenario earthquake, and compare it to that of the rest of the working population.

Four steps are required. First, calculate the mean PGA for each affected Public Use Microdata Area (PUMA). Second, identify the transportation and communications infrastructure restoration workforce by specifying appropriate Standard Occupational Classification (SOC) and North American Industry Classification System (NAICS) codes. To specify these codes, use the Emergency Support Function (ESF) Annexes for Transportation (ESF#1) and Communications (ESF#2) to clarify workers' roles and responsibilities. This listing of codes for specific ESFs is a novel contribution.

Third, via frequency table, calculate the mean and standard deviation of transportation and communications workers' exposure to PGAs in their PUMAs of residence. Finally, test the difference in mean PGA exposures between two populations: 1. transportation or communications workers and 2. the rest of the working population.

This study finds that for this scenario, transportation workers are exposed to statistically significant higher PGAs than non-transportation workers, and communication

workers to significantly lower PGAs. For practioners, knowing which worker categories a disaster disproportionately affects could justify pre-event investments in workforce preparedness and recovery planning efforts.

3.1 Introduction

After a significant adverse event such as an earthquake or a wildfire, prompt restoration of infrastructure – including transportation or communications – is critical to successful response and recovery. Restoration requires the public or private entities that own or operate infrastructure to mobilize their workforce. However, the event can impact this workforce, for example, by damaging their homes. The workers' ability to contribute to the restoration effort would thus be impeded.

For transportation agencies, physical infrastructure includes roadways, bridges, and critical facilities such as regional offices, maintenance yards, and Transportation Management Centers (TMCs). Worker categories such as highway maintenance workers and bridge inspectors become critical to restoring functionality. Any methodology that can determine the worker categories which a disaster event disproportionately affects could thus aid practitioners in planning for workforce preparedness, or for response and recovery operations.

Transportation infrastructure extends beyond the surface transportation infrastructure of public agencies and jurisdictions. For several transportation modes, private entities own and operate the infrastructure. For example, the Transportation Research Board maintains standing committees for eight modes ("Standing Committees by Mode and Topic", 2017) private ownership is standard for Aviation and Motor Carriers. In the *Transportation Systems Sector-Specific Plan* (2015), the Department of Homeland

Security recognizes seven modes as subsectors of the Transportation Critical Infrastructure Sector (CIS), including Maritime Transportation System, Mass Transit & Passenger Rail, Pipeline Systems, Freight Rail, and Postal & Shipping.

The Department of Homeland Security also recognizes Transportation as Emergency Support Function (ESF) #1. The scope of ESF#1 responsibilities is defined in the *National Response Framework* (2016) and its associated ESF Annex (*Emergency Support Function #1 – Transportation*, 2016). This study will employ the text of the ESF#1 Annex to assist in identifying the worker and industry categories responsible for implementing ESF#1 across both the public and private sectors. For worker and industry categories, this study will use the Bureau of Labor Statistics' Standard Occupational Classification (SOC) system and the North American Industry Classification System (NAICS), respectively.

However, resilient transportation operations increasingly rely upon communications infrastructure. For example, the Volpe Center found over 50 different systems and applications that depend upon GPS positioning, navigation, and timing services (Wallischeck, 2016). Another sign of interdependence is transportation infrastructure's vulnerability to cyber attacks. For example, the American Public Transportation Association publishes recommended practices on securing the control and communications systems of transit systems (APTA, 2010).

The rise of cloud or network computing in recent years means that increasingly, "control system components and networks are now accessible from anywhere and are increasingly connected to enterprise data" and thereby to human safety (CASE LLC and WMC LLC, 2015). First-generation Intelligent Transportation Systems (ITS) devices had fewer human safety ramifications (CASE LLC and WMC LLC, 2015). However, the near

future will see increases in both connected vehicles and connected vehicle infrastructure. In 2016, the National Highway Traffic Safety Administration (NHTSA) published its *Federal Automated Vehicles Policy* (2016). In December 2013, the Intelligent Transportation Society of America published a Market Report which found that 54% of survey respondents belonged to departments who have developed a regional or agency-specific Intelligent Transportation Systems (ITS) architecture; 63% of state governments had an ITS strategy in place, and 71% of survey respondents that have a state ITS plan said their agency implemented ITS to reduce congestion and traffic delays (ITS America, 2013b). Meanwhile, the 2013 National ITS Deployment Tracking survey suggests that one-half to three-fourths of the surveyed agencies planned to expand current deployments or deploy new technologies (ITS America, 2013a).

Consequently, restoring transportation infrastructure could depend upon restoring communications infrastructure. The Department of Homeland Security also recognizes Communications as ESF #2. The present study also employs the text of the ESF#2 Annex (*Emergency Support Function #2 – Communications*, 2016) to help identify the relevant worker and industry categories.

While Southern California is susceptible to other (and more frequent) natural hazards such as fire, the region is due for a major San Andreas earthquake (Corelogic, 2016). The present study uses this region as its study area. An 8.3 magnitude San Andreas earthquake could result in 1.6 to 3.5 million damaged homes (potentially costing $289 billion) (Corelogic, 2016). The United States Geological Survey's (USGS's) landmark 2008 ShakeOut Scenario report simulated a 7.8 magnitude San Andreas earthquake and found $213 billion

in economic losses; one simulation of that study demonstrated that this scenario could disrupt several Southern California highways (e.g. I-10, I-15, SR-14) (Jones et al, 2008).

3.2 Research Goals

This study seeks to achieve the following goals:

1. **Identify the workers likely to participate in restoring transportation and communications infrastructure after a Southern California earthquake.** That is, identify those workers whose occupational and industry categories correspond with the scopes and responsibilities described in the Transportation (ESF#1) and Communications (ESF#2) Emergency Support Function annexes. A literature search suggests that no such listing of worker and industry codes exists.
2. **Calculate the exposure of these workers to the Peak Ground Accelerations (PGAs) of the scenario earthquake, and compare these values to the exposure of the rest of the working population.** Are these workers exposed to statistically significant higher or lower levels of PGAs compared to their counterparts in other occupations and industries?

This study designates PGA exposure as the proxy for a worker's vulnerability to earthquake hazards. It assumes that exposure to PGAs at workers' areas of residence is positively correlated to damage to their homes, in turn affecting their ability to return to work restoring infrastructure. For example, in the Port of New York and New Jersey after Hurricane Sandy, Southworth et al (2014) highlighted one example action that would assist in recovery: arrange on-site housing for critical staff, emergency responders, and relief workers.

This study employs the Census Bureau's American Community Survey Public Use Microdata Sample (ACS PUMS), which uses Public Use Microdata Areas (PUMAs) as its geography level. PUMAs are statistical geographic areas that aggregate census tracts that contain a minimum of 100,000 people. Counts of ESF#1 and ESF#2 workers are estimated by their PUMA of residence.

3.3 Literature Review

This paper attempts to match SOC and NAICS codes to ESF roles and responsibilities. Thus, the keywords "Standard Occupational Classification" and "North American Industry Classification System" must accompany keywords relating to "emergency" and "disaster". Conversely, the keywords "Emergency Support Function" and "Peak Ground Acceleration" cannot be separated from keywords relating to "workers", "workforce", or "labor force". However, a search on the TRID database and the Annual Meeting Online compendium of papers suggests that such searches currently return few studies and publications.

Among studies mentioning both disasters and the NAICS, freight modeling studies are most common, such as freight commodity modeling (Lupa et al, 2015), goods movements estimation (Oliveira-Neto et al, 2013), aggregate freight generation modeling (Oliveira-Neto et al, 2012). These studies use NAICS as a means of identifying industry sectors. For example, one study needs NAICS codes to interpret the US Census Bureau's County Business Patterns date, where employment is categorized by industry (Lupa et al, 2015). In contrast, another study uses the Commodity Flow Survey (CFS), wherein freight activities by business establishments are classified by NAICS code (Oliveira-Neto et al, 2013). Two studies – Oliveira-Neto et al (2013) and Oliveira-Neto et al (2012) – mention the hazard that disasters pose in disrupting these modeled freight flows. However, only

Lupa et al (2015) raises the possibility of modeling disaster scenarios in the national freight model.

Neither TRID nor the Annual Meeting Online compendium returned any studies which employed the SOC system in an emergency or disaster environment.

No paper returned by TRID or the Annual Meeting Online compendium analyzes ESFs in terms of workforce or labor force planning. Whenever papers or presentations that mention ESFs also mention the keyword "worker", it is in the context of providing critical workers with waivers (Cook, 2017) or ensuring that they have proper credentialing (Sheehan, 2015).

When used alone, the phrase "peak ground acceleration" returns engineering papers in TRID or the Annual Meeting Online compendium. However, narrowing the search to include the keywords "workforce", "worker", or "labor force" returns no papers – thus demonstrating a gap of papers which employ PGAs to estimate effects to the workforce.

3.4 Data

The PGA data in this paper are taken from the USGS Southern California earthquake scenario catalog (*SCLEGACY Scenario Catalog*, 2017). To estimate the counts of the workers in ESFs #1 and #2, this analysis uses the Public Use Microdata Sample (PUMS) of the 2011-2015 American Community Survey from the U.S. Census Bureau.

3.4.1 Peak Ground Acceleration (PGA) Data: Ardent Sentry 2015

This paper uses PGAs that were simulated for the 2015 Ardent Sentry exercise. Ardent Sentry is an exercise program conducted jointly by North American Aerospace Defense (NORAD) and the U.S. Northern Command (USNORTHCOM) (Hagihara, 2015). In 2015, the Ardent Sentry scenario involved a magnitude 7.8 earthquake originating on the San

Andreas fault near the Salton Sea (*M 7.8 Scenario Earthquake - Ardent Sentry 2015 Scenario,* n.d.).

The Ardent Sentry scenario has the same magnitude and epicenter as the 2008 ShakeOut scenario (*M 7.8 Scenario Earthquake – Shakeout2 Full Scenario,* n.d.). However, the shaking intensity maps (Figure 11) differ slightly; for the ShakeOut scenario, the Violent and Extreme regions extend further away from the San Andreas fault.

2008

ShakeOut

2015

Ardent Sentry

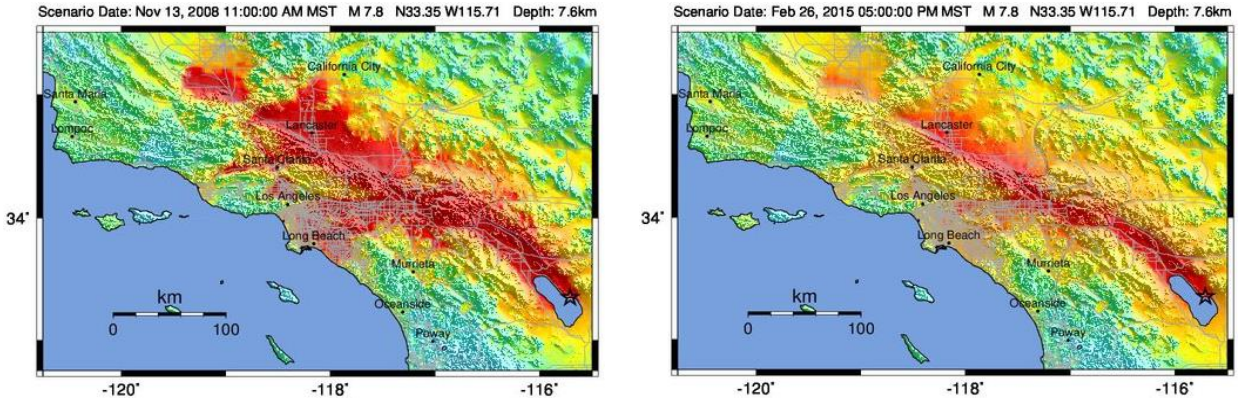

PERCEIVED SHAKING	Not felt	Weak	Light	Moderate	Strong	Very strong	Severe	Violent	Extreme
POTENTIAL DAMAGE	none	none	none	Very light	Light	Moderate	Mod./Heavy	Heavy	Very Heavy
PEAK ACC.(%g)	<0.05	0.3	2.8	6.2	12	22	40	75	>139
INSTRUMENTAL INTENSITY	I	II-III	IV	V	VI	VII	VIII	IX	X+

Scale based upon Worden et al. (2012)

Figure 11: Shaking intensity ShakeMaps for 2008 ShakeOut (R) and 2015 Ardent Sentry (L). Source: USGS.

3.4.2 Working Population Data

This study employs the five-year American Community Survey's Public Use Microdata Sample (ACS PUMS) from 2011 to 2015. Using the 5-year survey gives us smaller margins of error than using the 1-year survey, so we have the most accurate estimates available, even though not the most current (5-year averages from 2011-2015, as opposed to just the 2015 estimates).

In order to focus on the worker populations of interest in the study area, this study must first propose sets of SOC and NAICS codes which best correspond to ESF#1 (Transportation) and ESF#2 (Communications). Only after selecting these codes can one obtain counts and descriptive statistics at the PUMA level. This study uses the workers' PUMAs of residence. (These proposed SOC and NAICS codes are found in Table 3.)

For SOC and NAICS codes, this study uses the appropriate 2010 SOC or 2012 NAICS codes found within the *2011-2015 ACS PUMS Data Dictionary* (2017). While the NAICSP variable within the 2011-2015 ACS PUMS is based upon the 2012 NAICS codes, the NAICSP variable is subject to being abridged and thus losing the ability to distinguish between specialized industries or even industry groups. For example, all construction workers in PUMS are labeled as being in the NAICS sector "Construction" (NAICS = 23). This two-digit sector code is applied to all construction workers – from Highway, Street, and Bridge Construction workers (NAICS = 237310) to Industrial Building Construction workers (236210). It is thus not possible to isolate Highway, Street, and Bridge construction workers. In contrast, the entire 2010 SOC structure is available within those PUMS variables relating to SOC codes (SOCP10 and SOCP12).

Using the Public Use Microdata Area (PUMA) yields the smallest geographical resolution available with large enough sample sizes for both ESF#1 and ESF#2 workers. For all workers, this study uses the PUMA of residence variables (PUMA00 and PUMA10), not the Place of Work PUMA (POWPUMA). Rather than PUMA of employment, PUMA of residence is most of interest, since what the analysis seeks to capture is damage to homes, personal assets, and family life that could prevent a worker from being able to report to work in the event of a disaster. It is possible that the PUMA of residence and PUMA of employment is the same, particularly for those living far away from urban centers, or for those with very short commutes.

3.5 Methodology

3.5.1 Step 1) Determine the extent of PUMAs affected by the Ardent Sentry scenario earthquake. Calculate mean PGA for each PUMA.

First add two layers in ArcGIS 10.3.1: 1) the California state PUMA boundaries from the 2011-2015 ACS PUMS, and 2) the polygon shapefiles for the Ardent Sentry scenario's PGAs. The Intersect geoprocessing tool isolates the PGA contours into discrete regions within each PUMA boundary. Each of these discrete regions corresponds to a PGA value. Thus, to estimate the whole PUMA's mean PGA, each region's PGA is weighted by its area.

Initially, this procedure yielded PGAs for 152 PUMAs. However, the procedure did not capture four PUMAs in San Diego County: 0607318 San Diego City, 0607320 Sweetwater/Chula Vista, 0607321 National City, and 0607322 San Diego City. These were added manually by taking the mean PGA of the adjacent PUMAs. Ultimately, 156 PUMAs were affected by the Ardent Sentry scenario earthquake (Figure 11).

3.5.2 Step 2) Identify ESF#1 and ESF#2 workers in the study area. Calculate descriptive statistics.

To identify ESF#1 and ESF#2 workers, first produce a crosswalk with SOC and NAICS codes on the rows and ESF#1 and ESF#2 on the columns. This crosswalk is converted into a list of proposed SOC and NAICS codes for these ESFs. (The proposed SOC and NAICS codes for these two ESFs are found in Table 3.)

ESF#1 and ESF#2 workers are those workers 1) whose SOC is one of the SOC codes proposed for that ESF, *and* 2) whose NAICS code is one of that ESF's proposed NAICS codes, *and*, for ESF #1 only, 3) specifically those working in the public sector for those in architecture and engineering occupations. Subsequently, using the proposed SOC and NAICS codes, one can flag ESF#1 and ESF#2 workers within the California PUMS data. For each PUMA, counts are obtained for ESF#1, ESF#2, non-ESF#1, and non-ESF#2 workers who reside within. One can then also estimate distributions for housing type and household income (Figure 14 and Table 4). Figure 13 depicts the geographical distribution of ESF#1 and ESF#2 workers within the study area.

Both SOC and NAICS codes are necessary to identify both ESF#1 and ESF#2 workers within PUMS. For example, while Civil Engineers (SOC = 17-2051) could be employed in many industry sectors both public and private, the ones most relevant to ESF#1 would be those in such industries as Highway, Street, and Bridge Construction (NAICS = 237310), the Regulation and Administration of Transportation Programs (NAICS = 926120), and others.

For most SOC and NAICS codes, the relationship with the corresponding ESF is self-evident. For example, this study proposes that Radio and Telecommunications Equipment Installers and Repairers (SOC = 49-2020) are workers who would be part of ESF#2.

For those SOC and NAICS codes where the relationship to an ESF was less clear, one would consult the ESF#1 and ESF#2 Annexes. For example, a reference to pipelines in the ESF#1 Annex led to the crosswalk's inclusion of the Pipeline Transportation subsector (NAICS = 486XXX) in ESF#1.

3.5.3 Step 3) Construct a frequency table to calculate mean & standard deviation of PGA exposure to the average ESF#1 and ESF#2 worker.

If a frequency table is initialized with a PUMA's worker counts and mean PGA (calculated in Step 1), one can calculate the mean and standard deviation of PGA exposure for ESF#1, ESF#2, non-ESF#1, and non-ESF#2 workers. All four sets of means and standard deviations are necessary to maintain statistical independence between workers in an ESF and workers not in that ESF. Ultimately, this study uses these means and standard deviations to conduct hypothesis testing on the difference between the two population means.

The conventional formulae to obtain mean and standard deviation via a frequency table are given below (*Mean & Standard Deviation Calculator*, n.d.):

$$\bar{x} = \frac{\sum_{i=1}^{k} f_i x_i}{(n-1)} \tag{3-1}$$

$$s = \sqrt{\sum_{i=1}^{k} \frac{f_i\,(x_i-\bar{x})^2}{(n-1)}} \tag{3-2}$$

where in the context of this paper,

i = an index for the PUMA identifier.

k = the total number of PUMAs.

n = the total number of workers in study area.

Several worker categories of interest possible,

e.g. ESF#1, ESF#2, non-ESF#1, or non-ESF#2 workers.

x_i = mean PGA (in fraction of g) of PUMA i, calculated in Step 1.

f_i = worker count in PUMA i for the worker categories of interest.

$\bar{x}$ = mean PGA (% of g) to which workers are exposed in this category.

s = standard deviation of the PGA (% of g) exposure of the workers in this category.

Table 2 depicts an example frequency table to calculate the mean and standard deviation of ESF#1 workers' exposure to PGAs across nine PUMAs in the study area. The study then estimates the mean and standard deviation of PGA exposure for ESF#1, ESF#2, non-ESF#1, or non-ESF#2 workers across all 156 PUMAs of the study area (Table 5 in Results). To perform these calculations, SAS version 9.4 was used.

Table 2: Sample frequency table to calculate the mean and standard deviation of ESF#1 workers' PGA exposure.

PUMA ID	(x_i) Mean PGA (g)	(f_i) ESF#1 Count in PUMA	$f_i x_i$	$f_i\ (x_i - \mu)^2$
0602500	0.07	729	49.71	13.65
0602901	0.08	461	35.67	7.51
0602902	0.12	901	108.32	6.48
0602903	0.11	642	70.92	5.74
0602904	0.14	242	34.94	0.89
0602905	0.09	603	52.26	8.45
0603701	0.32	1131	356.40	13.71
0603702	0.21	1493	313.25	0.03
0603703	0.48	913	437.25	68.49
			$\boldsymbol{\bar{x} = 0.21g}$	$\boldsymbol{s = 0.13g}$

3.5.4 Step 4) Conduct a T-test to determine if PGA exposure is higher for ESF#1 and ESF#2 (than for the rest of the working population.

A T-test can determine if there is a statistically significant difference between the mean PGA exposures of ESF#1 and ESF#2 workers and those of non- ESF#1 and non-ESF#2 workers, respectively. The T-test formula is given in equation (3-3) below:

$$t = \frac{(\bar{x}_1 - \bar{x}_2) - (\mu_1 - \mu_2)}{\sqrt{\frac{{s_1}^2}{n_1} + \frac{{s_2}^2}{n_2}}} = \frac{(\bar{x}_1 - \bar{x}_2)}{\sqrt{\frac{{s_1}^2}{n_1} + \frac{{s_2}^2}{n_2}}} \qquad (3\text{-}3)$$

where in the context of this paper,

$\bar{x}_1$ = the estimated mean PGA exposure of either ESF#1 or ESF#2 workers, calculated in Step 3.

$\bar{x}_2$ = the estimated mean PGA exposure of either non-ESF#1 or non-ESF#2 workers, respectively, calculated in Step 3.

μ_1 = the true mean PGA exposure of either ESF#1 or ESF#2 workers.

μ_2 = the true mean PGA exposure of either non-ESF#1 or non-ESF#2 workers,

n_1 = the number of ESF#1 or ESF#2 workers in the estimate.

n_2 = the number of non-ESF#1 or non-ESF#2 workers in the estimate, respectively.

Note that if testing the null hypothesis $\mu_1 = \mu_2$, then the term $\mu_1 - \mu_2$=0.

Once Step 3 yielded the means and standard deviations of PGA exposure for this study's worker categories of interest, this study tested the following null hypotheses:

1. $\boldsymbol{H}_0{}^{\text{ESF\#1}}$: $\mu_{ESF\#1} = \mu_{non-ESF\#1}$, no statistically significant difference between the mean PGA exposure of ESF#1 (Transportation) workers compared with non-ESF#1 workers.

2. $\boldsymbol{H}_0^{\text{ESF\#2}}$: $\mu_{ESF\#2} = \mu_{non-ESF\#2}$, no statistically significant difference between the mean PGA exposure of ESF#2 (Communications) workers compared with non-ESF#2 workers.

Since the counts of ESF#1 and ESF#2 are sufficiently large (n > 100), the following t-statistic critical values would permit the rejection of these null hypotheses: $t > \pm 1.96$ for a 95% confidence level ($p<.05$), and $t > \pm 2.58$ for 99% confidence ($p<.01$). These critical values are for two-tailed tests. Table 5 in Results summarizes the outcome of these two hypothesis tests.

3.6 Results

3.6.1 Result 1: Mean Peak Ground Acceleration (PGA) for each PUMA

Figure 12 presents the mean PGAs for each of the 156 PUMAs in the study area. For reference, the figure also includes the PGA contours for the Ardent Sentry scenario. The dense PGA contours are generally collinear with the San Andreas fault. The PUMAs with the highest mean PGAs occur along the fault, through Imperial, Riverside, San Bernardino, Los Angeles, and Kern counties. Several PUMAs in northeast Los Angeles County are also subject to higher mean PGAs.

The maximum mean PGA in a PUMA is 0.70g, in Southwest San Bernardino County (PUMA ID = 0607108, San Bernardino City (West)). San Bernardino County claims 7 of the 10 PUMAs with the top 10 highest mean PGAs in the Ardent Sentry scenario.

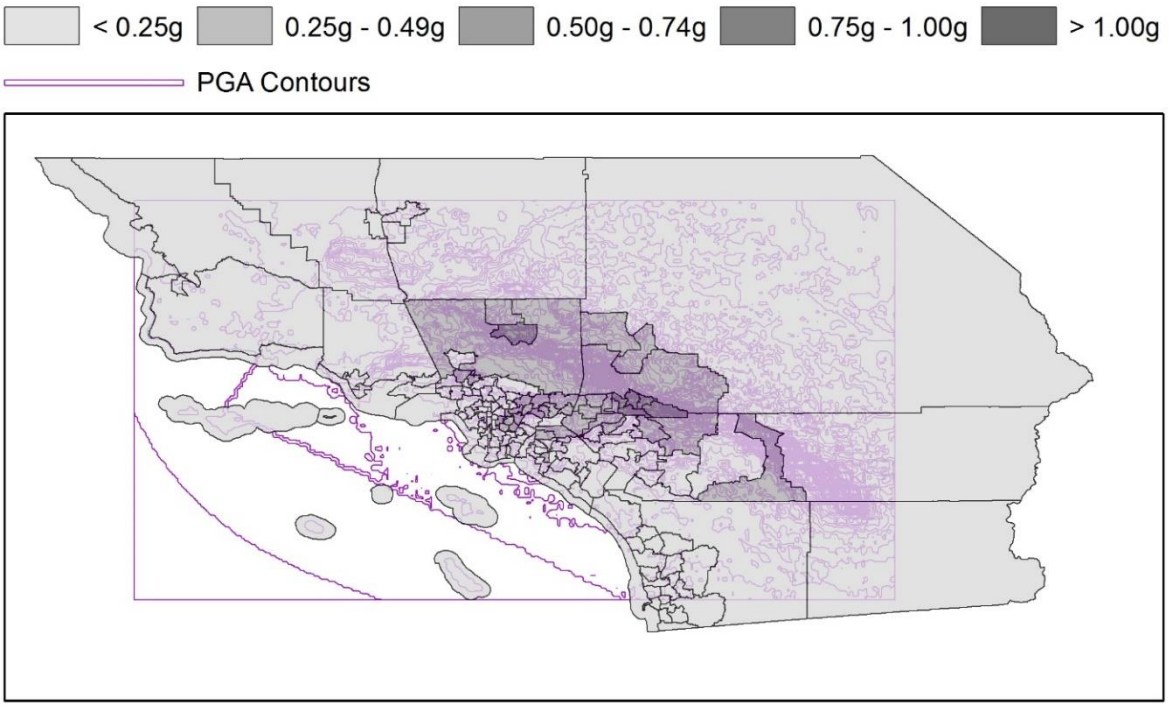

Figure 12: Mean Peak Ground Acceleration (in g) for each PUMA in study area.

Los Angeles (LA) County claims the 3 of the top 10. The two highest mean PGAs in LA County are 0.62*g* and 0.48*g*, in North Central LA County (PUMA IDs = 0603704 and 0603703, Palmdale City and Lancaster City, respectively). Meanwhile, the 10th highest mean PGA (at 0.46*g*) is in Central LA County (PUMA ID = 0603738, El Monte & South El Monte Cities).

3.6.2 Result 2: Proposed SOC & NAICS codes for ESF#1 & ESF#2, and comparison with the general working population

Table 3 shows the SOC and NAICS codes which this study proposes as corresponding to those workers and industry sectors (both private and public) who would perform the Transportation (ESF#1) and Communications (ESF#2) emergency support functions.

Italic entries indicate the 6-digit specialized industry NAICS codes which are not directly available as filtering values in the 2011-2015 ACS PUMS. Thus, the corresponding 2-digit sector or 3-digit subsector codes are marked with one asterisk "*". For example,

while this study deems the Highway, Street, and Bridge Construction NAICS (237310) to be within the scope of ESF#1, the 2011-2015 ACS PUMS merely indicates if a worker is in the Construction sector (NAICS = 23). Thus, Table 3 includes "23XXXX Construction*" among the NAICS codes for ESF#1.

Using these sector and subsector codes widens the scope of industries included in an ESF. When combined with SOCs in which many workers would be employed by both public and private entities, this widening of industry scope consequently includes many private sector workers which this study deems to be beyond the scope of the ESF of interest. One example SOC is Civil Engineers (17-2051).

Thus, Table 3 marks certain SOCs with "(p)" to indicate SOC codes for which only public-sector workers are considered for selection. In the 2011-2015 ACS PUMS public sector workers are those for whom the Class of Worker variable COW is 3, 4, or 5 – local, state, or federal government employee, respectively. This measure introduces the assumption that public-sector workers in these particular SOC codes are more likely to be critical to an emergency support function than private-sector workers. While imperfect, this study presents it as one possible solution to this issue.

Figure 13, Figure 14, and Table 4compare ESF#1 and ESF#2 workers against the general working population and against each other.

Figure 13 depicts the concentration of resident ESF#1 and ESF#2 workers in the study area, in terms of percentage of the total working population residing in the PUMA. While the greyscale color ramps for both are identical in the figure, the legend indicates that overall concentrations of ESF#2 workers are lower than those of ESF#1 workers.

The PUMA with the highest concentration of resident ESF#1 workers is in Southeast Orange County (PUMA ID = 0605915, Rancho Santa Margarita City (East) & Ladera Ranch). Among the top 10 PUMAs with the highest ESF#1 worker concentrations, Orange County claims two PUMAs, Los Angeles County claims three, San Bernardino County claims two, and San Diego, Ventura, and Riverside Counties claim one each. These concentrations range from 1.5% to 2%.

The PUMA with the highest concentration of resident ESF#2 workers is in Central San Diego County (PUMA ID = 0607308, San Diego (Northeast/Rancho Bernardo) & Poway). San Diego County claims three of top 10 the PUMAs in ESF#2 worker concentration, followed by San Bernardino and Riverside Counties (two each), and Orange, San Luis Obispo, and Los Angeles counties (one each). These concentrations range from 0.4% to nearly 0.6%.

Lancaster City (PUMA ID = 0603703) and Victorville & Adelanto Cities (PUMA ID = 0607102) are two PUMAs that are in the top 10 for both ESF#1 and ESF#2 worker concentrations. The former (Lancaster City) also ranks among the top 10 PUMAs with the highest mean PGA.

Table 3: SOC & NAICS codes proposed for identifying ESF#1 and ESF#2 workers.

Standard Occupational Classification (SOC) Codes	North American Industry Classification System (NAICS) Codes
ESF#1: Transportation	
11-3071 Transportation, Storage, and Distribution Managers 11-9021 Construction Managers 11-9041 Architectural & Engineering Managers 17-1022 Surveyors (p) 17-2051 Civil Engineers (p) 17-2121 Marine Engineers & Naval Architects (p) 17-3011 Architectural and Civil Drafters (p) 17-3022 Civil Engineering Technicians (p) 17-3031 Surveying and Mapping Technicians (p) 33-9093 Transportation Security Screeners 47-4011 Construction and Building Inspectors 47-4051 Highway Maintenance Workers 47-4061 Rail-Track Equip. Operators 49-2091 Avionics Technicians 49-2093 Electrical & Electronics Installers & Repairers, Transportation Equipment 49-2096 Electronic Equipment Installers & Repairers, Motor Vehicles 49-30XX Vehicle & Mobile Equipment Mechanics, Installers, Repairers 53-1011 Aircraft Cargo Handling Supervisors	23XXXX Construction* *237310 Highway, Street, and Bridge Construction* 481XXX Air Transportation 482XXX Rail Transportation 483XXX Water Transportation 484XXX Truck Transportation 485M Bus & Urban Transit* *485XXX Transit & Ground Passenger Transportation* 486XXX Pipeline Transportation 488XXX Support Activities for Air Transportation 92M2 Administration of Economic Programs and Space Research* *926120 Regulation & Administration of Transportation Programs*

53-20XX Air Transportation Workers 53-3020 Bus Drivers 53-3032 Heavy and Tractor-Trailer 53-3033 Light Truck or Delivery Services 53-40XX Rail Transportation Workers 53-50XX Water Transportation Workers 53-6011 Bridge and Lock Tenders 53-6041 Traffic Technicians 53-6051 Transportation Inspectors	
ESF#2: Communications	
11-3021 Computer & Information Systems Managers 15-11XX Computer Occupations 43-20XX Communications Equipment Operators 43-9011 Computer Operators 49-2020 Radio & Telecommunications Equipment Installers & Repairers 49-9052 Telecommunications Line Installers & Repairers	237130 Power & Communication Line & Related Structure Construction 5171 Wired Telecommunications Carriers 517Z Telecommunications, Except Wired Telecommunications Carriers 92M2 Administration of Economic Programs and Space Research* *926130 Regulation and Administration of Communications, Electric, Gas, & Other Utilities*

* The italicized entries below this entry are NAICS codes which are more specialized and relevant to this ESF, but which are not available in the *2011-2015 PUMS Data Dictionary* (2017).

(p) Only public-sector workers taken (Class of Worker = 3, 4, or 5)

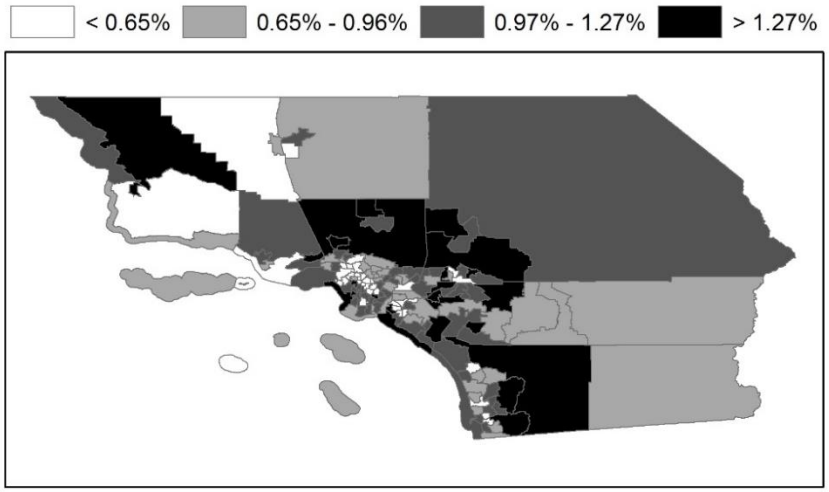

(a) ESF#1

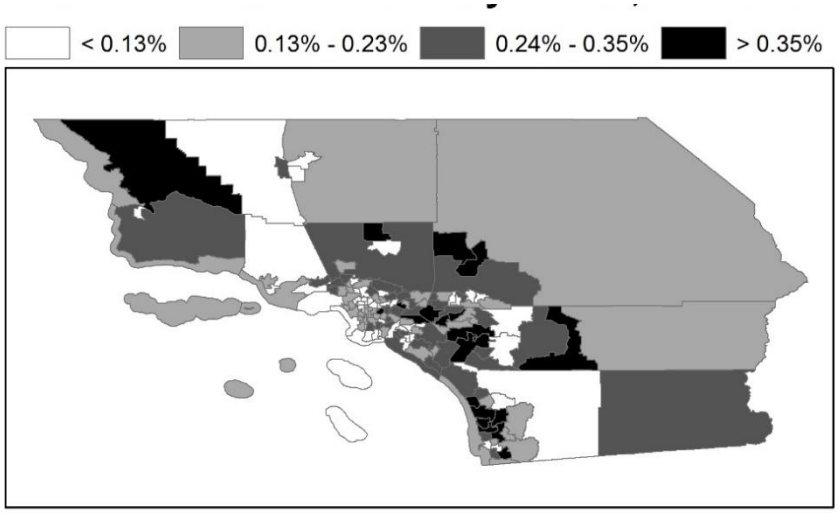

(b) ESF#2

Figure 13: Concentration of resident (a) ESF#1 and (b) ESF#2 workers. (In % of the total working population.)

Figure 14 shows the distribution of housing unit building types for the total working population, ESF#1 workers, and ESF#2 workers in Southern California. For all three building types, the percentage of workers with unknown housing unit building types is less than 3%. Furthermore, for each of the three building type categories, the percentage of workers who live in mobile homes is less than 2%. Mobile homes are a class of building which have been particularly vulnerable to earthquakes (e.g. Wein et al (2011) and Maison and Cobeen (2016). For all three worker categories, the category "Boat, RV, van, etc." was removed since the percentage was smaller than 1%.

At a glance, ESF#1 and ESF#2 workers are more like each other than to the general working population in their distribution between Single Family Detached and Condo, Apartment, and Townhouse (multifamily) housing. For example, whereas 70% of ESF#1 and 69% of ESF#2 workers live in Single Family Detached homes, only 60% of the total working population live in such homes.

Table 4 presents the household income distribution of the general working population, ESF#1 workers, and ESF#2 workers at the 10^{th}, 25^{th}, 50^{th} (median), 75^{th}, and 90^{th} percentiles. This study chose household income as opposed to the individual worker's income since the household income better reflects the resources that would be available to these workers in the event of an earthquake or fire. ESF#1 and ESF#2 household incomes are higher than that of the general working population from the 10^{th} to the 75^{th} percentiles – including the median household income. However, the 90^{th} percentile ESF#1 worker's household income is less than either the 90^{th} percentile ESF#2 worker or the 90^{th} percentile household income in the general working population. This paper does not attempt to determine if these differences are statistically significant.

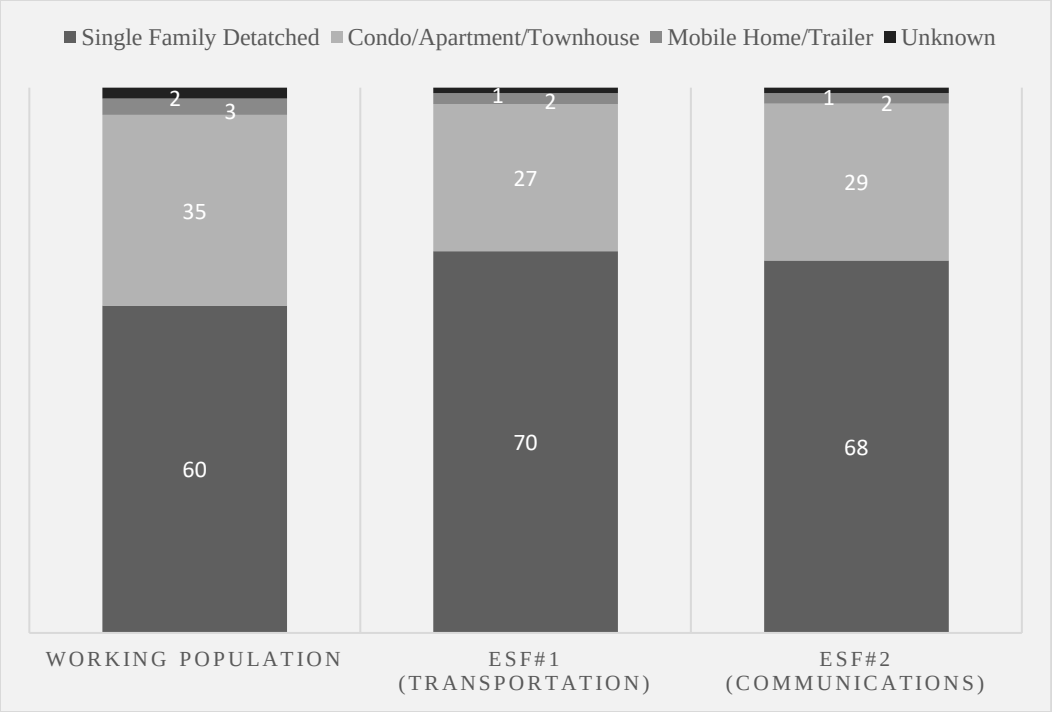

Figure 14: Distribution of Housing Unit Building Types for the total working population (left), ESF#1 workers (center), and ESF#2 workers (right) in Southern California, 2011-2015

Table 4: Distribution of Household Income (in percentiles) for the general working population, ESF#1 workers, and ESF#2 workers in Southern California, 2011-2015.

Worker Category	***Household Income Percentile (in 2015 dollars)***				
	10%	25%	**50% (Median)**	75%	90%
Working Population	$23,986	$45,220	**$82,103**	$136,092	$209,092
ESF#1 (Transportation)	$32,328	$57,748	**$95,607**	$144,911	$205,043
ESF#2 (Communications)	$39,778	$68,665	**$105,148**	$155,833	$217,775

3.6.3 Result 3: Means & Standard Deviations of PGA Exposure, and *t*-statistics for hypothesis tests

The top three rows of Table 5 summarize the means and standard deviations of PGA exposure for ESF#1 and non-ESF#1 workers, and for ESF#2 and non-ESF#2 workers. The bottom two rows present the resulting *t*-statistic values to test the two null hypotheses $\boldsymbol{H}_0^{\text{ESF\#1}}$ and $\boldsymbol{H}_0^{\text{ESF\#2}}$. For both *t*-statistics, the value is large enough to reject the null hypothesis, although to differing levels of confidence. Namely,

1. ESF#1 workers are exposed to *higher* mean PGAs than non-ESF#1 workers ($p<.01$), and
2. ESF#2 workers are exposed to *lower* mean PGAs than non-ESF#2 workers ($p<.05$).

ESF#1 workers are more exposed to PGAs in their PUMAs of residence than ESF#2 workers. In an earthquake similar to the 2015 Ardent Sentry scenario, ESF#1 workers may be more affected by damage to their homes than ESF#2 workers are. They could thus face more difficulty in returning to work and restoring transportation infrastructure.

This discrepancy may be due to the higher concentration of ESF#1 workers in southwest San Bernardino and northern Los Angeles Counties. The dark PUMAs of Figure 13(a) roughly correspond with the PUMAs of higher mean PGA in Figure 12. Of the PUMAs with the top 30 highest mean PGAs, twenty-seven are located in San Bernardino and LA Counties. Meanwhile, among the PUMAs with the top 30 highest concentrations of ESF#1 workers, fourteen are in those two counties. In contrast, only nine San Bernardino and LA county PUMAs are among the PUMAs with the highest ESF#2 worker concentrations.

Table 5: Mean and Standard Deviation exposure to PGA for ESF#1 and non-ESF#1 workers, and for ESF#2 and non-ESF#2 workers.

	Worker Category			
	ESF#1	Non-ESF#1	ESF#2	Non-ESF#2
Total count ***(n)***	102,991	10,695,776	22,360	10,776,407
Mean PGA exposure experienced in g ***($\bar{x}$)***	$0.193g$	$0.190g$	$0.188g$	$0.190g$
Standard Deviation of PGA exposure in g **(s)**	$0.141g$	$0.136g$	$0.133g$	$0.137g$
Hypothesis test	$\boldsymbol{H}_0^{\text{ESF\#1}}$: $\mu_{ESF\#1} = \mu_{non-ESF\#1}$		$\boldsymbol{H}_0^{\text{ESF\#2}}$: $\mu_{ESF\#2} = \mu_{non-ESF\#2}$	
***t*-statistic**	+5.67**		-2.18*	

* $p < .05$, ** $p < .01$, *** $p < .001$

3.7 Conclusion

This study aims to make two contributions. First, it proposes the use of SOC and NAICS codes as a means of identifying those worker and industry categories who would most likely participate in restoring damaged transportation and communications infrastructure. Specifically, this study lists those SOC and NAICS codes which most closely correspond to the Transportation (ESF#1) and Communications (ESF#2) Emergency Support Functions of the *National Response Framework* (2016).

Second, this study proposes one method to determine if any category of workers is exposed to higher PGAs in their PUMAs of residence. This method determines if the mean exposure to PGA of a worker category (e.g. ESF#1 or ESF#2) is equal to or different from the mean PGA exposure of the rest of the working population. For the 2015 Ardent Sentry

scenario, ESF#1 workers are found to be exposed to higher PGAs than non-ESF#1 workers, while ESF#2 workers are exposed to lower PGAs than non-ESF#2 workers. For both cases, the differences in PGA exposure are statistically significant.

For practitioners planning for disasters, awareness of which worker categories could be disproportionately impacted by a significant adverse event could facilitate pre-event response and recovery planning efforts. For example, public agencies can mitigate these potential worker shortfalls with investments in mutual aid agreements and worker preparedness. When established before a disaster, mutual aid agreements allow an affected jurisdiction to request resources (e.g. equipment, worker teams) from unaffected neighboring jurisdictions. For worker preparedness, measures would depend upon jurisdiction.

These results are subject to limitations. First, PUMAs are geographically large, with some PUMAs in this study over 1000 square miles. There can be significant variability in PGA even within a PUMA. These large PUMA sizes can distort the calculation for mean PGA in the PUMA. However, PUMAs were the finest geographic resolution for which SOC and NAICS data could be obtained for all worker categories and still achieve a sufficient sample size.

Second, while a San Andreas earthquake like the Ardent Sentry scenario is often used for planning purposes, large earthquakes could occur on other Southern California faults (e.g. the Northridge blind thrust fault). Ultimately, 2015 Ardent Sentry is only one of several scenario earthquakes in the USGS Southern California Legacy Catalog (*SCLEGACY Scenario Catalog*, 2017). Including scenario earthquakes of other magnitudes, locations,

and return periods can result in a more complete seismic hazard profile of mean PGA exposure for ESF#1 and ESF#2 workers.

Lastly, the NAICS codes available within the 2011-2015 ACS PUMS are only a subset of the full 2012 NAICS code structure from the Bureau of Labor Statistics. Consequently, in this this study, several 6-digit specialized industry NAICS codes are not directly available in the PUMS data. Out of necessity, this study uses the next-lowest-level NAICS code available (e.g. 4-digit industry group or 3-digit subsector code) and restricts the Class of Worker variable to public employees only.

There are other potential applications for applying this methodology in future research. For example, transportation infrastructure has interdependencies with energy infrastructure; thus, this methodology can be extended to include ESF#12 (Energy) workers. In addition, this methodology could be extended to all 14 ESFs. Similarly, the methodology could be applied to the six *National Disaster Recovery Framework (NDRF)* (2016) Recovery Support Functions (RSFs) and to the Department of Homeland Security's sixteen Critical Infrastructure Sectors (CISs). In these cases, the scope of the study would extend beyond transportation and cover other areas of emergency management.

The methodology could use another measure of worker vulnerability in place of PGA. For example, one could use risk measures of other hazards, such as wildfire or flood risk. In addition, another potential application for this methodology would be to conduct a case study in partnership with a transportation agency. Such a case study would allow the agency to tailor its strategy for mitigating potential worker shortfalls using data on its own employees (rather than general population data from PUMS).

4 STUDY 3: MODELING EXPECTED TRAVEL TIME CHANGES IN VEHICLE-CARRIED INFORMATION FLOW ALONG SELECTED ROUTES UNDER NETWORK DISRUPTIONS

4.1 Introduction

This study proposes a model for the travel time of information along communication-equipped vehicles that are physically traveling in a network. The study compares the expected travel time of information flowing along multiple paths connecting a specified pair of one sender and one receiver node in the fictional AZVille network. To estimate the information travel time, the methodology samples different proportions of simulated vehicles (10%, 20%, and 30%) as equipped vehicles. These samples' trajectories are analyzed to estimate link flow and turning movement counts of equipped vehicles, and to estimate the frequency of equipped vehicles encountering each other as they travel on links and through nodes. This study compares two scenarios: the baseline scenario and a work zone scenario that corresponds to a bridge being damaged in the network. Preliminary results suggest a difference in expected path travel times when 1. the representation of a specified subpath within the sample is increased and 2. when vehicles are routed along currently unused subpaths.

The initial motivation for this study is the continuing increase in both connected vehicles and connected vehicle infrastructure. The near-term development of a data-rich mobility environment prompted the consideration of the following question: If the conveyance of information were dependent upon being physically carried in vehicles that could transmit information only over short distances, is there some physically optimum way for the vehicles to move, or be routed, that optimizes that information flow in some

way? In other words, if information depended upon vehicles physically carrying it, can one route the vehicles to optimize the flow of information?

Study 3 emerged from that initial question. In terms of real world applications, MULEs (Mobile Ubiquitous LAN Extensions) served a starting point. As coined by Shah et al (2003), a "mule" is an entity which physically carries computer data between locations to create a data communication link – a pack animal for data, as the metaphor implies. They can be used to convey data to and from distant passive sensors in remote locations that monitor infrastructure such as wind farms or bridges.

Study 3 has diverged from this original vision. Ultimately, this study does not attempt a general routing problem. That is, this study does not propose a general routing algorithm to find the set of routes for equipped vehicles that optimizes either the flow or travel time of information between all origins and destinations of information (i.e. sending or receiving nodes). In addition, this study uses the more general term "equipped vehicles" rather than the term "mule".

Rather, this study proposes a model of information travel time along certain selected paths based upon the flows of communication-equipped vehicles along those paths. Equipped vehicles may only be traveling a portion of these specifically selected paths. This study explores how the expected information travel time can change when those underlying flows of equipped vehicles change.

For example, on links where expected travel time of information is greater than desired, then if more equipped vehicle flows are induced (i.e. over the already occurring mule flows), then the information expected travel time may decrease. These additional equipped vehicles are then entered into the simulation, which is repeated. However, these

additional equipped vehicles may change the flows and travel times on network links, and with them the information travel times as well.

While the methodology in this study does not solve a general information flow optimization problem, this study could be an important first step in developing a methodology to solve this problem.

4.2 Research Goals

This study assumes a transportation network, a set of sensors with information, a set of receivers to which the information must travel, vehicles that travel through the network, and a proportion ($\boldsymbol{\eta}$) of those vehicles equipped to act as mules that can

a. pick up information from sensors,
b. drop off that information at receivers, or
c. transmit that information to other equipped vehicles nearby.

With this context in mind, Study 3 has the following Research Goals:

1. Model the travel time of information on communication-equipped vehicles as the vehicles travel physically within a network.
2. Model the probability for information to make a specific turning movement as a function of equipped vehicle flows.
3. Model information travel times when the links are disrupted.

The primary goal of this study is to model the travel time of information on communication-equipped vehicles as the vehicles carry and pass the information in a network, on links or at nodes.

There are goals subordinate to this primary goal. First is to model the probability for information to make a specific turning movement as a function of the equipped vehicle

flows, especially their turning movements and their inflows into nodes. Second is to observe how this model behaves when specific links are disrupted. This study will use Work Zones to simulate traffic conditions during the recovery period.

4.3 Literature Review

The initial exploration for Study 3 was rooted in the literature for mules. Study 3 tries to fill the following gaps in the MULE literature.

First, Study 3 was intended to follow the growing number of data mule papers where the motion of the mules is not assumed to be random. The majority of the studies analyze simple or randomly generated networks with at most traces from small-scale real data. However, upon closer inspection, only a small set of papers depict the motion of mules as nonrandom or potentially nonrandom. These include Zhao, Ammar, & Zegura (2004), LeBrun et al (2005), Jea, Somasundara, & Srivastava (2005), Yazıcıoğlu et al (2013), and Yang, Adeel, & McCann (2013). Zhao, Ammar, & Zegura (2004) devised "message ferrying" where special mobile nodes exploit non-random motion to help deliver data. LeBrun et al (2005) found that where mules (in their case, buses) followed fixed routes, their location-based routing algorithm out-performed other algorithms in optimizing opportunistic forwarding performance. Jea, Somasundara, & Srivastava (2005) assign mules ("mobile elements") to specific sensor nodes in order to balance the load that each mule services. In Yazıcıoğlu et al (2013), the mules act as agents and move to different parts of the network to maximize a potential function. While Yang, Adeel, & McCann (2013) assumes the "spatial regularity of human mobility", their paper explores the introduction of incentives for mules to direct themselves within the network in order to trade sensor data.

Second, Study 3's origins are rooted in a domain-specific application for mules: bridge monitoring. A literature search for the keywords "bridge monitoring" and "data mules" returns few papers on Google Scholar and in the TRB Paper Compendia 2015 through 2017. Ghaleb et al (2014) notes that mules are a method of data gathering in wireless sensor networks (WSNs), and that WSNs have been used for civil infrastructure (including bridges). However, Ghaleb et al does not explicitly note an application where the two have been combined. Lattanzi et al (2017) demonstrates the feasibility of using unmanned aerial vehicles (UAVs) as data mules for bridge inspections. However, the focus is on the quality of 3D bridge models produced by the UAV, rather than on the design of a system that deploys UAVs as mules. This gap in mule research additionally justifies the inclusion of bridge monitoring as an application.

Third, Study 3 is intended to contribute to the domain of emergency or disaster applications within data mule literature. As early as 2001, Nasipuri, Castañeda, & Das (2001) posited an emergency rescue or exploration application for their multipath routing protocol, specifically "where cellular infrastructure is unavailable or unreliable". Since then, a handful of studies have explicitly suggested emergency or disaster applications for mules – few enough to suggest room for growth in this domain for data mules. Such studies include Zhao, Ammar, & Zegura (2001), Meghanathan (2007), and Ghaleb et al (2014). Zhao, Ammar, & Zegura (2004) specifically mention earthquake as an application of interest. Meghanathan (2007) recommends its own associativity-based routing scheme for applications deployed in energy constrained and disaster relief environments. In its review, Ghaleb et al (2014) cites a different study which uses wireless sensor networks for forest fire monitoring.

It is necessary to distinguish the goals and methodology of Study 3 against those of similar studies that use simulation in modeling intervehicle communication. The main distinction is that Study 3's focus is on information travel times that arise from flows of communication-equipped vehicles within the network. The purpose of focusing on these information travel times is to facilitate future formulations where equipped vehicles can be routed so as to optimize information travel times within a network.

For example, Yang and Recker (2006) models the potential benefits of dynamic vehicle routing where vehicle-to-vehicle communications enable a distributed traffic information system. Using both real-time and historic traffic information, vehicles in Yang and Recker (2006) optimize their routes independently. A "self-organizing traffic information overlay" emerges from these equipped vehicles rerouting themselves in response to the information they receive from their interactions with the distributed information system.

However, the vehicles are not themselves routed to optimize the distributed system's information travel time, or connectivity, or other metric of information system performance (rather than the performance of the vehicles). Study 3, in contrast, focuses on the changes in information travel time that result from changes in the flows of equipped vehicles in terms of their link-level flows and turning movements. This focus is rooted in the future goal of formulating a scheme to route equipped vehicles such that they optimize information travel times within a network.

4.4 Model Data

4.4.1 Network Model for Baseline Scenario

This study uses the DynusT demonstration model AZVille for its simulation and analysis. It uses the default input files for the Baseline scenario. Origin-Demand entries and Work Zone disruptions are added in the Disruption scenario.

AZVille is a fictitious network that combines parts of the Phoenix and Tucson networks, and was created by Prof. Yi Chang Chiu. In personal correspondence with me, he stated that his purpose for creating this network Was to test different diversion strategies along 3 complimentary corridors. The AZVille network was selected due to difficulties with converting either the West LA network of Study 1, or a smaller demonstration Irvine Triangle network. Since it is a fictitious network, for the purposes of Study 3, the analysis can assume that the region has a seismic hazard profile similar to Southern California. This will be important for translating the disruption modeling to a Southern California context.

The network contains 174 nodes, 374 links, and 5 zones (Figure 16). However, in DynusT, just as in Dynasmart, zones are assigned generation links to generate trips from the origin zone and destination nodes to accept trips into the destination zone. Between these 5 zones, there are 103 generation links and 23 destination nodes. In Figure 16, starting nodes of generation links are indicated by stars, the destination nodes are indicated by circles, and differing colors distinguish one zone from another (purple for Zone 1, red for Zone 2, green for Zone 3, blue for Zone 4, and black for Zone 5).

The scenario being modeled is a PM Peak Period (See Table 7 for the baseline Origin-Demand Table). Zone 1 (in the downtown portion of the network) has 1000 trips destined primarily for zones 4 and 5 (smaller outbound zones). Zone 2 (also downtown) has 2000 trips destined for Zone 5. And Zone 3 has 200 trips destined for Zone 1, and 1000

destined for Zone 2. For this study, trips are added in the reverse direction, from Zone 4 to Zone 1, in an attempt to use an intersecting flow of equipped vehicles to improve information travel time along a selected path.

4.4.2 Disruption Scenario

Since AZVille is a fictitious network, this analysis assumes that the region has a seismic hazard profile similar to Southern California. A key link is assumed to hold a bridge, and a plausible fragility curve is assigned to the bridge. The PM Peak period means that any equipped vehicles are outbound from the downtown area.

For this scenario, the disruption occurs at an earthquake-damaged onramp bridge on Link 146-69 (a two-lane link of speed limit 55 mph and of capacity 1800 veh/hr/lane). It is indicated by the blue curved link in Figure 17 labeled “Damaged Bridge”. The analysis in this study will examine vehicles that travel on paths between the Sender Node 127 and the Receiver Node 79, indicated by black squares here. Equipped vehicle flows (and hence expected information travel times) between these two nodes are affected by the Work Zone on the damaged onramp bridge.

In the workzone.dat file, the capacity, speed limit, and queue discharge rate of the link is reduced. Namely, the capacity is reduced to 50% of the undisrupted link, the speed limit is lowered from 55 mph to 30 mph, and the queue discharge rate from 2200 veh/hr/lane to 1300. These workzone.dat input values are adapted from the work zone scenario use case (Case III) in the *DynusT (2017 Build) Use Case Guide* (2017).

The workzone.dat file input values suggest that one lane has been taken away. The link has not been closed, but traffic restrictions have been applied. DesRoches et al (2012) contains a table which estimates that this level of traffic restrictions corresponds to a

Moderate damage state (BSST-1). This table is reproduced in Table 6. At the Moderate damage state, the link would likely be open to limited traffic (with speed/weight/lane restrictions), though a closure or detour may be unlikely. For emergency repair, shoring and bracing would likely not be required, but roadway level may be necessary. This study takes the simplifying assumption in looking at the damage system of the bridge as a whole. The damage state of individual components (e.g. abutment seats, joint seals, columns) is not considered. However, in DesRoches et al (2012), the most vulnerable component is used in designating the fragility curve for the bridge as a system.

Table 6: General description of bridge system level damage states along with component damage thresholds. Source: Table 5.7, DesRoches et al (2012).

Bridge system damage states	BSST-0 MINOR	BSST-1 MODERATE	BSST-2 EXTENSIVE	BSST-3 COMPLETE
ShakeCast Inspection Priority levels	Low	Medium	Medium-High	High
Likely Immediate Post-Event Traffic State	Open to normal public traffic – No Restrictions	Open to limited public traffic – speed/weight/lane restrictions	Emergency vehicles only – speed/weight/lane restrictions	Closed (until shored/braced) – potential for collapse
Traffic Operation Implications				
Is closure/detour needed?	Very unlikely	Unlikely	Likely	Very likely
Are traffic restrictions needed?	Unlikely	Likely	Very Likely	Very Likely - Detour
Emergency Repair Implications				
Is shoring/bracing needed?	Very unlikely	Unlikely	Likely	Very likely
Is roadway leveling needed?	Unlikely	Likely	Very Likely	Very Likely - Detour

The level of ground motion that produces a Moderate damage state depends upon the bridge's fragility curve. Since the AZVille network is fictional, the analysis can assume a bridge of any type for the disruptable link 146-69. DesRoches et al (2012) has several types of multispan continuous concrete bridges: Slab (S), Box girder (BG), T-girder (TG), and I-girder (IG) bridges. For the latter three types, DesRoches et al (2012) also classifies fragility curves by bent type: multi-column bent (M), single-column bent (S), and pile extensions (P). DesRoches et al (2012) also classifies fragility curves for different:

- Design Eras: Pre-1971 Sylmar earthquake (E1), 1971-1990 (E2) i.e. between the 1971 Sylmar and 1989 Loma Prieta earthquakes, and post-1990 (E3)
- Abutment Types: Diaphragm, Seat
- Seat Width Class: None (S0), 4-12 in (S1), 12-18 in (S2), 18-24 in (S3), >24 in (S4)
- Gap Size: NA, Small (S), and Large (L)

This study uses the fragility curves of DesRoches et al (2012) since the fragility curves of ShakeCast are based upon the work performed in these compiled reports. That is, "the primary focus of" DesRoches et al (2012) "was to demonstrate that improved (fragility curve) models could be developed for use in emergency-alerting applications such as ShakeCast".

This study assumes a simple model of bridge: the multispan continuous concrete slab bridge. DesRoches et al (2012) has a set of fragility curves for these types of bridges (MSCC-SL). These curves apply to slab bridges of all design eras (E1, E2, E3). The bridges in the fragility model have seat abutments (rather than diaphragm abutments) and the "pile extensions" bent type. It is important to choose the curves which correspond to the damage state of the disruption scenario – the Moderate damage state, BSST-1.

These curves are reproduced in Figure 15. The x-axis is the Peak Spectral Acceleration (PSA) at one second, $S_a(1.0)$. The y-axis is the probability $P[BSST\text{-}1|S_a(1.0)]$ that a bridge enters the Moderate damage state BSST-1, given a certain value $S_a(1.0)$ of PSA at one second. This figure shows both the system fragility curve (for the bridge as a whole) and the fragility curves for components such as columns, joint seals, etc. The curves of interest are the red "Bridge" fragility curves.

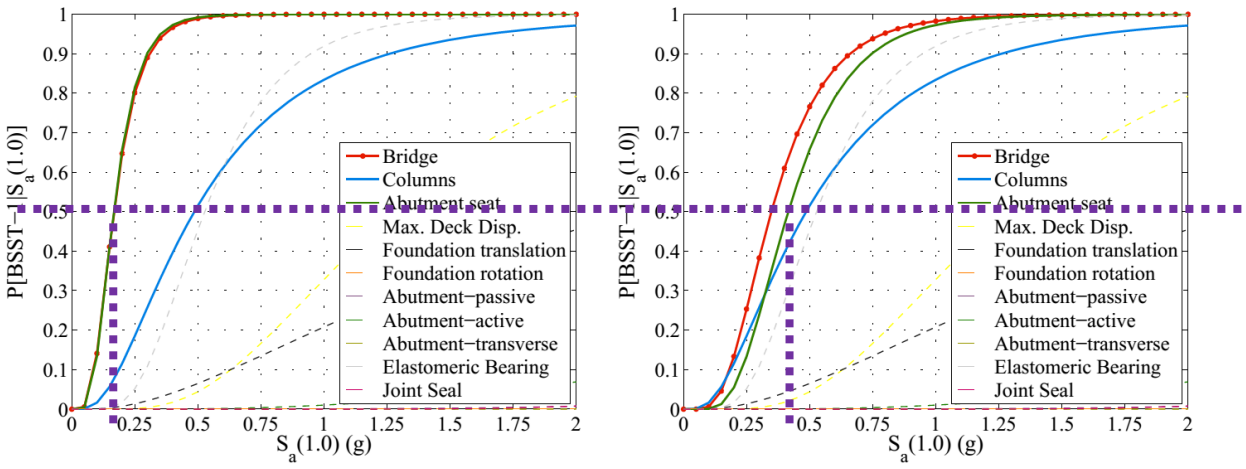

(a) 4-12 in seat width (S1) (b) 18-24 in seat width (S3)

Figure 15: System and component level fragility curves for MSCC-SL bridges with seat type abutments and seat width class S1 and S3. Sources: Figure 6.3, DesRoches et al (2012).

To find the one-second PSA that corresponds to the Moderate damage state (BSST-1) that in turn leads to the traffic restrictions in the workzone.dat file, one must find the PSAs where $P[BSST\text{-}1|S_a(1.0)] > 0.50$. That is, one must find the $S_a(1.0)$ value where the probability of a bridge entering the BSST-1 damage state equals or exceeds 50%. Figure 15 indicates this threshold with the purple dotted line. For seat widths of 4-12 in (seat width class S1), the probability $P[BSST\text{-}1|S_a(1.0)]$ equals or exceeds 0.50 starting at approximately $S_a(1.0)=0.15g$. For seat widths of 18-24 in (seat width class S3), the same probability $P[BSST\text{-}1|S_a(1.0)]$ equals or exceeds 0.50 starting at approximately $S_a(1.0)=0.33g$.

For a basis of comparison, Figure 18 and Figure 19 are contour maps of PSA at one second for the 2015 Ardent Sentry scenario earthquake and the 1994 Northridge earthquake, respectively. On the 2015 Ardent Sentry scenario contour map, there are no visible contours below 0.60g. This means PSAs in this scenario that are much greater than the threshold values of 0.15g for S1 seat abutments and 0.33g for S3 seat abutments,

suggesting damage to multispan continuous concrete slab bridges that could far exceed the Moderate (BSST-1) damage state.

On the 1994 Northridge contour map, one-second PSA contours that exceed 0.15g are generally restricted to Northwest Los Angeles county south of the San Gabriel mountains. These contours do not seem to extend further south and east than Huntington Beach in Orange County.

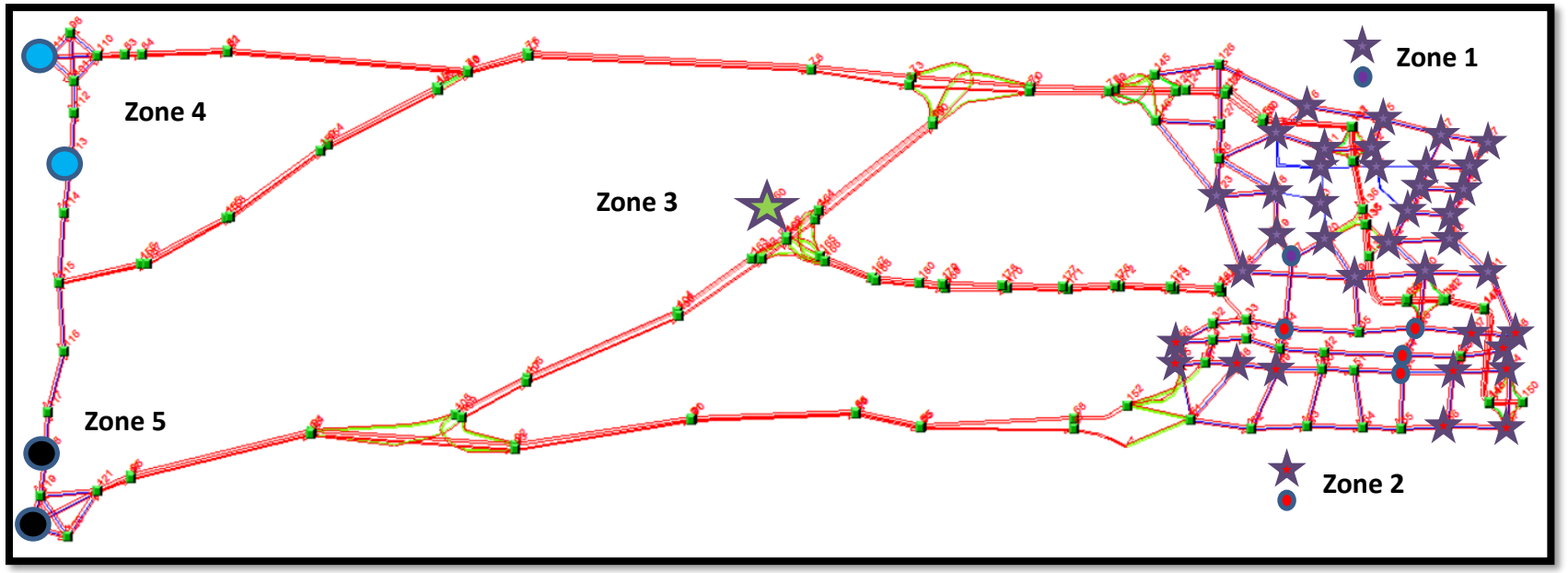

Figure 16: AZVille demonstration network for Baseline scenario. 174 nodes, 374 links, 5 zones (103 generation links, 23 destination nodes).

Table 7: Baseline scenario Origin-Demand tables (a) for single-occupant vehicles and (b) for high occupancy vehicles.

(a) single-occupant vehicles

Veh/hr	Zone 1	Zone 2	Zone 3	Zone 4	Zone 5
Zone 1	0	**5**	0	**1000**	**1000**
Zone 2	0	0	0	**2000**	0
Zone 3	0	**200**	**1000**	0	0
Zone 4	0	0	0	0	0
Zone 5	0	0	0	0	0

(b) High-occupancy vehicles

Veh/hr	Zone 1	Zone 2	Zone 3	Zone 4	Zone 5
Zone 1	0	**5**	0	**1000**	**1000**
Zone 2	0	0	0	0	0
Zone 3	**2000**	0	0	**200**	**1000**
Zone 4	0	0	0	0	0
Zone 5	0	0	0	0	0

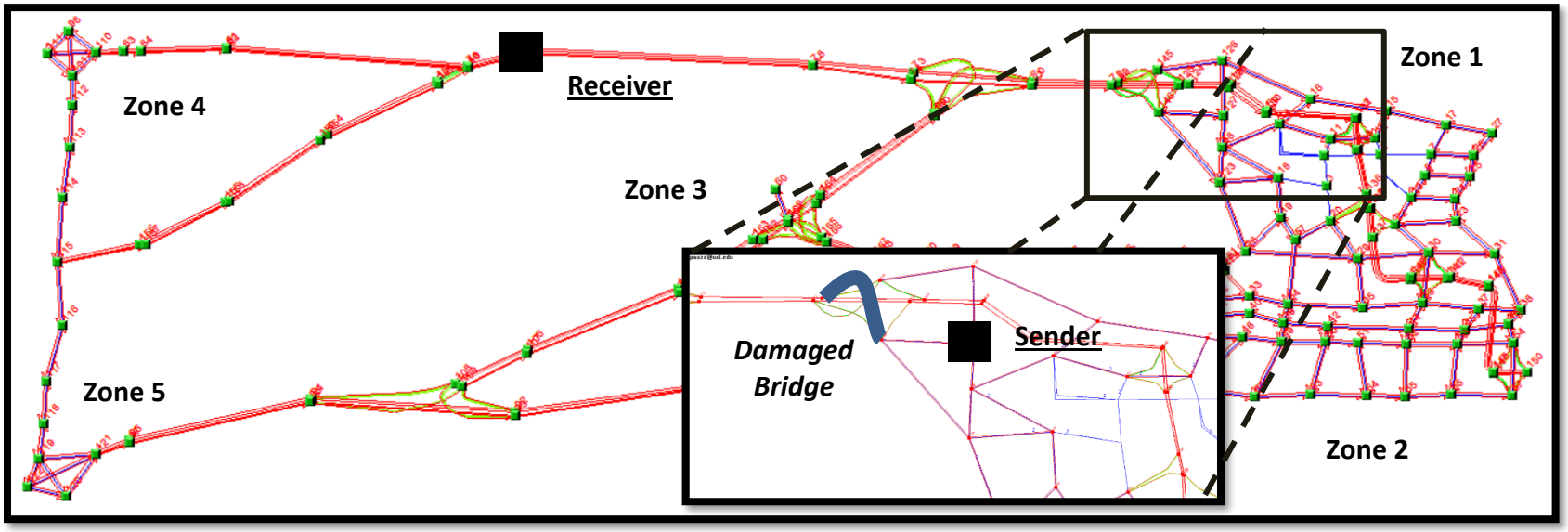

Figure 17: Disruption case. Location of damaged onramp bridge on link 146-69.

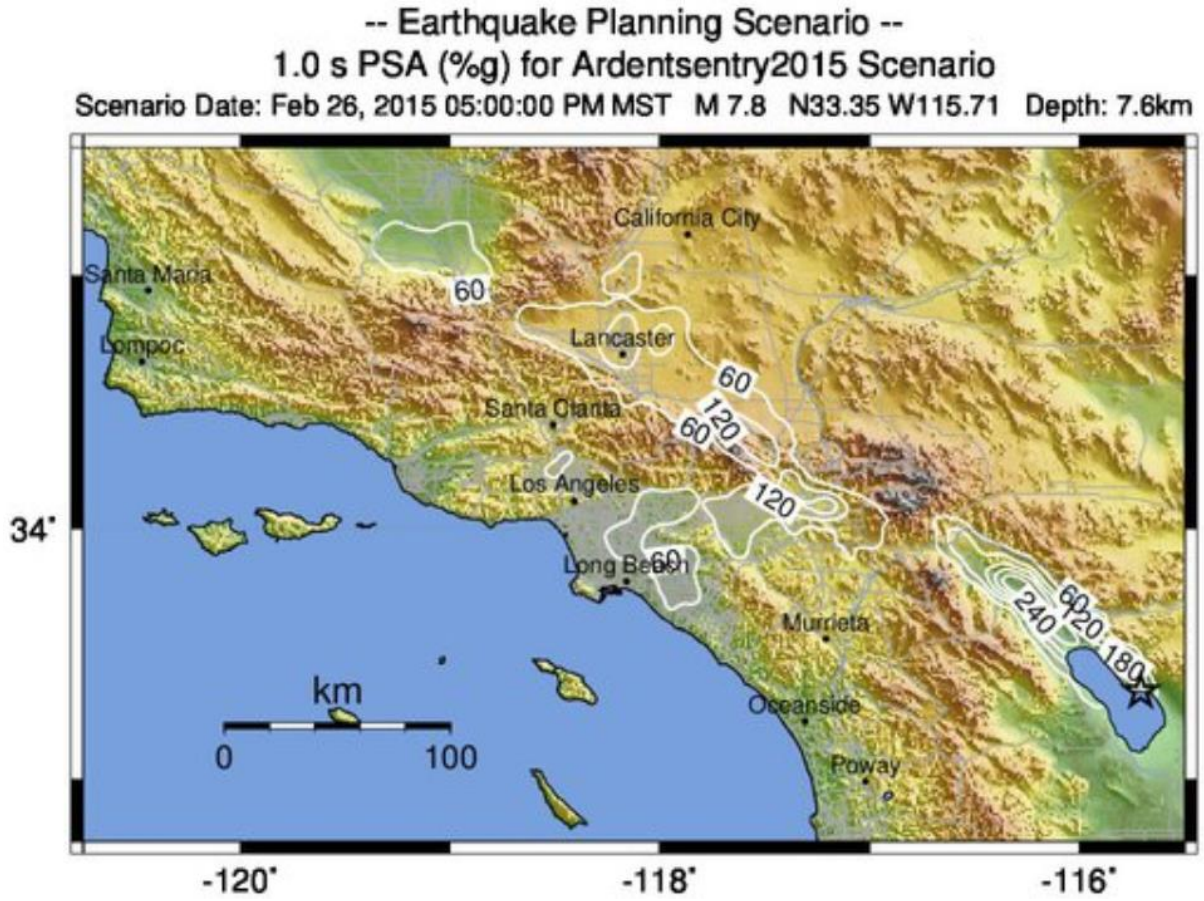

Figure 18: Contours of Peak Spectral Acceleration (PSA) at one second, $S_a(1.0)$, for the 2015 Ardent Sentry scenario. Source: M 7.8 Scenario Earthquake - Ardent Sentry 2015 Scenario (n.d.).

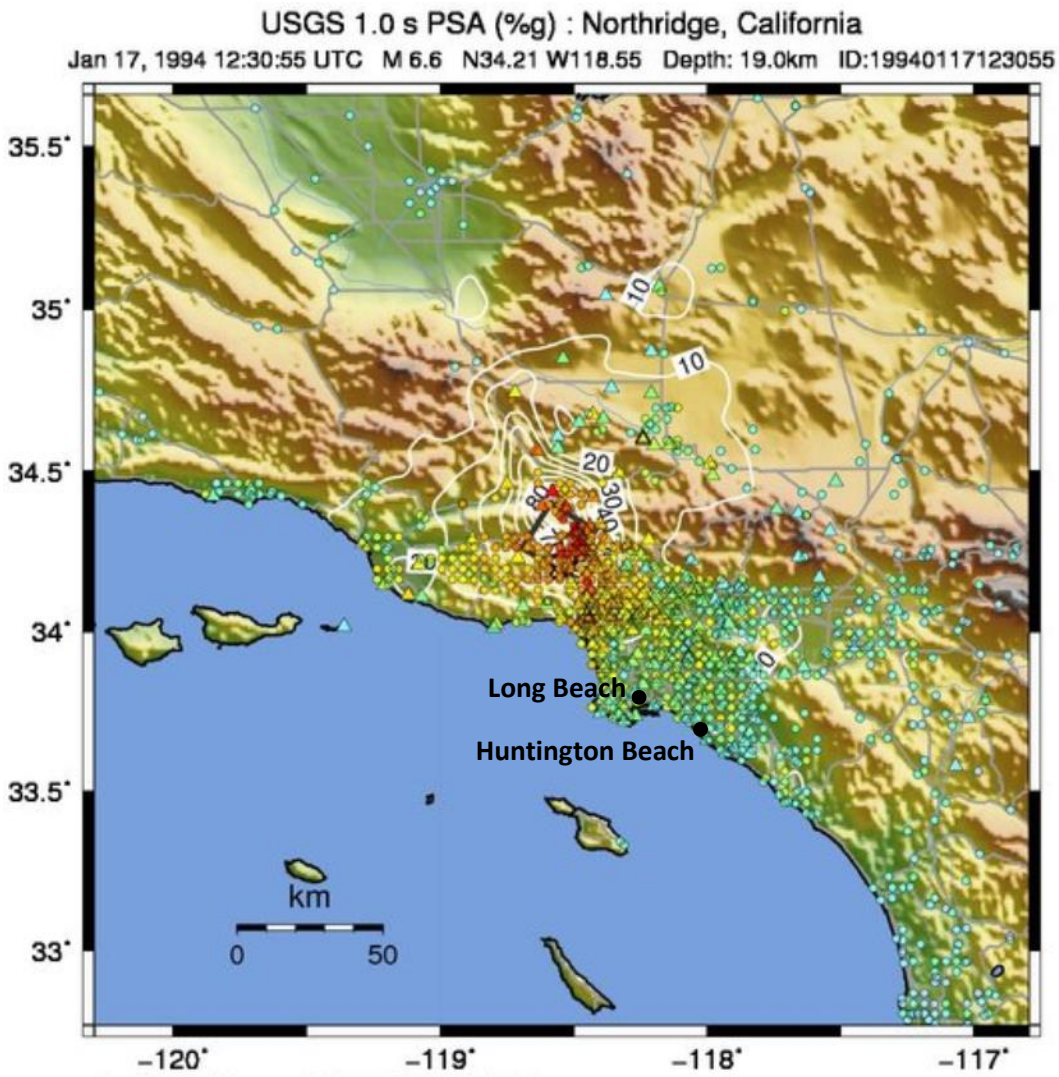

Figure 19: Contours of Peak Spectral Acceleration (PSA) at one second, $S_a(1.0)$, for the 1994 Northridge earthquake. Source: M 6.7 - 1km NNW of Reseda, CA. (n.d.).

4.5 Methodology

This study's methodology begins with the overall Framework, and its specific definitions and uses of scenarios, cases, and phases.

Next come various Elements of the study's methodology for modeling information travel times. First are the most fundamental elements, the expected travel time of information and the propagation of gaps in the flow of information. The study samples of vehicles in the vehicle trajectory file to act as equipped vehicles in order to estimate link-level counts and turning movement counts of equipped vehicles. These link counts and turning movements are then used in estimating the probability of information successfully making a specific turning movement ("information turning flow probability").

The methodology concludes with the Simulation and Analysis plan used in processing the baseline and disruption scenarios. It specifies the specific control and treatment cases conducted for each scenario.

4.6 Simulation & Analysis Framework

In order to model the expected travel time of information in the model network, this study requires both a traffic modeling component and an information flow modeling component that work iteratively. Figure 20 depicts the iteration of traffic modeling and information travel time modeling that must occur. Link travel times and vehicle trajectories are the output of the traffic model and the input into the information flow model. The information travel time model then returns routes that improve information travel times back into the traffic flow model.

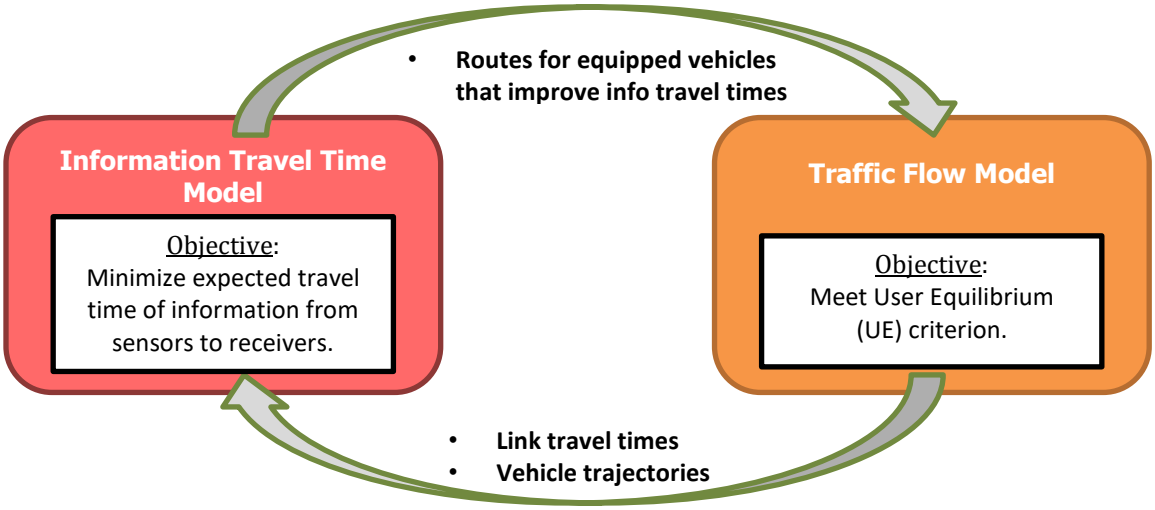

Figure 20: Iterative relationship between Traffic Flow and Information Flow models.

This concept was the kernel that evolved into the study's current framework, depicted in Figure 21. This figure illustrates the approach required to analyze one particular scenario, and shows the relationship between *scenarios*, *phases*, and *cases*. The analysis of a scenario occurs in three phases, though the specific case being analyzed may not require the execution of all three.

For a given network model, there are at least two scenarios: the Baseline scenario, and at least one Disruption scenario for each network disruption of interest that one wishes to compare against the baseline scenario. This study has two scenarios: the Baseline scenario, and only one Disruption scenario (where the link 146-69 has been disrupted with a Work Zone to repair the onramp bridge).

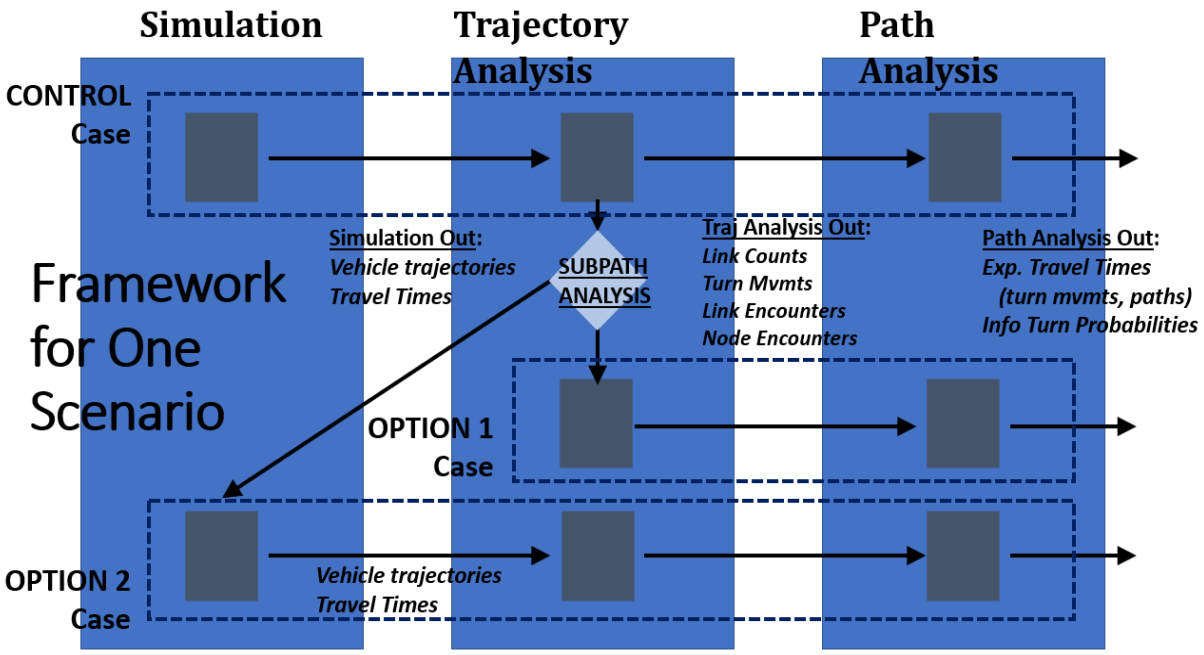

Figure 21: Simulation and Analysis Framework for Study 3, for one scenario. Relationship between scenarios, cases, and phases.

To analyze a scenario, there are three phases: Simulation, Trajectory Analysis, and Path Analysis. In the Simulation phase, DynusT is used in generating vehicle trajectories and link travel times. During the Trajectory Analysis phase, the vehicles are sampled within the vehicle trajectories file. This sampling marks these vehicles as equipped vehicles. Sampling occurs at three different rates: η=0.10 (i.e. 10% equipped vehicles), η=0.20, η=0.30. The samples are then processed in SAS in order to estimate the 1) link counts and turning movements of equipped vehicles, and the 2) number of link and node encounters of equipped vehicles. In the Path Analysis phase, one manually calculates the information turning probabilities and the expected travel times along turning movements. Ultimately, it builds the turning movement expected travel times into Path expected travel times.

In order to move from one phase to another, it is necessary to break the scenario down into Cases: The Control case, and the Treatment cases. In the Control case, all vehicles

(traversing all paths) have an equal probability of being sampled during the Trajectory Analysis phase. However, in the Treatment cases, vehicles from a specified path are sampled at a higher rate. The result of this higher sampling is an Incremental Assignment of equipped vehicles on that path. There are two options by which to specify Treatment Cases:

- Option 1: Increasing representation along a specific path.
- Option 2: Introducing flows of equipped vehicles on a specific path, and then including those vehicles in the sample.

The Treatment cases are all compared to the Control case.

Before deciding on a Treatment Option, it is necessary to conduct a Subpath Analysis. This step finds all the paths leading to and from a specified pair of one Sender and one Receiver node. Once the subpaths between the Sender and Receiver are obtained, then the analyst can choose between the two Treatment case options.

Option 1 increases the representation of a particular subpath from the Subpath Analysis during the sampling process. Doing so would increase the information flow along that path because this option increases the proportion of equipped vehicles along it. The result of this higher sampling is an Incremental Assignment of equipped vehicles on this specified path – and no vehicles are introduced in order to achieve this incremental assignment. Such an outcome would occur if, for example, drivers already traveling that route were to volunteer to act as equipped vehicles before an event, and were then activated as equipped vehicles in the event's aftermath.

Option 2 introduces vehicles that have a trajectory which intersects the paths already present. An intersecting trajectory is one that shares at least one node and/or link

with another trajectory. This study achieves Option 2 by introducing an OD flow in the fictitious network *into* the downtown zones 1 and 2. The analysis is then programmed to include all of these introduced vehicles within every sample (not merely at a higher rate than the Control case). The result of including all introduced vehicles into every sample is an Incremental Assignment of equipped vehicles on this introduced path.

For all three cases (Control, Treatment Option 1, and Treatment Option 2), one can conduct Trajectory Analysis and Path Analysis. Trajectory Analysis requires vehicle trajectory and travel time output from the simulation. The Path Analysis then uses the Trajectory Analysis output to examine information travel times along the paths of interest.

4.7 Elements of the Information Travel Time Model

4.7.1 Example Network

While discussing various elements of the information travel time model, this study may reference the following eight-node, nine-link example in Figure 22. There is initially only one OD pair, from node 5 to node 7. The traffic is assigned to two different routes:

1. Path J-A-B-G through nodes 5, 1, 2, 3, & 7, and
2. Path J-C-D-G through nodes 5, 1, 4, 3, & 7.

On each path, there is a proportion η of equipped vehicles. In the figure, they are represented by the white cars. These vehicles can communicate with each other.

Initially, there is no cross flow between nodes 6 and 8. However, in this example, an intersecting path flow (one which shares at least one link and/or node with another path) can be i*ntroduced* between those nodes, for OD pairs 6-8 and 8-6. In this case, this introduced flow would consist of equipped vehicles only.

None of these introduced equipped vehicles travel over any of the same links as the two initial path flows JABG and JCDG. However, their purpose is to allow information to potentially cross from the first path to the second path, or vice versa. The exchange of information would occur at nodes 2 and 4.

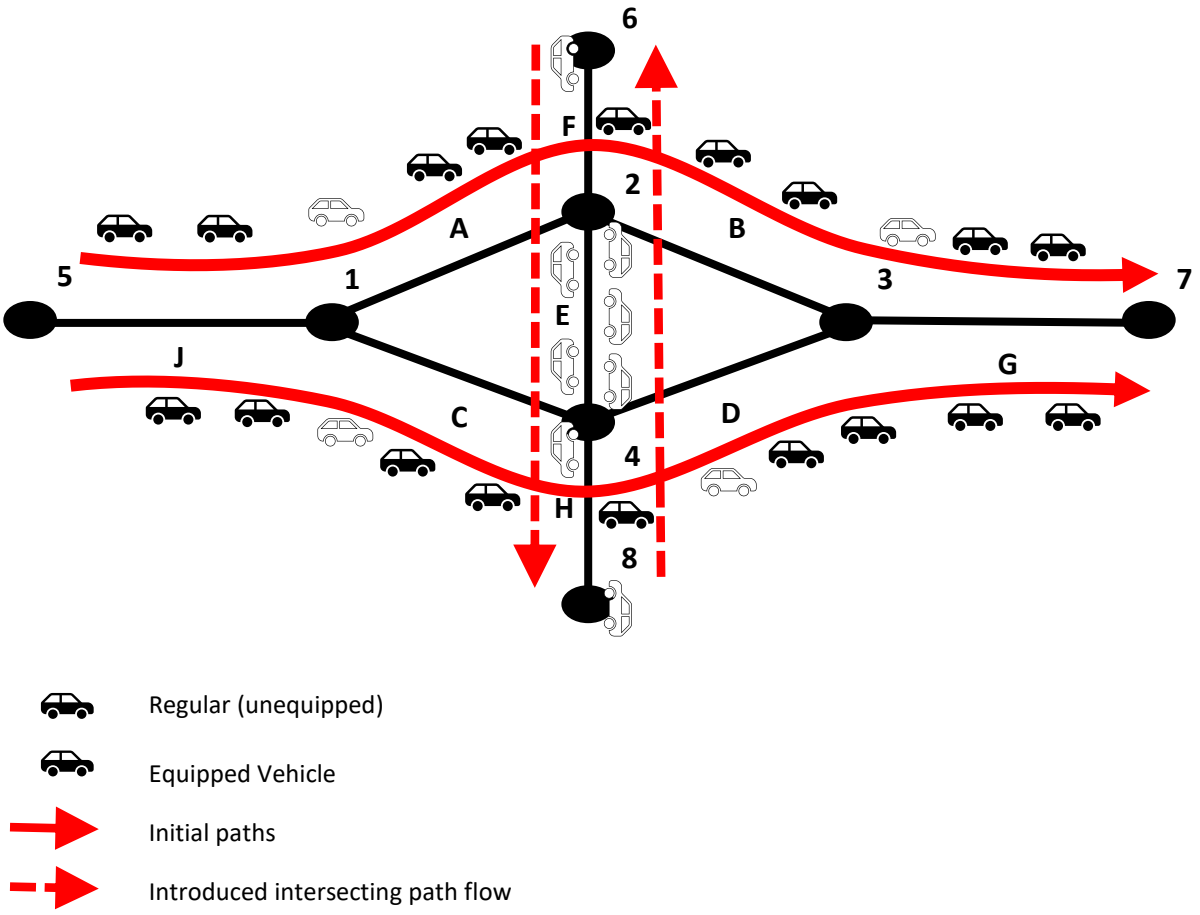

Figure 22: Small example network.

4.7.2 Expected Travel Time of Information

This study's model of information travel time makes a key assumption. Namely, if an equipped vehicle is in range of another equipped vehicle, it transmits its message successfully. It creates the connection instantaneously, and the message is small enough to be transmitted in that brief time they are interconnected. This case is depicted in Figure 23(a).

The focus in this study is the motion of the equipped vehicles themselves. If an equipped vehicle is not in contact with another equipped vehicle, then the information it is carrying will remain with it. The information then travels at the speed of the vehicle. This case where a gap forms is depicted in Figure 23(b).

For every potential link turning movement, one can thus write an expression of the expected travel time of the information to make that turn. Since there are two possibilities of travel time, and travel time is zero for the No Gap case, the expected travel time simplifies to a product of the travel time on link J and the probability that a gap forms:

$$E[\tau_J] = (0)(p_{No\ Gap}) + t_J\ (p_{Gap}) \\ = t_J\ (p_{Gap}) \quad (4\text{-}1)$$

Where τ_J= travel time of gap formed on link J

t_J= travel time on link J

$p_{No\ Gap}$ = probability that no gap forms

p_{Gap} = probability that a gap forms

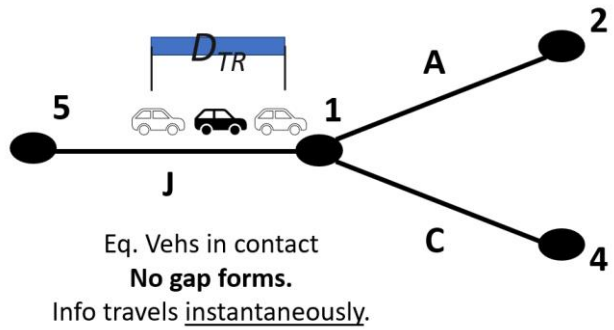

(a) No gap forms, and information travels instantaneously.

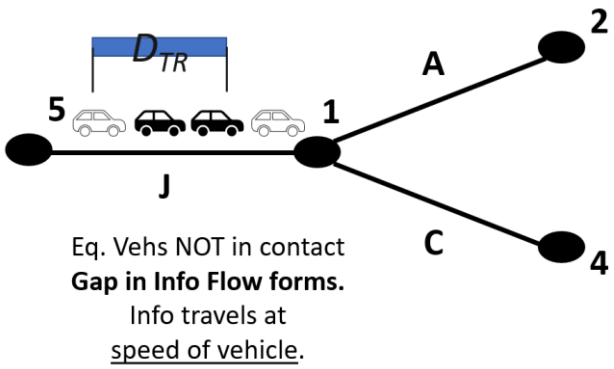

(b) Gap forms within the information flow. Information travels at the speed of the vehicle.

Figure 23: Situations where (a) no gap forms, and (b) a gap forms within the information flow.

4.7.3 Information Flow Gaps

The presence of p_{Gap} in the expected travel time expression warrants a closer look at the probability of a gap to form in the information flow. In general, once the density of equipped vehicles on a link reaches 18 per mile per lane, the probability of a gap forming drops below 1%. At 18 equipped vehicles per mile per lane, the gaps are practically eliminated, and the expected travel time of information on that link will drop to zero.

This probability assumes that the standard deviation of the gap size is 30% of the mean gap between equipped vehicles. Both quantities decrease as the density of equipped vehicles increases, driving the gap formation probability below 1%. Also assumed is that the gap size between equipped vehicles is normally distributed. There are additional assumptions regarding the fundamental flow, speed, and density relationships on the hypothetical link, namely:

- a Triangular flow-density relationship in which the free flow speed is 70 mph, and
- critical and jam densities are 30 and 150 vehicles per mile per lane, respectively.

However, these equipped vehicles are traveling in a traffic flow with unequipped vehicles. The smaller the ratio of equipped to unequipped vehicles, the longer the mean distances between mules (as depicted schematically in Figure 24). As a result, the density at which gap formation drops below 1% probability will only decrease as the equipped/unequipped vehicle ratio η increases.

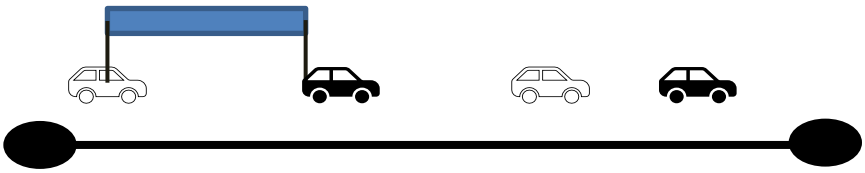

(a) Gap has formed

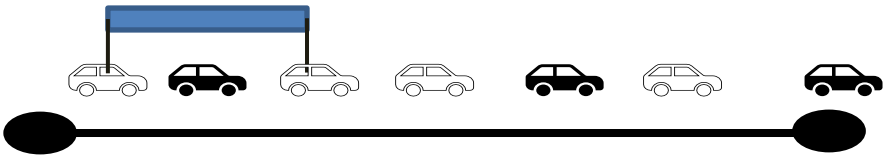

Gap eliminated

(b) Gap eliminated

Figure 24: As ratio of equipped to unequipped vehicles increases, the mean distances between them decrease. In (a), a gap has formed, whereas in (b) with its higher ratio, the gap is eliminated.

Two quantities decrease as the proportion of equipped vehicles η increases: 1) the probability P(Gap>500ft) that the gap between equipped vehicles is greater than 500 feet, and 2) the expected travel time of information over the mean gap. The latter quantity (i.e. expected information travel time) is obtained by multiplying the former quantity, P(Gap>500ft), by the travel time (in seconds) for an equipped vehicle to traverse the mean gap. The relationship of both quantities with the average density of all vehicles (including both equipped and unequipped vehicles) is presented in Figure 25 and Figure 26, respectively.

At η=0.10, in Figure 25(a), there is still an 8% probability that there is a gap larger than 500 ft between equipped vehicles at the jam density of 150 vehicles per mile per lane. For this proportion η, the expected travel time of information over the mean gap never decreases below 1 second. In Figure 26(a), the expected travel time reaches a minimum of

approximately 17 seconds when the average density of all vehicles is 30 veh/mi/lane (meaning an equipped vehicle density of 3 equipped vehicles per mile per lane).

At $\eta=0.20$, the gap formation probability drops below 1% at 90 veh/mi/lane, corresponding to 18 equipped vehicles per mile per lane (Figure 25(b)). The expected travel time of information over the mean gap decreases below 1 second at 80 veh/mi/lane (16 equipped vehicles per mile per lane) (Figure 26(b)).

At $\eta=0.30$, the gap formation probability drops below 1% at 60 veh/mi/lane, corresponding to 18 equipped vehicles per mile per lane (Figure 25(c)). The expected travel time of information over the mean gap decreases below 1 second at 46.7 veh/mi/lane (14 equipped vehicles per mile per lane) (Figure 26(c)).

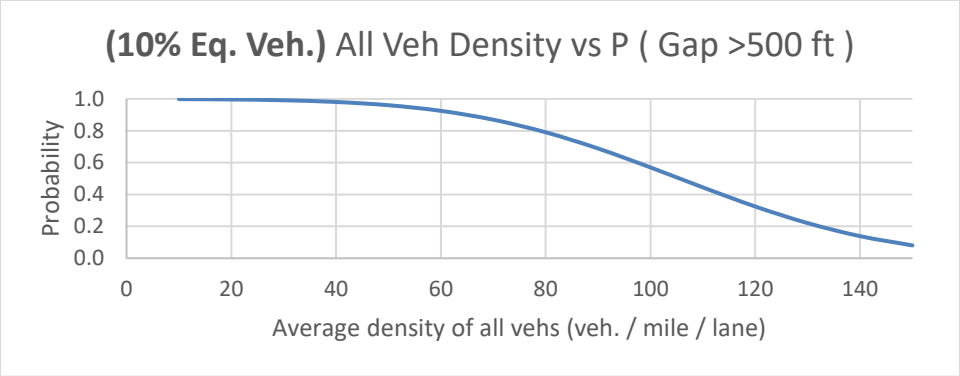

(a) η = 0.10

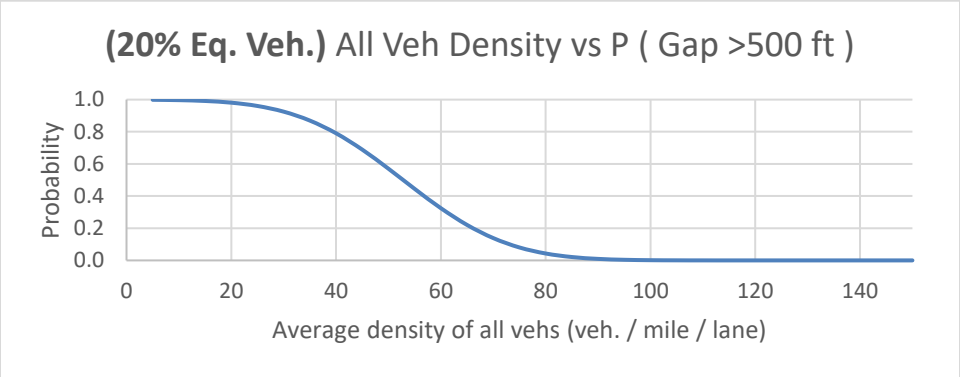

(b) η = 0.20

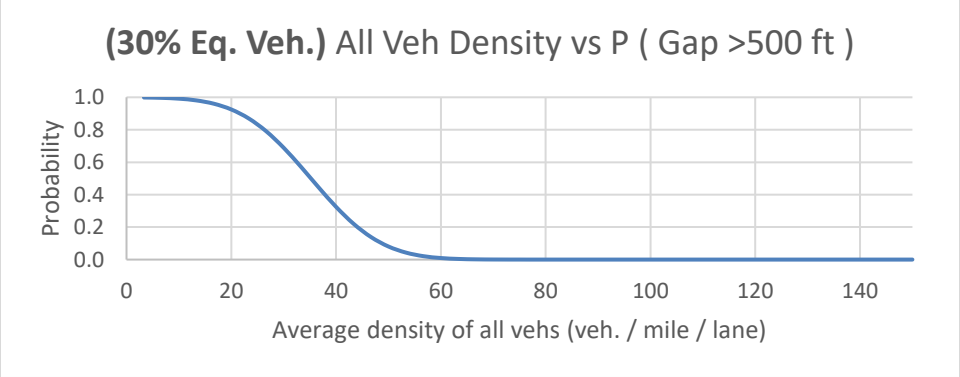

(c) η = 0.30

Figure 25: Probability P(Gap>500ft), of gap between equipped vehicles exceeding 500 ft, for (a) η = 0.10, (b) η = 0.20, and (c) η = 0.30.

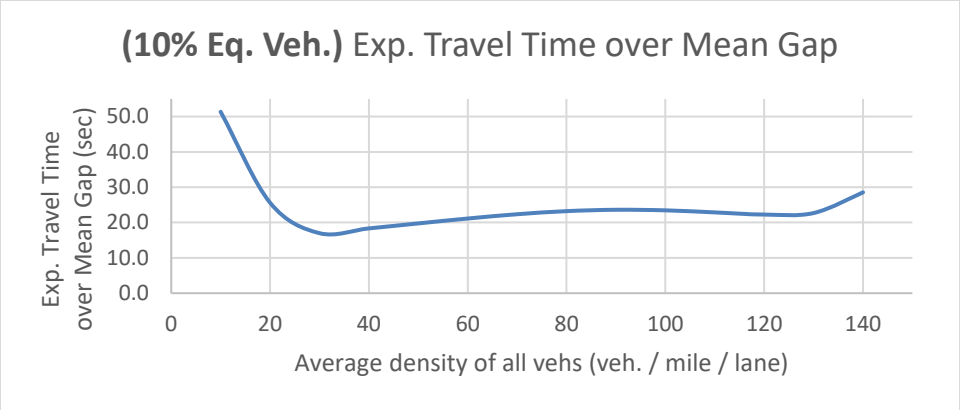

(a) η = 0.10

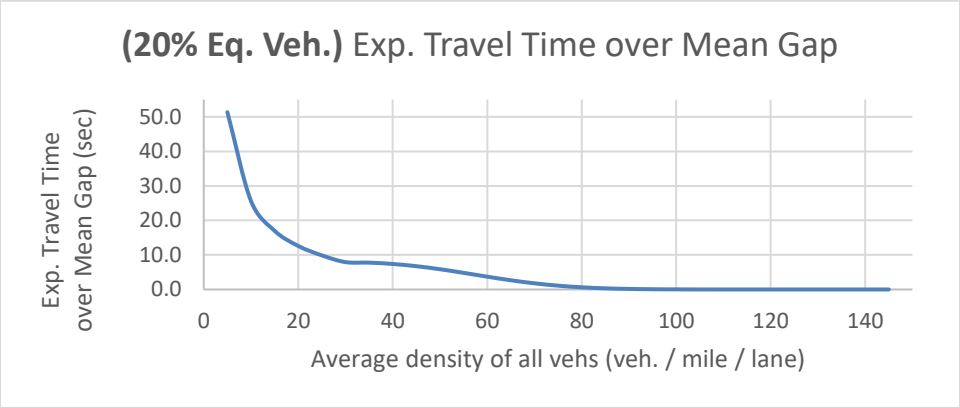

(b) η = 0.20

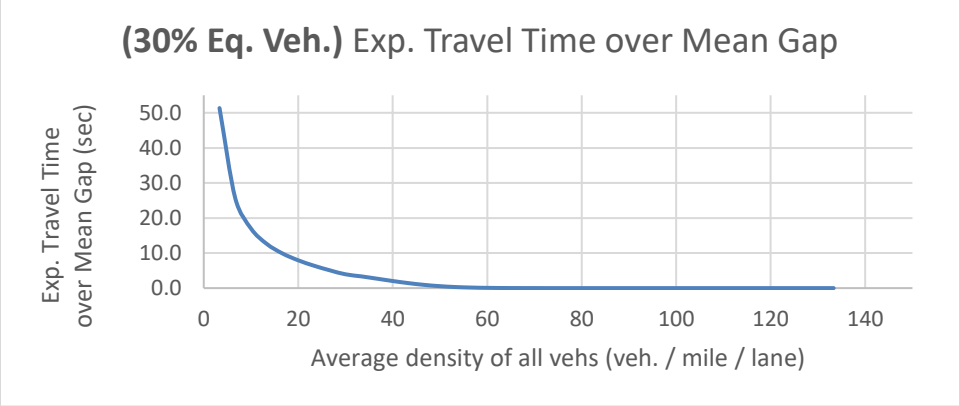

(c) η = 0.30

Figure 26: Expected travel time of information over the mean gap between equipped vehicles, for (a) η = 0.10, (b) η = 0.20, and (c) η = 0.30.

Gaps in information flow can also be eliminated by equipped vehicles traveling on intersecting flows. In Figure 27, there are equipped vehicles on link A and link B. They are not within transmission distance D_{TR} of each other.

However, there is an equipped vehicle traveling the intersecting path FE. It is within transmission distance of both of those equipped vehicles. It is important to note that this vehicle is continuing onto link E, and is not turning onto link B. Nonetheless, the gap is filled in and any message on the link A equipped vehicle can transmit to the one on link B.

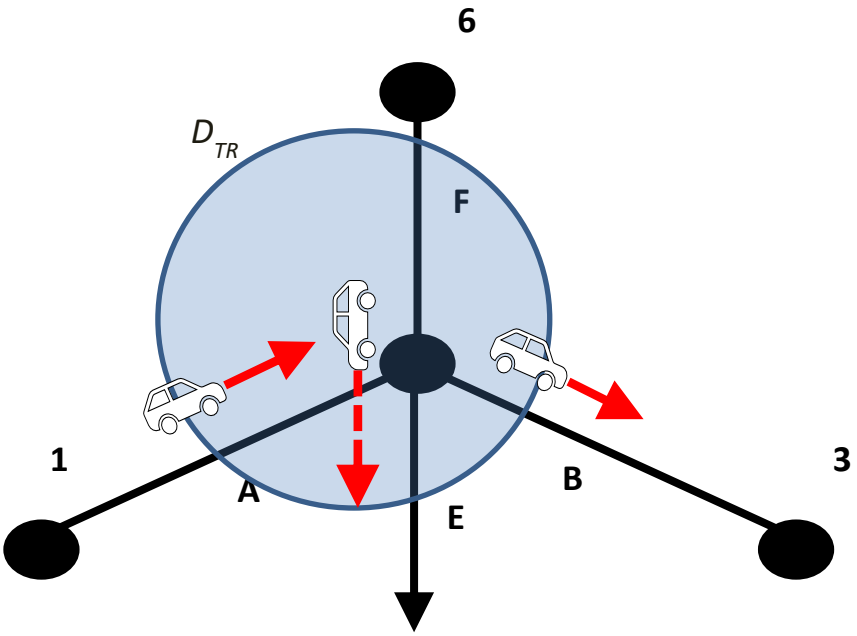

Figure 27: Gap in information flow from link A to link B is eliminated by an intersecting flow from link F to link E.

4.7.4 Sampling of Equipped Vehicles

In order to simulate the presence of equipped vehicles among the population of simulated vehicles, this study uses the software SAS to

1. take 50 samples of vehicles from the vehicle trajectory output,
2. designate them as equipped vehicles, and then
3. perform the Trajectory Analysis macros.

These trajectory analysis macros estimate the turning movements and link counts of equipped vehicles, then estimate the number of equipped vehicle encounters that occur at links and on nodes.

There are three different sampling rates: 10, 20, and 30 percent ($\eta = 0.10, 0.20, 0.30$). This study takes samples of equipped vehicles in two ways. First, all vehicles in the vehicle trajectory output can have an equal probability of being sampled. This is the Control Case.

However, after establishing the Control Case, one can designate specific subpaths so that one can sample the vehicles that use those subpaths at a greater rate. This is the Treatment Case. In the Treatment Case, it is imperative that one calculate the size of the subset so that it is represented at the desired level for the analysis.

4.7.5 Link Counts and Turning Movement Counts of Equipped Vehicles

Once the samples are drawn, one can begin the Trajectory Analysis. The Trajectory Analysis is supposed to produce link and turning movement counts of equipped vehicles, and estimate the equipped vehicle encounters at each node and link.

Every link *ij* has a count of equipped vehicles, ξ_{ij}, and every turning movement *ijk* has a turning movement count of equipped vehicles, φ_{ijk}. For each sample drawn, the list of nodes visited by every vehicle in the sample is broken into 2- and 3-node sequences. The SAS procedure `freq` then sums up these sequences to obtain the link counts and turning movements.

In the example in Figure 28, the link-level equipped vehicle count for link J (ξ_J) splits into two equipped vehicle turning movement counts φ_{JA} and φ_{JC}.

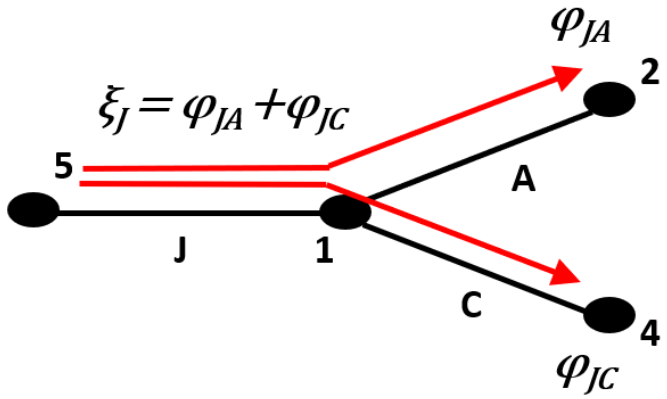

Figure 28: Example of relationship between link counts of equipped vehicles (here, ξ_J) and equipped vehicle turning movement counts (φ_{JA} and φ_{JC}).

4.7.6 Link and Node Equipped Vehicle Encounters

Other important quantities to estimate are the numbers of equipped vehicle encounters that occur on each link and node. For each sample, every node *A* has a count of equipped vehicle node encounters, ω_A. Likewise, every link *ij* has a count of equipped vehicle link encounters, θ_{ij}. These values are necessary in order to calculate expected information travel time along specific turning movements made by equipped vehicles.

Figure 29 demonstrates link and node equipped vehicle encounters in the same portion of the example network as Figure 27.

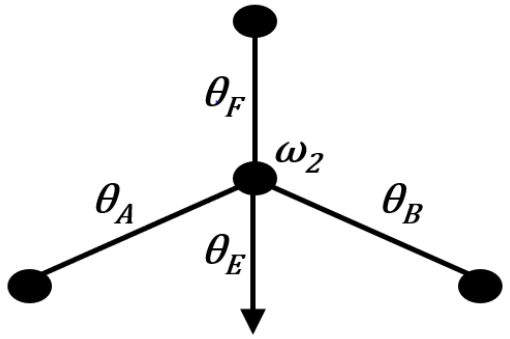

Figure 29: Link and node equipped vehicle encounters in a portion of the example network.

Links A, B, F, and E have equipped vehicle link encounters θ_A, θ_B, θ_F, and θ_E, respectively. Though this figure is focused on node 2 and shows node 2 as having a count ω_2 of equipped vehicle node encounters, there would also be equipped vehicle node encounter counts at the other three nodes shown. These counts would be ω_6, ω_3, and ω_1 proceeding clockwise from the 12 o'clock position.

The key to finding the link and node encounters of equipped vehicles is to sort vehicles by their node exit time, and then to check if vehicles come within a specified interval of each other. The procedure is slightly different for nodes and for links.

For nodes, the procedure to find equipped vehicle node encounters $\boldsymbol{\omega_A}$ is relatively straightforward. For each node and for each sample:

1. Sort the vehicles in the sample according to node exit time.
2. Create a lag variable to examine the vehicle directly behind.
3. Check if the two equipped vehicles are **within 6 sec** of each other (one DynusT simulation interval).

First, it is necessary to sort the vehicle in the sample according to when they exit that node. These node exit times are quantities which can be found in the vehicle trajectory output files generated by DynusT simulations during the simulation phase. Second, one then creates a lag variable to examine the vehicle directly behind. One can place multiple lag variables if one wants to determine if a vehicle is in contact with the vehicle 2, 3, 4, or even 5 places behind it, though the addition of additional lag variables can increase the computation time. Finally, one then checks if the two equipped vehicles are within 6 seconds of each other. Six seconds is equal to one DynusT simulation interval. At a free-flow speed of 60 mph, one DynusT simulation interval corresponds to approximately 500 feet (a reasonable transmission range). At slower speeds during congested flow, the 6-second interval represents an even smaller distance, well within transmission range.

To find the equipped vehicle link encounters $\boldsymbol{\theta_{ij}}$, the procedure is less straightforward because it requires the node exit times to be associated to the specific link for which it is the downstream node. That is, the node exit times must become link exit times. The procedure requires an extra step:

1. Match node exit times to the links for which those nodes are the downstream nodes. These node exit times become *link* exit times.

2. For each link, sort the vehicles in the sample according to link exit time.
3. For each link in the sample, create a lag variable to examine the vehicle directly behind.
4. For each link in the sample, check if the two equipped vehicles are **within 6 sec** of each other (one DynusT simulation interval).

The last two steps above (3 and 4) correspond to the last two steps (steps 2 and 3) of the procedure to find equipped vehicle node encounters ω_A. The first step is the most complicated to execute, but the second step follows logically from the shift in focus from nodes to links. The second, third, and fourth steps are repeated for each link and for each sample.

4.7.7 Information Turning Probability

The preceding quantities (link-level equipped vehicle counts ξ_{ij}, equipped vehicle turning movements φ_{ijk}, and link & node encounters ω_A and θ_{ij}) are necessary to calculate the probability that information can make a specified turning movement *ijk*. These probabilities are then multiplied with the steady state link travel time to calculate the expected travel time.

For each turning movement *ijk*, there are two types of information turning probabilities, π_{ijk} and ν'_{ijk}.

In the first type of information turning movement (π_{ijk}), information is passed to an equipped vehicle heading to the downstream link *jk* from an equipped vehicle within the upstream flow. To calculate this type of information turning probability, one distributes the link encounters on the upstream link, θ_{ij}, by the proportion of equipped vehicles φ_{ijk} making each downstream turning movement ijk.

In the second type of information turning movement (ν'_{ijk}), information is passed to a vehicle heading to the downstream link *jk* from an equipped vehicle that is at the same node. To calculate ν'_{ijk} requires several formulas, which are given in the example below.

Figure 30 and Figure 31 show examples of calculating these two types of information turning probabilities at two different portions of the example 8-node network.

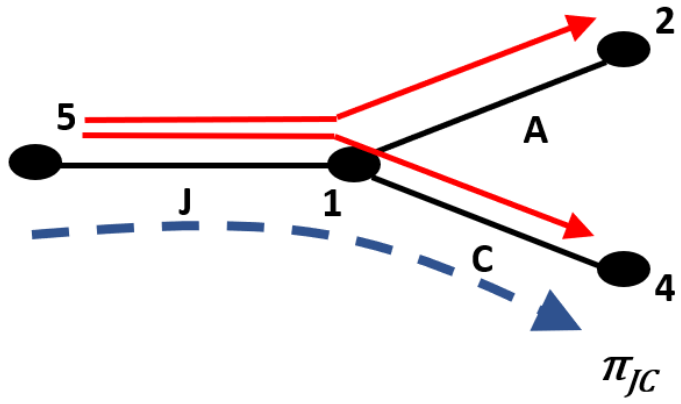

Figure 30: Example for calculating information turning probability π_{JC} from link J.

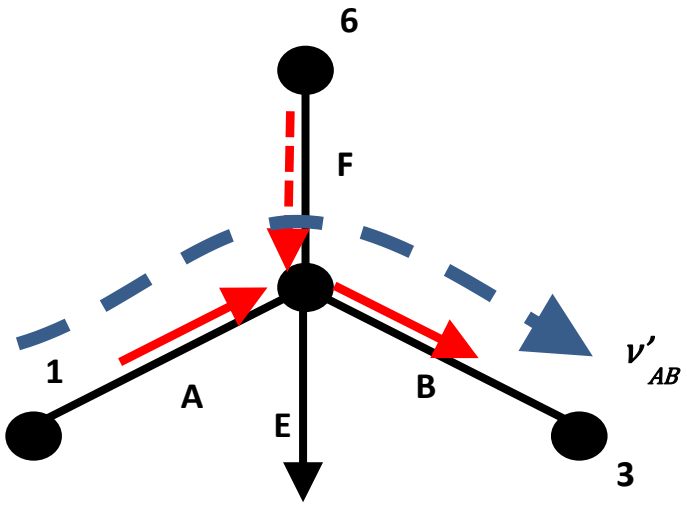

Figure 31: Example for calculating information turning probability ν'_{ijk} from node 2.

Equation (4-2) shows how to calculate $\boldsymbol{\pi}_{JC}$ from its contributing equipped vehicle link encounter $\boldsymbol{\theta}_J$, link count $\boldsymbol{\xi}_J$, and turning movement $\boldsymbol{\varphi}_{JC}$.

$$\boldsymbol{\pi}_{JC} = \frac{\boldsymbol{\theta}_J}{(\boldsymbol{\xi}_J)^2}(\boldsymbol{\varphi}_{JC}) \tag{4-2}$$

Equation (4-3) shows how to calculate $\boldsymbol{\nu}'_{JC}$ for the turning movement JC centered about node 2, though it requires the intermediary equations (4-4) to incorporate the equipped vehicle link encounters, link counts, and turning movements that contribute to node 2.

$$\boldsymbol{\nu}'_{JC} = \frac{\boldsymbol{\omega}_2}{\boldsymbol{V}_2}(\mathbf{1} - \boldsymbol{u}_A - \boldsymbol{b}_{B,i\neq 1}) \tag{4-3}$$

where

$$b_{B,i\neq 1} = \frac{1}{V_4}\sum_{\substack{jk=B \\ ij\neq A}} \varphi_{ijk} = \frac{1}{V_4}(\varphi_{EB} + \varphi_{FB}) = 0 \tag{4-4a}$$

$$u_A = \frac{1}{V_4}\sum_{ij=A} \varphi_{ijk} = \frac{1}{V_4}(\varphi_{AB}) \tag{4-4b}$$

$$V_4 = \sum_{j:2} \xi_{ij} = \xi_A + \xi_E + \xi_F \tag{4-4c}$$

4.8 Results

This study accomplished the following cases and phases for the baseline and disruption cases. Time constraints precluded the completion of Path Analysis for this study. For the Baseline scenario, the following phases were conducted for each case:

- Control Case: Simulation, Trajectory analysis
- Option 1 Cases:
    - Path 1 Increment 1 (+5%): Trajectory analysis
    - Path 1 Increment 2 (+10%): Trajectory analysis
    - Path 2 Increment 1 (+5%): Trajectory analysis
    - Path 2 Increment 2 (+10%): Trajectory analysis
- Option 2 Cases:
    - Path 3 Increment 1 (+5): Simulation, Trajectory analysis
    - Path 3 Increment 2 (+10): Simulation, Trajectory analysis

For the Disruption scenario, only the Simulation and Trajectory analysis phases of the Control case were conducted.

- Control Case: Simulation, Trajectory analysis

For each simulation performed, vehicle trajectories and link travel times are retained. Figure 32 is an example of Link Travel Time output from the simulation of Baseline Scenario, Treatment Case Option 2, Path 3, Increment 2.

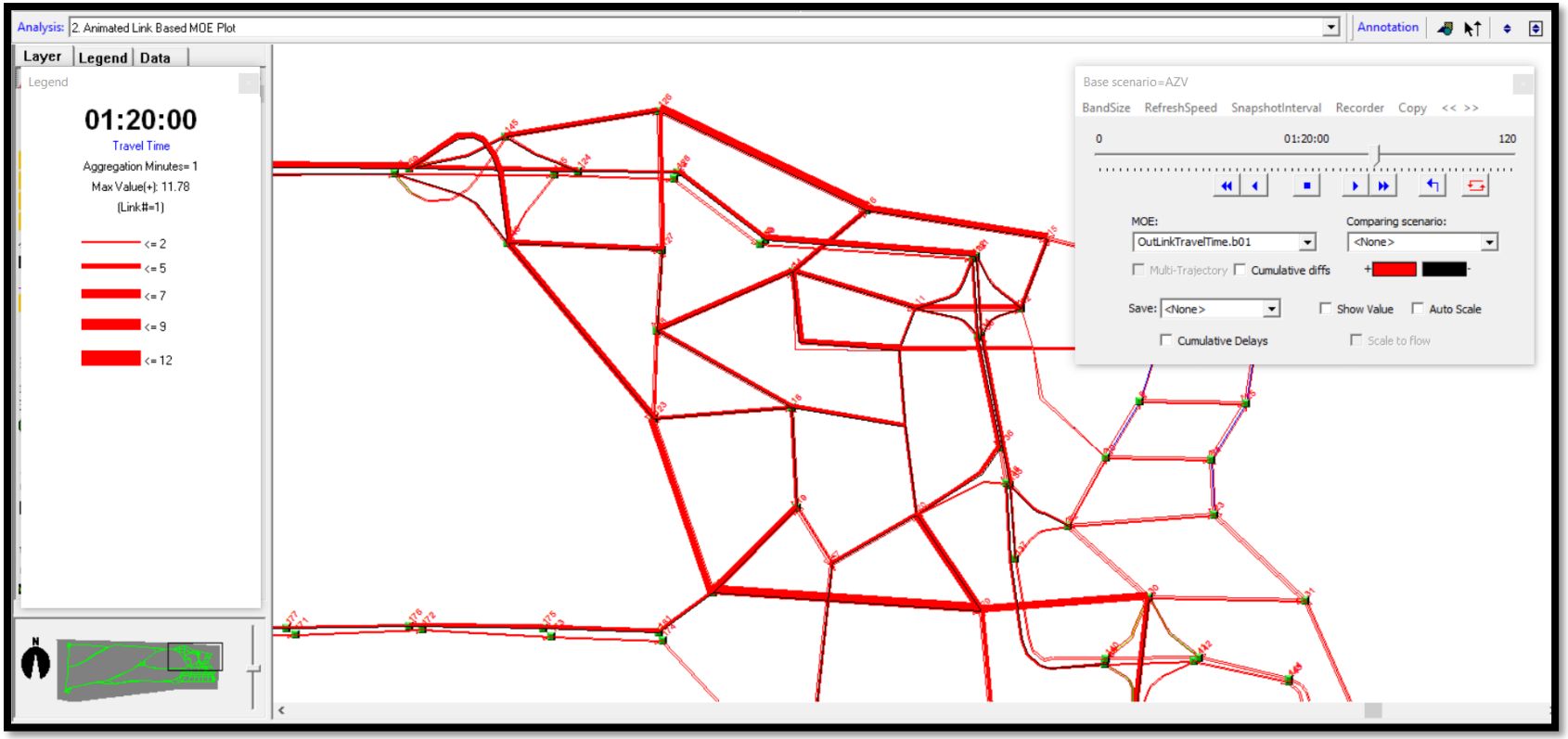

Figure 32: Link Travel Time output for Baseline Scenario, Treatment Case Option 2, Path 3, Increment 2 (10%).

With the vehicle trajectories in hand, it is possible to conduct Trajectory Analysis for all Cases, Options, Paths, and Increments in the Baseline Scenario. The most crucial segment of all three paths is found in this section of the network depicted in Figure 33. After conducting Subpath Analysis to find all paths being used between Sender node 127 and Receiver node 79, two paths were observed among the vehicle trajectories. The first is Path 1 (in goldenrod), which traverses nodes 127, 146, and 69. The second is Path 2 (in green), which traverses nodes 127, 126, 145, and 69.

These two paths represent two arterial paths to the freeway. For each of these two paths, Incremental Assignment was performed using Treatment Option 1. Two increments were performed: 5% and 10% increases in representation over the observed path flows in the Control case.

For Treatment Option 2, it was necessary to introduce an intersecting flow. The intersecting flow of Path 3 (in blue) was chosen. Path 3 was induced by adding trips into the OD matrix that travel from Zone 4 into Zone 1. This path exits the freeway link to traverse nodes 146, 123, 58, 127, and finally ending at 126. It intersects with Path 2 at nodes 146 and 127. Path 3 also intersects with Path 1 at node 127, link 127-126, and node 126.

Incremental Assignment was performed within Treatment Option 2. Instead of basing flow upon observed path flows in the Control case, increments in Treatment Option 2 (where a flow is introduced) are based upon percentages of the total number of trips in the OD matrix in the Control case. Two increments were performed: 5% and 10% of the total OD trips were introduced on Path 3. For each increment, a Trajectory Analysis was conducted.

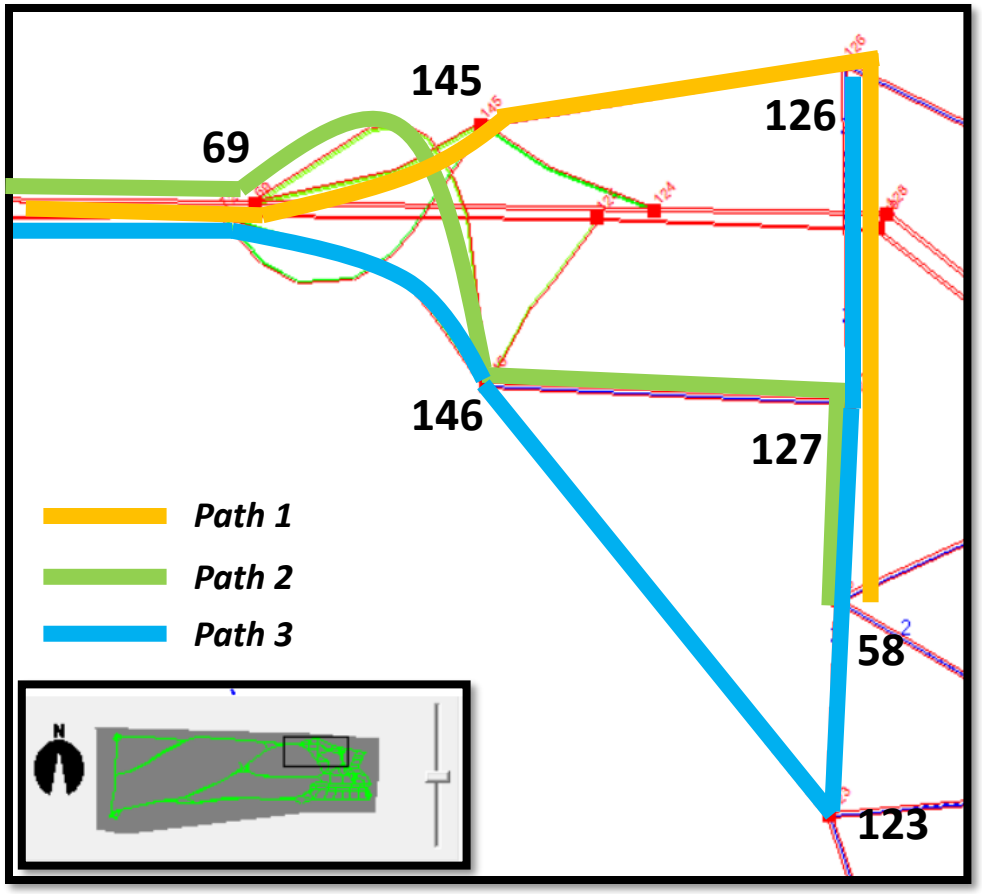

Figure 33: Paths emphasized during the Trajectory Analysis.

4.9 CONCLUSION

The desired contribution of Study 3 is to propose a model of information travel time along certain selected paths. The information travel time is based upon the flows of communication-equipped vehicles along those paths. These are vehicles that may only be traveling a portion of those paths. To calculate expected travel time of information along the selected paths, the simulation and analysis framework of this study proposes three phases (simulation, trajectory analysis, and path analysis). The analyst can elect to increase

representation of paths already found in the vehicle trajectories, or introduce new paths – these give rise to the treatment cases that are compared to the control case.

For a given control or treatment case, the methodology samples different proportions of simulated vehicles (10%, 20%, and 30%) as equipped vehicles. These samples' trajectories are analyzed to estimate link flow and turning movement counts of equipped vehicles, and to estimate the frequency of equipped vehicles encountering each other as they travel on links and through nodes. It is hypothesized that there would arise a difference in expected path travel times when 1. the representation of a specified subpath within the sample is increased and 2. vehicles are routed along currently unused subpaths.

However, this study does not yet attempt to optimize either the flow or travel time of information according to an objective function, algorithm, or heuristic. This study ultimately does not propose a general routing algorithm to find the set of routes for equipped vehicles that optimizes either the flow or travel time of information between all origins and destinations of information (i.e. sending or receiving nodes). Study 3 leaves such research questions for future work.

Nonetheless, while this optimization problem is beyond the scope of this study, the approach in this study could constitute a first step toward developing a methodology that can solve this more general formulation.

5 CONCLUSIONS

5.1 Contributions

The ability to model the disruptions of adverse events on various systems, such as infrastructural and social, is an important tool to assessing these systems' resilience. While previous research on system resilience concentrated on physical infrastructure such as transportation systems, two recent research topics include social resilience and dependencies across many infrastructure systems. For example, transportation is dependent on such systems as power, communications, and the workforces that are key to restoring these infrastructure systems.

This dissertation contains three disruption modeling studies that have followed the evolution of resilience research over the past decade from physical systems to interrelated topics.

The first study (Study 1) uses mesoscopic traffic simulation to evaluate seismic risk of potential travel time increases from earthquake damage to bridges in a roadway network. This analysis successfully obtained system risk curves of network-wide travel time increases. This study's main contribution was to extend the methodology of Shinozuka et al (2005) to include a mesoscopic traffic simulation model, and thereby achieve an unprecedented level of disaggregation in the seismic risk analysis of transportation lifelines.

The second study (Study 2) shifts focus towards workforces that participate in restoring infrastructure systems. It identifies transportation and communications workers and calculates these workers' exposure to the Peak Ground Accelerations (PGAs) of a 7.8 magnitude Southern California scenario earthquake. Indeed, for this scenario,

transportation workers are exposed to statistically significant higher PGAs than non-transportation workers, and communication workers to significantly lower PGAs.

Study 2 aims to make two contributions. First, it proposes the use of SOC and NAICS codes as a means of identifying those worker and industry categories who would most likely participate in restoring damaged transportation and communications infrastructure. To this end, this study produced a table that lists those SOC and NAICS codes which most closely correspond to the Transportation (ESF#1) and Communications (ESF#2) Emergency Support Functions of the *National Response Framework* (2016). Second, this study proposes one method to determine if any category of workers is exposed to higher PGAs in their PUMAs of residence. This method determines if the mean exposure to PGA of a worker category (e.g. ESF#1 or ESF#2) is equal to or different from the mean PGA exposure of the rest of the working population. The significance of these contributions is that for practitioners planning for disasters, awareness of which worker categories could be disproportionately impacted by a significant adverse event could facilitate pre-event response and recovery planning efforts.

The third study proposes a model for the travel time of information along communication-equipped vehicles physically traveling in a network. Vehicles are sampled as equipped vehicles, then their trajectories are analyzed to (1) estimate equipped vehicle link flow and turning movement counts and (2) estimate the frequency of equipped vehicles encountering each other on links and at nodes. This study compares two scenarios: the baseline scenario and a work zone scenario that corresponds to a bridge being damaged in the network. It is hypothesized that there would arise a difference in

expected path travel times when (1) the representation of a specified subpath within the sample is increased and (2) when vehicles are routed along currently unused subpaths.

The desired contribution of Study 3 is to propose a model of information travel time along certain selected paths. The information travel time is based upon the flows of communication-equipped vehicles along those paths. These are vehicles that may only be traveling a portion of those paths.

Study 3 does not yet attempt to optimize either the flow or travel time of information according to an objective function, algorithm, or heuristic. That is, this study ultimately does not propose a general routing algorithm to find the set of routes for equipped vehicles that optimizes either the flow or travel time of information between all origins and destinations of information (i.e. sending or receiving nodes).

Nonetheless, while this optimization problem is beyond the scope of this study, the approach in this study could constitute a first step toward developing a methodology that can solve this more general problem.

5.2 Future Work

Each of the three studies has potential for novel future work.

Study 1 was an early study conducted in 2009. Many advances have been made in both scholarship and practice regarding fragility curve modeling, the calculation of ground motion measures, and the emergence of sophisticated transportation system models. For example, if Study 1 were conducted in the present day, instead of using attenuation functions, the study would employ ground motion ShakeMaps produced by USGS – an improvement made possible with modern improvements in Geographical Information Systems (GIS). Instead of using fragility curves based on Peak Ground Acceleration (PGA),

the study would use fragility curves based upon Peak Spectral Acceleration (PSA) at one second. These PSA-based curves are used in the USGS ShakeCast system which has been adopted by such agencies as the California Department of Transportation (Caltrans) (DesRoches et al, 2012). Another potential improvement is to use an Activity Based Model in place of either a static model or a mesoscopic traffic simulation model, should an agency allow access to its model.

For Study 2, there are other potential applications for applying the study's methodology in future research. For example, transportation infrastructure has interdependencies with energy infrastructure; thus, this methodology can be extended to include ESF#12 (Energy) workers. In addition, this methodology could be extended to all 14 ESFs. Similarly, the methodology could be applied to the six *National Disaster Recovery Framework (NDRF)* (2016) Recovery Support Functions (RSFs) and to the Department of Homeland Security's sixteen Critical Infrastructure Sectors (CISs). In these cases, the scope of the study would extend beyond transportation and cover other areas of emergency management.

In addition, Study 2's methodology could use another measure of worker vulnerability in place of PGA. For example, one could use risk measures of other hazards, such as wildfire or flood risk. In addition, another potential application for this methodology would be to conduct a case study in partnership with a transportation agency. Such a case study would allow the agency to assess exposure of its own employees to its most high-priority hazards. The agency can thereby tailor its strategy for mitigating potential worker shortfalls using data from its own employees (rather than general working population data from PUMS).

For Study 3, the clear next step in future work would be a general routing scheme that finds the set of routes for equipped vehicles that optimizes either the flow or travel time of information between all origins and destinations of information. Study 3 does not yet attempt to optimize either the flow or travel time of information according to an objective function, and to an algorithm or heuristic. Nonetheless, the approach in this study could constitute a first step toward developing a methodology that can solve this more general formulation.

6 References

2011-2015 ACS PUMS Data Dictionary. (2017, Jan 19). Washington, D.C.: U.S. Census Bureau. Retrieved from https://www2.census.gov/programs-surveys/acs/tech_docs/pums/data_dict/PUMS_Data_Dictionary_2011-2015.pdf.

"After Action-Corrective Action Reporting". (no date). California Governor's Office of Emergency Services (Cal OES). Retrieved from http://www.caloes.ca.gov/cal-oes-divisions/planning-preparedness/after-action-corrective-action-reporting

American Public Transportation Association (APTA). (2010). *Recommended Practice: Securing Control and Communications Systems in Transit Environments.* APTA-SS-CCS-RP-001-10. Washington, D.C.: American Public Transportation Association. Retrieved from *http://www.apta.com/resources/standards/Documents/APTA-SS-CCS-RP-001-10.pdf*

California Department of Transportation (Caltrans) Structure Maintenance and Investigations. (2009). *California Log of Bridges on State Highways: District 7*. http://www.dot.ca.gov/hq/structur/strmaint/brlog/logpdf/logd07.pdf. Accessed June 29, 2009.

Campbell, K.W. (1997). Empirical near-source attenuation relationships for horizontal and vertical components of peak ground acceleration, peak ground velocity, and pseudo-absolute acceleration response spectra. *Seism. Res. Lett.* **68**, 154–179.

Campbell KW, Bozorgnia Y. (2006). *Campbell-Bozorgnia NGA empirical ground motion model for the average horizontal component of PGA, PGV, PGD and SA at selected spectral periods ranging from 0.01 – 10.0 seconds (Version 1.0)*.

http://peer.berkeley.edu/lifelines/repngamodels.html. Berkeley, CA: Pacific Earthquake Engineering Center.

Chang, S.E., Shinozuka, M. and Moore, J. (2000). Probabilistic Earthquake Scenarios: Extending Risk Analysis Methodologies to Spatially Distributed Systems. *Earthquake Spectra*, Vol.16, No.3, pp.-557-572.

Chiu, Y.-C., E. Nava, H. Zheng and B. Bustillos. (no date). *DynusT Online User's Manual*. Retrieved from http://dynust.net/wikibin/doku.php. Accessed May 29, 2009.

Cho, S., Fan, Y.Y., and J.E. Moore. (2003). Modeling Transportation Network Flows as Simultaneous Function of Travel Demand, Earthquake Damage, and Network Level of Service. *Proceedings, Sixth U.S. Conference and Workshop on Lifeline Earthquake Engineering*, American Society of Civil Engineers (ASCE), August 10–13, 2003, Long Beach, CA, pp 868–877.

Cook, Kevin. (2017) Ports, Impact Assessments, and Emergency Management. Washington, D.C.: *Transportation Research Board 96th Annual Meeting*.

Countermeasures Assessment and Security Experts (CASE) LLC and Western Management and Consulting (WMC) LLC. (2015). *NCHRP Report 221/TCRP Report 67: Protection of Transportation Infrastructure from Cyber Attacks: A Primer*. Washington, D.C.: Transportation Research Board. Retrieved from http://www.trb.org/Main/Blurbs/174382.aspx.

Corelogic. (2016). *California Earthquake Risk Report*. Retrieved from http://www.corelogic.com/about-us/researchtrends/california-earthquake-risk-report.aspx#.WNGvePkrJEY

DeBlasio, A.J., Zamora, A., Mottley, F., Brodesky, R., Zirker, M.E., and M. Crowder. (2002). Northridge Earthquake – January 17, 1994. *Effects of Catastrophic Events on Transportation System Management and Operations*. Federal Highway Administration (FHWA), U.S. Department of Transportation.

DesRoches, R., Padgett, J., Ramanathan, K., Dukes, J. (2012, September). *Feasibility Studies for Improving Caltrans Bridge Fragility Relationships*. Report CA12-1775. California Department of Transportation. Retrieved from http://www.dot.ca.gov/newtech/researchreports/reports/2012/t1775_final_report_cjr_v2.pdf

"Disasters | FEMA.gov". (no date). Federal Emergency Management Agency (FEMA). Retrieved from https://www.fema.gov/disasters

DynusT (2017 Build) Use Case Guide. (2017, Oct 02). Tucson, AZ: Metropia.

Emergency Support Function #1 – Transportation. (2016, June). Washington, D.C.: Federal Emergency Management Agency (FEMA). Retrieved from https://www.fema.gov/media-library-data/1470148635327-75b99900ae83949a9c5577c1dc99ccdd/ESF_1_Transportation_20160705_508.pdf.

Emergency Support Function #2 – Communications. (2016, June). Washington, D.C.: Federal Emergency Management Agency (FEMA). Retrieved from https://www.fema.gov/media-library-data/1473679033823-d7c256b645e9a67cbf09d3c08217962f/ESF_2_Communications_FINAL.pdf.

Federal Automated Vehicles Policy (2016). National Highway Traffic Safety Administration (NHTSA).

Ghaleb, M. M., Subramaniam, S., Othman, M., & Zukarnain, Z. (2014). Static and mobile data gathering techniques in wireless sensor networks: A Survey. *International Journal of Advancements in Computing Technology*, 6(3), 47.

Hagihara, Ken. (2015, May 05). U.S. 3rd Fleet Participates in Exercise Ardent Sentry 2015. *Navy News Service*. http://www.navy.mil/submit/display.asp?story_id=87132. Accessed July 15, 2017.

HAZUS-MH MR Technical Manual. (2003). Federal Emergency Management Agency (FEMA). Washington, D.C.: Department of Homeland Security Emergency Preparedness and Response Directorate.

ITS America. (2013a). *2013 Deployment Tracking Survey Results*. Retrieved from http://www.itsdeployment.its.dot.gov/Default.aspx

ITS America. (2013b, Dec.). *Market Report: State ITS Trends*. Retrieved from http://itsamerica.org/state-dot-its-trends/

Jayakrishnan, R., Mahmassani, H., Hu, T-Y. (1993). An evaluation tool for advanced traffic information and management systems in urban networks. *Transportation Research* 2C(3), 129–148.

Jea, D., Somasundara, A., & Srivastava, M. (2005, June). Multiple controlled mobile elements (data mules) for data collection in sensor networks. In *international conference on distributed computing in sensor systems* (pp. 244-257). Springer Berlin Heidelberg.

Jones, L.M., Bernknopf, R, Cox, D, Goltz, J, Hudnut, K, Mileti, D, Perry, S, Ponti, D, Porter, K, Reichle, M, Seligson, H, Shoaf, K, Treiman, J, and Wein, A. (2008). *The ShakeOut Scenario*. U.S. Geological Survey Open-File Report 2008-1150 and California Geological Survey Preliminary Report 25.

Lattanzi, D., Khaloo, A., Cunningham, K., Riley, M., Dell'Andrea, R. (2017). Integrating UAVs and photogrammetry to support bridge inspections, *96th Annual Meeting of the Transportation Research Board*, Washington, DC, January 8-12, 2017.

LeBrun, J., Chuah, C. N., Ghosal, D., & Zhang, M. (2005, May). Knowledge-based opportunistic forwarding in vehicular wireless ad hoc networks. In *Vehicular technology conference, 2005. VTC 2005-Spring*. *2005 IEEE 61st* (Vol. 4, pp. 2289-2293).

Lupa, M.R, R.W. Eash, P. Mescher, J.T. von Brown, and C.A. Clymer. (2015). Rail Freight Commodity Model for Iowa: Methodology & First Steps. Washington, D.C.: *Transportation Research Board 94th Annual Meeting*.

M 6.7 - 1km NNW of Reseda, CA. (no date). United States Geological Survey (USGS). Retrieved from https://earthquake.usgs.gov/earthquakes/eventpage/ci3144585

M 7.8 Scenario Earthquake - Ardent Sentry 2015 Scenario. (no date). United States Geological Survey (USGS). Retrieved from https://earthquake.usgs.gov/scenarios/eventpage/sclegacyardentsentry2015_se.

M 7.8 Scenario Earthquake – Shakeout2 Full Scenario. (no date). United States Geological Survey (USGS). Retrieved from https://earthquake.usgs.gov/scenarios/eventpage/sclegacyshakeout2full_se.

Mahmassani, H. S., Qin, X., and X. Zhou. (2004a). DYNASMART-X evaluation for real-time TMC application: Irvine test bed. *TREPS Phase 1.5B Final Rep*. College Park, MD : Maryland Transportation Initiative, University of Maryland.

Mahmassani, H.S., Sbayti, H., and X. Zhou. (2004b). *DYNASMART-P Version 1.0 User's Guide*. College Park, MD: Maryland Transportation Initiative, university of Maryland.

Maison, B. and K. Cobeen. (2016, Feb). Analytical Study of Mobile Home Response to the 2014 South Napa Earthquake. *Earthquake Spectra*, Vol. 32, No. 1, pp. 1-22.

Mean & Standard Deviation Calculator for Frequency Table & Grouped Data. (no date). KNOWPAPA.COM. Retrieved from http://knowpapa.com/sd-freq/. Accessed July 15, 2017.

Meghanathan, N. (2007, March). Stability-energy consumption tradeoff among mobile ad hoc network routing protocols. In *Wireless and Mobile Communications, 2007. ICWMC'07. Third International Conference* on (pp. 9-9). IEEE.

Nasipuri, A., Castañeda, R., & Das, S. R. (2001). Performance of multipath routing for on-demand protocols in mobile ad hoc networks. *Mobile Networks and applications*, 6(4), 339-349.

National Disaster Recovery Framework (NDRF) (2016, 2nd Ed). US Department of Homeland Security.

National Infrastructure Protection Plan (2013). US Department of Homeland Security.

National Preparedness Goal (NPG) (2015, 2nd Ed). US Department of Homeland Security.

National Response Framework (NRF) (2016, 3rd Ed). US Department of Homeland Security.

Oliveira-Neto, F.M., S.M. Chin, H.L. Hwang. (2012). Aggregate Freight Generation Modeling: Assessing Temporal Effect of Economic Activity on Freight Volumes with Two-Period Cross-Sectional Data. Washington, D.C.: *Transportation Research Record*, Issue 2285, pp 145–154.

Oliveira-Neto, F.M., S.M. Chin, H.L. Hwang, B. Peterson. (2013). Methodology for Estimating Ton-Miles of Goods Movements for U.S. Freight Multimodal Network System. Oak Ridge, TN: Oak Ridge National Laboratory.

SCLEGACY (Scenario Catalog): Southern California Legacy Catalog. (2017). United States Geological Survey (USGS). Retrieved from https://earthquake.usgs.gov/scenarios/catalog/sclegacy/. Accessed July 15, 2017.

Shah, R. C., Roy, S., Jain, S., & Brunette, W. (2003). Data mules: Modeling and analysis of a three-tier architecture for sparse sensor networks. *Ad Hoc Networks*, 1(2), 215-233.

Sheehan, Terrence. (2015). St. Louis County, Minnesota, June 2012 Floods: Critical Connections of Low-Volume Roads. Washington, D.C.: *Transportation Research Board 94th Annual Meeting*.

Shinozuka, M., Zhou, Y., Kim, S., Murachi, Y., Banerjee, S., Cho, S., and H. Chung. (2005). *Socio-economic Effect of Seismic Retrofit Implemented on Bridges in the Los Angeles Highway Network.* Report F/CA/SD-2005/03. California Department of Transportation. Retrieved from http://www.dot.ca.gov/newtech/researchreports/reports/2008/06-0145.pdf

Sisiopiku, V.P., Li, X., Abro, A.M., and R.W. Peters. (2007). *Transportation Facilities Management Under Emergencies*. UTCA Report 06202. University Transportation Center for Alabama.

Southworth, F., J. Hayes, S. McLeod, and A. Strauss-Wieder. (2014). *Making US Ports Resilient as Part of Extended Intermodal Supply Chains*. National Cooperative Freight Research Program Report 30. Washington, D.C.: Transportation Research Board. Retrieved from http://onlinepubs.trb.org/onlinepubs/ncfrp/ncfrp_rpt_030.pdf.

"Standing Committees by Mode and Topic". (2017). Transportation Research Board. Washington, DC. http://www.trb.org/AboutTRB/StandingCommitteesMT.aspx. Accessed July 15, 2017.

State of California Emergency Plan (2017). California Governor's Office of Emergency Services (Cal OES).

"Top 20 Deadliest California Wildfires". (2018, August 20). California Department of Forestry and Fire Protection (Cal Fire). Retrieved from http://calfire.ca.gov/communications/downloads/fact_sheets/Top20_Deadliest.pdf

"Top 20 Largest California Wildfires". (2018, August 27). California Department of Forestry and Fire Protection (Cal Fire). Retrieved from https://www.fire.ca.gov/communications/downloads/fact_sheets/Top20_Acres.pdf

"Top 20 Most Destructive California Wildfires". (2018, August 20). California Department of Forestry and Fire Protection (Cal Fire). Retrieved from http://www.fire.ca.gov/communications/downloads/fact_sheets/Top20_Destruction.pdf

Transportation Systems Sector-Specific Plan. (2015). Washington, D.C.: US Department of Homeland Security and US Department of Transportation. Retrieved from https://www.dhs.gov/publication/nipp-ssp-transportation-systems-2015.

US Geological Survey (USGS). (2009). New Study Shows Odds High for Big California Quakes. Retrieved from www.usgs.gov/newsroom/article.asp?ID=1914. Accessed July 28, 2009.

Wachs, M., L.L. Cove, T.B. Dean, G.B. Dresser, R.W. Eash, R.A. Johnson, E.J. Miller, M.R. Morris, R.H. Pratt, C.L. Purris, G. Rousseau, M.J. Tischer, and R.E. Wallker. (2007). *Metropolitan Travel Forecasting: Current Practice and Future Direction*. Transportation Research Board Special Report 288. Washington, D.C.: Transportation Research Board of the National Academies.

Wallischeck, Eric. (2016). *GPS Dependencies in Transportation: An Inventory of Global Positioning System Dependencies in the Transportation Sector, Best Practices for Improved Robustness of GPS Devices, and Potential Alternative Solutions for Positioning, Navigation and Timing*. Publication DOT-VNTSC-NOAA-16-01. Volpe National Transportation Systems Center and National Oceanic and Atmospheric Administration. Retrieved from http://ntl.bts.gov/lib/60000/60400/60433/DOT_VNTSC_NOAA_16_01.pdf.

Wein, A., L. Johnson, and R. Bernknopf. (2011, May). Recovering from the ShakeOut Earthquake. *Earthquake Spectra*, Vol. 27, No. 2, pp. 521-538.

Werner, S.D., Lavoie, J.P., Eitzel, C., Cho, S., Huyck, C., Ghosh, S., Eguchi, R.T., Taylor, C.E. and J.E. Moore. (2008). *REDARS 1: Demonstration software for seismic risk analysis of highway systems*. Buffalo, NY: MCEER University of Buffalo. mceer.buffalo.edu/publications/resaccom/03-sp01/02werner.pdf. Accessed September 16, 2008.

Werner, S.D., Taylor, C.E., Cho, S., Lavoie, J.P., Huyck, C., Eitzel, C., Chung, H., and R.T. Eguchi. (2006). *Technical Manual: REDARS 2 Methodology and Software for Seismic Risk Analysis of Highway Systems*. Buffalo, New York: Multidisciplinary Center for Earthquake Engineering Research (MCEER).

Yang, S., Adeel, U., & McCann, J. A. (2013). Selfish mules: Social profit maximization in sparse sensornets using rationally-selfish human relays. *IEEE Journal on Selected Areas in Communications*, 31(6), 1124-1134.

Yang, X., & Recker, W. W. (2006). Modeling dynamic vehicle navigation in a self-organizing, peer-to-peer, distributed traffic information system. *Journal of intelligent transportation Systems*, *10*(4), 185-204.

Yazıcıoğlu, A. Y., Egerstedt, M., & Shamma, J. S. (2013). A game theoretic approach to distributed coverage of graphs by heterogeneous mobile agents. *IFAC Proceedings Volumes*, 46(27), 309-315.

Zhao, W., Ammar, M., & Zegura, E. (2004, May). A message ferrying approach for data delivery in sparse mobile ad hoc networks. In *Proceedings of the 5th ACM international symposium on Mobile ad hoc networking and computing* (pp. 187-198). ACM.